RESEARCH & DEVELOPMENT

Development of a New Chip Seal Mix Design Method

Y. Richard Kim, Ph.D., P.E., F. ASCE

Javon Adams, Ph.D.

Dept. of Civil, Construction, & Environmental Engineering

North Carolina State University

NCDOT Project 2008-04

FHWA/NC/2008-04

December 2012

Development of a New Chip Seal Mix Design Method

FINAL REPORT
(Report No. FHWA/NC/2008-04)

Submitted to the North Carolina Department of Transportation
(Research Project No. HWY-2008-04)

Submitted by

Y. Richard Kim, Ph.D., P.E., F.ASCE
Distinguished University Professor
Campus Box 7908
Department of Civil, Construction, & Environmental Engineering
North Carolina State University
Raleigh, NC 27695-7908
Tel: 919-515-7758, Fax: 919-515-7908
E-mail: kim@ncsu.edu

Javon Adams
Graduate Research Assistant / Ph.D. Candidate
Campus Box 7908
Department of Civil, Construction & Environmental Engineering
North Carolina State University
Raleigh, NC 27695-7908
E-mail: jmadams2@ncsu.edu

Department of Civil, Construction, & Environmental Engineering
North Carolina State University
Raleigh, NC

December 2012

Technical Report Documentation Page

1. Report No. FHWA/NC/2008-04	2. Government Accession No.	3. Recipient's Catalog No.
4. Title and Subtitle Development of a New Chip Seal Mix Design Method		5. Report Date December 2012
		6. Performing Organization Code
7. Author(s) Y. Richard Kim and Javon M. Adams		8. Performing Organization Report No.
9. Performing Organization Name and Address Campus Box 7908, Dept. of Civil, Construction, & Environmental Engrg. NCSU, Raleigh, NC 27695-7908		10. Work Unit No. (TRAIS)
		11. Contract or Grant No.
12. Sponsoring Agency Name and Address NC Department of Transportation Research and Analysis Group 1 South Wilmington Street Raleigh, NC 27601		13. Type of Report and Period Covered Final Report July 2007 – December 2010
		14. Sponsoring Agency Code 2008-04
15. Supplementary Notes		

16. Abstract

This report presents a new performance-related mix design method for chip seal construction. The components of this method include the determination of an optimal aggregate application rate (AAR) using the modified board test and determination of an optimal emulsion application rate (EAR) using the laser profiler. The board test used in the Modified Kearby chip seal mix design method has been modified further to accommodate an optimal board size and a minimum number of board test replicates to yield the least variability and most representative AAR to fill the board tray with a single layer of aggregate. The main concept used in the determination of the optimal EAR is that the initial embedment depth of the aggregate particles should be 50% of the total depth. The 50% embedment concept is validated by the aggregate loss and bleeding test results using the third scale Model Mobile Loading Simulator (MMLS3). This validation study used Granite 78M and lightweight aggregate with CRS-2L emulsion to fabricate the chip seal specimens in the laboratory. Three different gradations with vastly different performance uniformity coefficients (PUCs) were used for each of the two aggregate types. An optimum AAR for each gradation was determined by the modified board test. Chip seal specimens were fabricated using the laboratory scale chip spreader, ChipSS, and EARs were varied from 0.1 to 0.3 gal/yd^2 at increments of 0.05 gal/yd^2. It was found from the bleeding test that the optimal EARs determined by the NCSU mix design method for the different chip seal specimens were the maximum EARs that did not cause bleeding, thus validating the NCSU mix design concept. The final optimum EAR is determined after accounting for the aggregate absorption and existing pavement surface absorption via the percentage of absorption of the aggregate and the surface texture measurements obtained from the laser profiler. A comparison of the mix design rates with the rates used by the NCDOT Divisions reveals that the mix design AARs and EARs are about 40% and 20% lower than the field rates, respectively. Various factors explain these differences, including wet aggregate and traffic whip-off to explain the AARs, and the absorption of both the aggregate and existing pavement surface to explain the EARs. Finally, further research is suggested to conduct field calibration and validation of the performance-related chip seal mix design method in order to take full advantage of the performance-related mix design method so that the NCDOT can implement the proposed method in routine chip seal construction.

17. Key Words Chip Seal, Performance-Related, Mix Design, Board Test, Laser, Embedment	18. Distribution Statement		
19. Security Classif. (of this report) Unclassified	20. Security Classif. (of this page) Unclassified	21. No. of Pages 104	22. Price

Form DOT F 1700.7 (8-72) **Reproduction of completed page authorized**

DISCLAIMER

The contents of this report reflect the views of the authors and are not necessarily the views of North Carolina State University. The authors are responsible for the facts and the accuracy of the data presented herein. The contents do not necessarily reflect the official views or policies of the North Carolina Department of Transportation at the time of publication. This report does not constitute a standard, specification, or regulation.

ACKNOWLEDGEMENTS

This research was sponsored by the North Carolina Department of Transportation. The Steering and Implementation Committee was comprised of Dennis Wofford (Chair), Judith Corley-Lay, Ph.D., P.E.; Jack Cowsert, P.E.; Terry McLaurin; Averette Moore; Christopher Peoples, P.E.; James Phillips, P.E.; Vann Price; Jackson Provost, P.E.; Archie Smith, Jr.; David Spainhour, P.E.; and Todd Whittington, P.E. These advisors have given invaluable direction and support to the research team throughout the project.

Table of Contents

1. INTRODUCTION

1.1 Research Needs and Significance

In the last decade, the NCDOT has placed a great emphasis on pavement preservation. The Department has formally trained field personnel on the importance of “placing the right treatment on the right road at the right time.” One of the most cost-effective preservation treatments is the chip seal. The NCDOT has expanded its chip-sealing operation and is paving approximately 3,000 centerline miles annually. In July 2006, the General Assembly added a line item to the NCDOT budget, which specifically funds “System Preservation.” With this great interest in and emphasis on pavement preservation, there is a need to research further preservation treatments.

The importance of chip seals in serving the North Carolina public is demonstrated by three research projects that have been funded by the NCDOT since 2003. These research projects include: (1) Optimizing Gradations for Surface Treatments (NCDOT Project HWY-2004-04); (2) Quantifying the Benefits of Improved Rolling of Chip Seals (NCDOT Project HWY-2006-06); and (3) Performance-Based Analysis of Polymer-Modified Emulsions in Bituminous Surface Treatments (NCDOT Project HWY-2007-06). The overarching goal of these projects is to improve the performance of chip seals in North Carolina by investigating three major components involved in the construction of chip seals: the aggregate (HWY-2004-04), emulsion (HWY-2007-06), and rolling procedure (HWY-2006-06).

During the course of conducting these research projects, existing chip seal test methods and design procedures were carefully reviewed and evaluated. The review of existing design procedures has revealed a clear need for a new chip seal design procedure that can encompass newer materials and is based on performance. Specifically, the existing design methods do not take into consideration lightweight materials, which are used throughout the State, and the use of polymer-modified emulsion, the use of which is gaining support in more Divisions.

The earliest design procedure for asphalt surface treatments (ASTs) was developed by Hanson (Hanson 1934, 1935). His design methodologies are used in all major AST designs in current use. In North Carolina, the most generally accepted AST design methods are the Kearby method and the McLeod method. Although a few North American agencies have developed their own formal design procedures that are not based on either method, most use either an empirical design method or no formal method at all (Gransberg 2005). The two existing mix design methods for chip seals (Kearby and McLeod) are old and have not been refined in years.

Another critical need for improvement that was identified during the three chip seal research projects at North Carolina State University (NCSU) is a reliable test method that can better represent the conditions in the field. Most test methods are empirical in nature and yield more qualitative results than quantitative results. Although the hot mix asphalt (HMA) community has adopted more recent technologies in evaluating the performance of HMA, the chip seal community has not. Several test methods have been developed or are under development at

NCSU. One of the major accomplishments in this area is the aggregate retention and bleeding test using the third-scale Model Mobile Loading Simulator (MMLS3). This test method has been used in the NCDOT HWY-2004-04 project to successfully evaluate the effect of fine contents and aggregate gradation on aggregate loss. Because the MMLS3 test is capable of evaluating both the aggregate retention and bleeding performance of the chip seal under realistic loading conditions, it is ideal for evaluating the reliability of the mix design procedure.

Other test methods that are available at NCSU include: a digital imaging technique to evaluate bleeding; a cross-sectional digital imaging technique of chip seals reinforced by epoxy to determine the aggregate embedment depth; and a laser surface profiling system to determine the aggregate exposure depth. These test methods are designed to be applicable to both laboratory and field conditions. These new test methods can play a major role in developing a chip seal mix design procedure that is based on reliable, quantitative and objective measures of design parameters.

This report describes research efforts for developing a performance-based chip seal design procedure using the experience and results obtained from the previous research projects at NCSU and the newly developed performance test methods.

1.2 Research Objective

The objective of the research project is to develop a new chip seal mix design method that can evaluate lightweight aggregate and polymer-modified emulsion, as well as normal aggregate and emulsion, and can be utilized efficiently by field personnel.

1.3 Report Organization

This report is composed of nine chapters. Chapter 1 presents the research needs and objectives. Chapter 2 summarizes the literature review of distress types in chip seal pavements, factors that affect the performance of chip seals, and existing chip seal mix design methods. Chapter 3 describes the sample fabrication procedure and experimental test methods employed in this study. In Chapter 4, the three-dimensional laser profiler is introduced as a means of measuring the surface texture of chip seals from which the mean profile depth (MPD) is determined. Chapter 5 introduces the underlying concepts and the framework of the performance-related chip seal mix design procedure. Chapter 6 reports the laboratory performance testing effort and its results to validate the developed chip seal mix design method. Chapter 7 discusses the field test section fabrication efforts. This performance evaluation of the field test sections is documented in Chapter 8. Conclusions from this research and future research recommendations are given in Chapter 9.

2. LITERATURE REVIEW

2.1 General

Several terms are used for asphalt surface treatments (ASTs) in the literature; these terms include chip seal, seal coat, surface treatment, bituminous surface treatment, spray seal (Austria), and surface dressing (United Kingdom). The official term used in the North Carolina Department of Transportation (NCDOT) specifications is *asphalt surface treatment* (NCDOT Standard Specifications for Roads and Structures 2002).

Over the years, continuous efforts have been made by state highway agencies (SHAs) and government agencies worldwide with regard to pavement preservation. Preventive maintenance, implemented via regular surface treatments, has increased steadily as cost-effective measures to extend the life of pavements have become a high priority. Therefore, it is imperative for the agencies that utilize AST alternatives to optimize their usage to extend the service life, decrease life cycle costs and increase safety. In a previous study (Ksaibati et al. 1996) directed at evaluating the use of surface treatments in the United States, twenty-five highway agencies rated their surface treatments as good, seven (including the NCDOT) rated their ASTs as average, and three rated them as fair. Not a single highway agency believed its AST operations were excellent. Several agencies, including those in Minnesota, Virginia, South Dakota, Wyoming, and Saskatchewan in Canada, recognized the need to improve overall pavement performance and therefore invested funds into evaluating their AST operations (Ksaibati et al. 1996, Roque et al. 1991, Shuler 1986).

Originally, chip seals and other ASTs were used exclusively for the construction of low traffic volume roads, but with advances in emulsion quality, construction techniques, and overall knowledge, ASTs have evolved into a maintenance alternative that can be successful for both low and high traffic volume pavements (Gransberg 2005).

The intended purpose of ASTs is not to improve the structural capabilities of the pavement section, and therefore, they should not be applied to roads that exhibit severe distress. Any structural deficiencies must be remedied prior to the application of an AST. However, various triggers, such as surface wear, decreased skid resistance, and water infiltration, serve to initiate the selection and construction of an AST. In North America, physical evidence of distress and water infiltration constitutes the most common triggers for the necessity of ASTs (Gransberg 2005).

In this section, major distress types in ASTs are first reviewed because the objective of AST mix design method is to select materials and application rates properly to ensure satisfactory performance of AST over its design life within the available resources and the performance is primarily governed by these distresses. Also reviewed in this section are existing AST mix design methods.

2.2 Distresses in ASTs

2.2.1 Debonding

The most common failure modes associated with ASTs are streaking (the debonding of the existing surface and the new AST), flushing/bleeding, and the loss of cover aggregate. Streaking is caused by the failure to apply asphalt uniformly inch by inch across the road surface, as shown in Figure 1. Streaking is usually caused by the asphalt sprayer's nozzle being clogged or inoperable during the emulsion spraying phase of construction. With regard to debonding failure, a new AST may not have a good bond with an existing roadway surface after construction. This debonding can occur for various reasons, including the presence of high amounts of dust (fine content) on the existing surface, the existing surface being wet or too cold, or the asphalt being too hard. Normally, this failure to establish a good bond with the existing surface causes a problem on a small area of only a few square inches to a few square feet. Occasionally, however, a few square yards or even the entire surface treatment can fail for these reasons (McLeod 1969). A typical debonding failure of an AST is shown in Figure 2.

Figure 1 Example of streaking of an asphalt surface treatment

Figure 2 Typical example of debonding failure

2.2.2 Bleeding

Another major long-term distress that appears in ASTs is bleeding, or flushing (as seen in Figure 3). This failure is usually caused by the application of excessive asphalt in the mix design phase, which causes the excess asphalt to rise out of the cover aggregate onto the road surface. Flushing or bleeding may also result from the loss, or so-called ‘whip-off’, of the aggregate for any number of reasons, such as a rainfall shortly after construction, asphalt that is too hard and fails to develop adequate adhesion with the cover aggregate, and use of cover stone that is too dirty or too wet to establish good adhesion to the asphalt. The main issue with bleeding is the loss of skid resistance associated with the distress, which in turn decreases the overall safety of the road as well as the effectiveness of the AST (McLeod 1969, Gransberg 2005).

Figure 3 Example of partial bleeding failure

2.2.3 Aggregate Loss

Aggregate loss is one of the most critical AST failure distresses. Generally, most of the aggregate loss of an AST occurs during the initial traffic passes once a road is newly opened to traffic. Other major causes of aggregate loss include excessive aggregate application, poor traffic control during construction, inadequate embedment of the aggregate particles into the emulsion, poor aggregate gradation qualities, and dusty aggregate (Shuler 1990, Gransberg 2005). Aggregate loss issues due to construction problems usually occur within a few months, and an AST with this type of problem should be repaired rather than resealed because a reseal alone will not normally last the expected life of the AST (Transit New Zealand 2005). The aggregate properties used in the surface treatment, such as gradation, shape, moisture condition, and dust, play a major role in aggregate retention. Also, the McLeod procedure (McLeod 1969) recognizes that some of the cover aggregate will be forced to the side of the roadway by the initial passing vehicles while the newly sprayed seal coat is still in its initial curing phase. The amount of aggregate that is whipped off in this manner is related to the speed and number of vehicles on the new seal coat. To account for this occurrence, a traffic whip-off factor is included in the aggregate design equation.

Reasonable values to assume are 5% for low volume residential types of traffic and 10% for higher speed roadways, such as county roads (McHattie 2001).

2.2.4 Loss of Skid Resistance

Loss of skid resistance associated with an existing asphalt surface is one of the common road conditions that trigger the need for a new surface treatment. One of the major roles of surface treatments, in general, is to provide an increase in skid resistance (Gransberg 2005). Existing surface conditions that indicate that the existence of a potential safety hazard include bleeding and rutting, among others.

Skid resistance changes as a function of time. Usually, skid resistance increases in the first two years following construction as the asphalt is worn away by traffic, then decreases over the remaining life of the pavement as the surface aggregate becomes more polished. Skid resistance tends to increase in winter when wet and cold weather roughens the surface, and tends to decrease in the summer. This seasonal variation in skid resistance is significant and should be taken into account when considering the skid resistance of respective locations. Additionally, it is believed that the winter recovery in skid resistance is not enough to balance out the summer polishing of the road surface (Jayawickrama and Thomas 1998, Hunter 2000).

2.3 Factors Affecting AST Performance

2.3.1 Aggregate and Emulsion Application Rates

One of the most important components of AST design and construction is the selection of appropriate application rates. In particular, the application of an excessive amount of aggregate can be problematic in AST field construction. If too much aggregate is applied, excess aggregate is whipped off by rapidly moving traffic, which creates a safety hazard and wastes materials. An incorrect assumption often made regarding the over-application of aggregate is that the excess aggregate can simply be swept off the surface, leaving the correct application quantity in place. Although it is reasonable to assume that some traffic whip-off will occur during the initial traffic loading, lack of care and the application of excessive aggregate can be detrimental, resulting in at least two major forms of distress, pavement distress and vehicular distress.

Pavement distress occurs when more than one layer of aggregate is present and the excess aggregate on the surface is forced into the layer below. This action causes the aggregate in the first layer to dislodge, therefore leading to loss of aggregate. This dislodgement, in addition to creating early aggregate loss, can potentially lead to flushing issues as well (Shuler 1990). When large quantities of aggregate are applied, the small stones adhere and the large stones are likely to be brushed off (Benson and Gallaway 1953), which affects the grading of the aggregate layer as well. It has been reported that an excess of aggregate material is often more detrimental than a slight shortage of aggregate, in that with an excess of cover material the amount of fines applied is also increased (Kearby 1952).

2.3.2 Aggregate Gradation

Aggregate gradation also plays an important role in the design, construction, and ultimately the performance of ASTs. Ideally, the specified gradation should be such that the texture of the seal is consistent. Tight gradation bands, which ensure a uniformly graded aggregate with minimal fines and dust, are desirable for an effective treatment. The literature and field surveys indicate that single-sized aggregate with less than 2% fine passing the No. 200 sieve is considered ideal (Gransberg 2005). One advantage of using a single-sized aggregate in an AST is that it maximizes the contact area between the tire and the seal surface. This contact increases the frictional area, and in effect, improves the skid resistance as long as the emulsion application rate (EAR) is appropriate (Herrin et al. 1968).

Ideally, the aggregate should be as close to uniform size as possible and be economically reasonable, so that the surface treatment has a single aggregate layer. If there is a significant difference between the largest and the smallest particles, the asphalt film may completely cover the smaller aggregate and thus prevent the proper embedment of the larger particles. As a general rule, the largest size aggregate in a surface treatment should be no more than twice the smallest sized aggregate, with a reasonable allowable tolerance for both oversize and undersize to allow for economical surface treatment production (The Asphalt Institute 1964). As the magnitude of the tolerance is increased (for budgetary reasons), it is believed that overall performance quality is decreased. Therefore, depending on the economic conditions, it may be favorable to have higher initial construction costs and obtain close to one size of aggregate that performs well rather than have lower initial construction costs with poor performance. Such poor performance will ultimately lead to high annual maintenance expenses (McLeod 1960). Therefore, state agencies must find a balance between the two alternatives.

Additionally, Benson and Gallaway (1959) found that an increase in the fine content from 0 to 30% of the total aggregate causes 10% more aggregate loss. This gradation issue, as discussed earlier, is tied directly to economic considerations, because aggregate costs increase as the gradation requirements for AST construction become more restricted. However, in the case where two aggregates are otherwise the same in price and quality, the aggregate that has the uniform gradation is preferred.

Kandhal (1987) also reports a reduction in the aggregate retention capabilities of a surface treatment with the use of graded aggregate. These graded stones contain additional smaller particles that tend to fill the voids between large particles and, thus, may not become effectively embedded into the applied asphalt.

2.3.3 Material Selection

Material selection for AST design and construction generally is based on product availability, aggregate/emulsion quality, and the climate of the potential construction site. Aggregate selection is a function of geological availability and the distance that the aggregate must be transported. The existing pavement's surface, the size of the job, the aggregate gradation, and local climate must be taken into consideration for the asphalt selection process (Gransberg 2005).

The specifications for ASTs in North Carolina call for granite (No. 78M for the aggregate size) and CRS-2 or CRS-2L/2P (latex/polymer-modified emulsion) for the emulsion type (NCDOT Standard Specifications for Roads and Structures 2002). The most commonly used size of aggregate for a single seal is a nominal maximum aggregate size (NMAS) of 3/8 in. (9.525 mm) (Gransberg 2005). Lightweight aggregate is often used as the aggregate material in AST construction in North Carolina because it provides a highly skid-resistant surface, good color contrast to improve visibility in daylight and at night, a surface that reduces paint striping maintenance, and it completely eliminates windshield damage caused by flying loose aggregate, which is a major concern associated with chip seal surface treatments (Epps et al. 1974).

2.4 Asphalt Surface Treatment Design Methods

The earliest mix design procedure for ASTs was developed originally by F. M. Hanson (1934/35) in New Zealand. The fundamentals of his mix design methodology are incorporated in all of the major AST mix design methods that are currently used worldwide. The newest mix design method to be developed based on the original Hanson method is the 2004 Chip Seal Design Guide from New Zealand (also known as the New Zealand method). In North America, the modified Kearby method and McLeod method are the most widely used AST mix design methods (Gransberg 2005). The main components of the Hanson, McLeod, 2004 New Zealand, Kearby, and modified Kearby design methods are provided in Table 1.

2.4.1 Hanson Method

The Hanson method was designed originally for cutback liquid asphalt, and it is based on the average least dimension (ALD) parameter of the aggregate source used in the mix. The ALD is calculated by using calipers on a representative amount of the aggregate source (at least 200 pieces or more) to obtain a value that represents the aggregate layer in essentially its rolled, compacted state. Hanson observed that when aggregate is dropped from an aggregate spreader onto newly applied fresh asphalt, the voids between the aggregate particles are approximately 50%, meaning 50% of the available aggregate voids are filled with emulsion. His theory was that when the layer is compacted, this value is reduced to 30%, and it is reduced further to 20% when the aggregate is compacted under traffic loading, as displayed in Figure 4. Hanson specified the percentage of voids to be filled by residual asphalt to be between 60% and 75%, depending on the type of aggregate and traffic level (Hanson 1934/35).

Table 1 Summary of Design Methods

	Modified Kearby	McLeod	2004 New Zealand
Factors for AAR	• Board test	• Aggregate gradation • Flakiness index • Bulk-specific gravity of aggregate • Loose unit weight of aggregate • Wastage	• Aggregate gradation • Flakiness index • Bulk-specific gravity of aggregate • Wastage
Factors for EAR	• AAR • Bulk-specific gravity of aggregate • Loose unit weight of aggregate • Traffic correction • Surface condition correction • Seasonal adjustment • Percentage of residual asphalt in emulsion	• Aggregate gradation • Flakiness index • Traffic correction • Bulk-specific gravity of aggregate • Loose unit weight of aggregate • Surface condition • Aggregate absorption • Percentage of residual asphalt in emulsion • Traffic volumes	• Aggregate gradation • Flakiness index • Average daily traffic (ADT) • Percentage of heavy commercial vehicles per day • Texture depth • Soft substrate • Absorptive surfaces • Steep grades • Aggregate shape • Traffic volumes
Reference voids for AAR	Voids at the board test condition, approximately 50%	Voids at ultimate compacted AST state, 20%	Voids at two-year light traffic volumes, approximately 40%
Reference voids for EAR	Voids at the board test condition, approximately 50%	Voids at ultimate compacted AST state, 20%	Voids at the first major frost day, normally higher than 40%
Embedment depth	Variable in terms of AST mat thickness and aggregate type	65-80%	35%
Lightweight aggregate	Considered in EAR	Not considered	Not considered
Multilayer Seals	N.A.	Available with empirical guideline	Available with empirical guideline

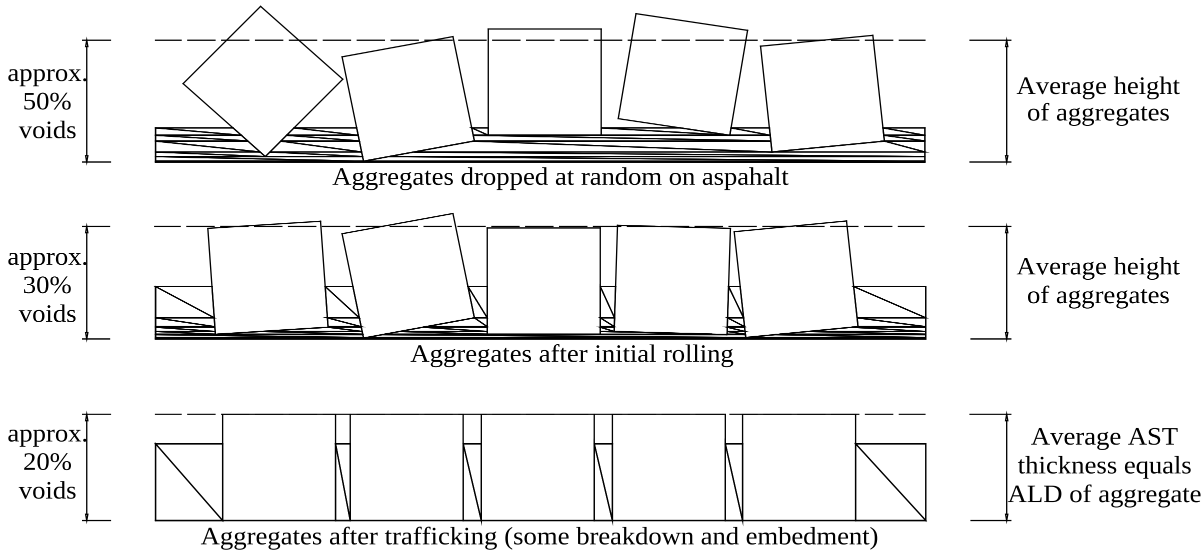

Figure 4 States of embedment of AST in asphalt

2.4.2 2004 New Zealand Method

The Hanson method, over time, has evolved into the 2004 New Zealand Design Method. This method was developed as a performance-based AST design method that considers the aggregate loss during the first winter after construction as well as the AST voids reduction model (Transit New Zealand 2005). One of the major difficulties involved in the design of material application rates, which is addressed in the 2004 New Zealand Method, is non-uniformity of the substrate. The 2004 New Zealand employs a substrate correction factor using the sand circle (sand patch) test for the texture depth of the substrate and the ball penetration test to measure the substrate hardness. The ball penetration test involves measuring the penetration that a 19 mm ball bearing makes in a sample of the substrate after the ball is struck one time with a Marshall hot mix-compaction hammer (The Asphalt Institute 1997). New Zealand reports that, for its location, typical ball penetration values for reseal surfacing are in the range of 2 to 3 mm. In cases where the ball penetration value is greater than 5 mm, the substrate is deemed to be too soft for a chip seal to be constructed. Soft substrates are said to occur when the resealing is over a previous chip seal, or when an asphalt or pavement repair has not fully cured or hardened. The problem with substrate softness is that it can lead to a deeper embedment of the aggregate than if the surface treatment was constructed on a hard substrate. This problem increases the likelihood of premature flushing of the surface.

2.4.3 McLeod Method

Throughout the 1960s, McLeod (1969) developed an AST design procedure based partially on Hanson's previous work in the field, and also based on empirical relationships and observations of his own. His method covers both single and multilayer surface treatments and determines the quantity of aggregate, quantity and type of asphalt, and rate of asphalt application. These quantities are determined based on several equations McLeod developed (1969).

The equations used to determine the quantity of aggregate needed for a given surface treatment course are based on the assumption that 80% of the aggregate will ultimately be embedded into the pavement, the aggregate is single-sized (with a slight modification to the equation for graded aggregate), and the aggregate will ultimately be arranged so that the thickness of the aggregate layer is equal to approximately the ALD of the aggregate source. With this method, additional consideration must be given to the type of aggregate, type of supporting layer, climatic variations, etc.

The equation used to determine the quantity of asphalt emulsion also is based on several assumptions. One assumption is that 20% of the total surface treatment will be comprised of asphalt (80% embedment of aggregate). Also, it is assumed that the aggregate is single-sized, as with the determination of the aggregate quantity (also containing a modification to the equation for graded aggregate). Lastly, the temperature during measurement is 60°F (otherwise the value must be adjusted).

The appropriate asphalt type and grade to be used depends on the aggregate size and surface temperature at the time of application, and are determined by a chart developed by McLeod. The Asphalt Emulsion Manufacturers Association and the Asphalt Institute have adapted and furthered McLeod's work by providing recommendations for asphalt types and grades for various aggregate gradations, and for correction factors to the AAR based on existing surface conditions.

2.4.4 Kearby Method

One of the initial efforts in the United States toward AST mix design was made by Jerome P. Kearby (1953). Kearby developed a design method that determines both the amounts and types of asphalt and aggregate for single seal surface treatments. Kearby's work resulted in the development of a monograph that provides an asphalt cement application rate in gallons per square yard for the input data of average thickness, percentage of aggregate embedment, and percentage of voids (Kearby 1953). Kearby recommends the use of a uniformly graded aggregate by outlining eight grades of aggregate based on gradation and associated average spread ratios. He also recommends that the combined flat and elongated particle content not exceed 10% of any aggregate gradation requirement. Furthermore, the Kearby method accounts for the effects of existing pavement conditions and traffic volume on the optimal aggregate embedment depth. The percentage of embedment should be increased for hard aggregate and reduced for soft aggregate in the case of ASTs being constructed on an existing hard surface. For ASTs under heavy traffic, the percentage of embedment should be decreased, along with the use of large-sized aggregate particles; and under low volume traffic, the percentage of embedment should be increased, with the use of mainly medium-sized aggregate particles.

2.4.5 Modified Kearby Method (Texas)

In 1974, Epps and his associates proposed a further change to the design curve developed by Kearby for use in ASTs by incorporating the use of synthetic aggregate such as lightweight aggregate (Epps et al. 1974). Based on the high porosity of synthetic aggregate, Epps et al. proposed a curve showing approximately 30% more embedment than the Benson–Gallaway curve (Benson and Gallaway 1953). The rationale for this increase is that high friction lightweight aggregate may turn over and subsequently ravel under traffic. In a separate research effort, Epps et al. (1980) continued the work done in Texas by Kearby (1953) and Benson and Gallaway (1953) by undertaking a research program to conduct field validation of Kearby's design method. During this study, it was observed that the Kearby design method predicted lower asphalt application rates than those used in the Texas practice, and so the Epps study proposed two changes to the design procedure. The first one was a correction to the asphalt application rates based on the level of traffic and existing pavement conditions. The second change justified the shift of the original design curve proposed by the Kearby and Benson-Gallaway methods, as suggested for lightweight aggregate (Epps et al. 1974). Since then, practitioners and researchers have labeled this design approach the *modified Kearby method*.

In this method, the aggregate application rate (AAR) is determined using the laboratory board test method whereby only one aggregate layer is placed in a ½ yd^2 area. The dry loose unit weight and the bulk-specific gravity of the aggregate are determined and used to convert the amount of aggregate to cover the ½ yd^2 area to an AAR in the field. The test board is made of plywood with sides framed by 12 mm (1/2 in.) molding strips. The asphalt application rate is determined by an equation that includes the traffic level (vehicles per day per lane), the existing surface conditions, the residual quantity of asphalt in the emulsion or cutback, and field factors based on field experience.

According to the study conducted by Epps (1974) on ASTs with lightweight aggregate, the modified Kearby method appears to be the most effective methodology for the prediction of the AAR.

3. TEST PROCEDURES AND ANALYSIS CONCEPTS

3.1 Sample Fabrication Procedure

The process of fabricating chip seal samples in a laboratory setting involves simulating the chip seal construction process as closely as possible. The North Carolina State University (NCSU) research facilities contain various tools to replicate the chip seal sample construction process. These resources are discussed in detail in the following sections.
The first step in constructing chip seal specimens in the lab is to obtain a felt disk in the desired size/shape of the chip seal specimen to be fabricated. In the case of this mix design project, these felt disks were 12 in. x 14 in. on which 7 in. x 12 in. samples were fabricated. In order to make the 7 in. x 12 in. samples on the felt disk, a template was created and placed on top of the sample during the emulsion spraying process to ensure consistent dimensions and rates for each sample replicate. The template ensures that the emulsion reaches only the desired area. In addition, in order to apply the emulsion to the felt disk in a manner that simulates the emulsion being sprayed from the truck in the field, a paint spray gun is used. It is recommended that this paint gun shoots at a rate of, or exceeds, 5.4 gallons per hour (ideally higher than 7.2 gallons/hour to spray polymer-modified emulsion, which is more viscous). Lastly, a weight scale is used to keep track of the amount of emulsion that has been sprayed onto the felt disk (to ensure accurate emulsion application rates (EARs) during sample fabrication). The complete emulsion spraying process is detailed in Figure 5.

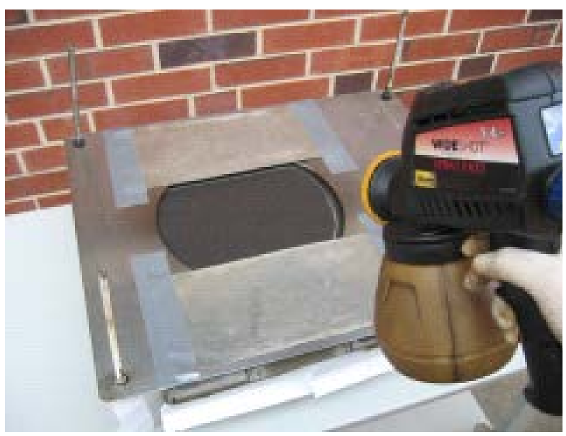

Figure 5 Chip seal emulsion spraying procedure

The figure shows the first step in the sample fabrication process, which is the emulsion being sprayed onto the felt disk with a template over the felt disk to control the shape and size of the chip seal specimen. Following this step, the felt disk with newly applied emulsion is then positioned underneath the chip seal spreader (ChipSS). The automated aggregate spreader is displayed in Figure 6.

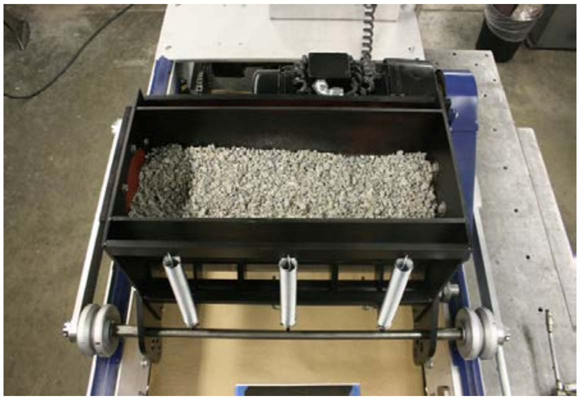

(a) Filled aggregate into hoper

(b) Ready to spread aggregate on the felt disk

(c) Spreading aggregate on the felt dsik

(d) Spread aggregate on the felt disk

Figure 6 ChipSS aggregate spreading machine

Figure 6 shows the process of spreading the aggregate onto a felt disk after the initial application of emulsion. Figure 6 (d) shows the aggregate being spread by the ChipSS across the felt disk. After the application of the emulsion onto the felt disk (in the 7 in. x 12 in. area), only the section of the felt disk covered by emulsion will retain aggregate, and the excess is swept off by a small brush. Through this process a single layer of aggregate is obtained that completely covers the specimen.

Prior to the beginning of sample fabrication, the aggregate spreading machine is calibrated to drop the amount of aggregate required to achieve the desired AAR for the sample being fabricated to ensure the desired rate is applied. The AAR is controlled by two parameters: the box and drum speeds. The box speed is the speed at which the box moves across the sample, and the drum speed is the speed at which the rotating drum (located inside the aggregate hopper) rotates and drops the aggregate. At lower box speeds, more aggregate is dropped onto the sample, and vice versa at high speeds. At lower drum speeds, less aggregate is dropped out of the hopper, and vice versa for high drum speeds. Using these concepts, the AAR can be controlled effectively during specimen fabrication.

After the aggregate is applied, and the excess outside of the designated sample area is swept away, the aggregate weight is measured (to determine the exact amount of aggregate that was applied), and the sample is compacted. The compaction device is shown in Figure 7.

Figure 7 Chip seal sample compactor

The compactor shown in Figure 7 is used to compact the chip seal specimen directly after the aggregate is applied to the hot emulsion. This machine simulates the compactor that follows behind the aggregate truck in the field. Specifically, the compactor shown in Figure 7 is used in conjunction with a rubber mat in order to replicate a combination roller (a combination of steel wheel and pneumatic tires), which has been found to be the most effective type of roller in the field. This procedure is necessary because the steel supplies great compaction force, while the rubber material helps minimize the breaking of chips that occurs when the steel wheel is used alone for compaction.

The compaction procedure involves three compaction passes across the horizontal face of the sample, and the additional compaction passes perpendicular to the first three passes. This compaction procedure is repeated for each sample fabricated in the lab to ensure a consistent and effective compaction of the aggregate into the emulsion layer.

Following compaction, the newly fabricated sample is then cured in the oven undisturbed at 35°C for 24 hours to allow the sample to cure. After the curing period is complete, the sample fabrication is complete, and the sample is ready to be tested.

3.2 Complete Temperature Control for Sample Fabrication and Testing

In order to eliminate temperature as a variable in fabricating and testing chip seal specimens in the lab, it is important to be able to control the temperature throughout the entire process. Such control is vital because it ensures that each sample is subjected to the same temperature during the fabrication, curing, and testing processes. Pivotal to achieving this level of temperature control is a closed facility that can host the fabrication process. The NCSU research team has constructed such a facility: a 16 ft. by 8 ft. greenhouse made of wood and polycarbonate glass.

This greenhouse, pictured in Figure 8, ensures a consistent temperature for the specimens during the sample fabrication process.


Figure 8 Greenhouse for temperature control

A few modifications were made to the greenhouse to increase its efficiency in maintaining the temperature that the research team specifies. One major adjustment is the addition of insulating foam in all crevices and small openings of the greenhouse. This insulating foam ensures no unnecessary flow of air in or out of the greenhouse. A picture of the foam insulation can be seen in Figure 9.

Figure 9 Foam insulation used to seal all openings in greenhouse

In addition to building a greenhouse for temperature control, it was important to find a method of properly and effectively heating the greenhouse to the desired temperature in a reasonable amount of time. In order to perform this task many alternatives were considered, but ultimately, after consulting with the president of a heating solutions company, a heat gun was chosen as the main heat source for the greenhouse. The heat gun that was selected delivers a direct stream of heat and produces a temperature of up to 1,100°F. Initially, a fan was used to circulate this direct heat throughout the greenhouse, but the research team soon found the fan to be unnecessary. To ensure that a consistent temperature is maintained once the greenhouse is heated to the desired temperature, a special thermometer was obtained that allows the temperature to be set and controlled. The heat gun is powered through this particular thermometer, and once the desired temperature is reached, the thermometer ceases to deliver power to the heat gun. If the greenhouse temperature falls below the desired temperature, the thermometer begins to deliver the power needed for the heat gun to operate again. Thus, the greenhouse and heat gun/thermometer combination allows the research team to have control of the temperature during the sample fabrication process. A picture of the heat gun and thermometer setup is shown in Figure 10.

Figure 10 Thermometer and heat gun used for temperature control

Additionally, an oven (that is tested and calibrated regularly for accuracy) is used to ensure that the 24-hour curing temperature of 35°C for newly created samples is consistent. Further, a temperature chamber and thermocouple ensure that the MMLS3 machine retains a constant temperature during the testing of chip seal specimens. The emulsion is stored in a large oven at 140°F until it is needed for sample fabrication. Prior to fabrication, it is placed in a separate oven (at 160°F) for two hours to be heated to the desired sample fabrication temperature.

3.3 Third Scale Model Mobile Load Simulator (MMLS3) Aggregate Loss Test

The MMLS3 machine simulates the traffic loading conditions experienced by ASTs under field traffic loading conditions. The MMLS3 applies repeated wheel loads to the asphalt surface at a consistent and accelerated rate (990 wheel loads applied every 10 minutes) and causes the AST to respond similarly to its response under field loading conditions. Also, the MMLS3 machine has the ability to wander across the sample to simulate the actual wandering of vehicles across the wheel path. For the performance testing conducted in this project, the MMLS3 wandering feature was enabled. It takes approximately 10 minutes for the MMLS3 to wander across the whole 7 in. width of the chip seal specimens. For the aggregate loss testing, the MMLS3 machine is placed inside a temperature chamber that allows the temperature to be controlled during testing, thus enabling the simulation of field temperature conditions during traffic loading in the laboratory setting. A maximum of three samples (at 12 in. lengths per sample) can be secured underneath the MMLS3 to be trafficked under MMLS3 loading conditions. The cumulative sample length (36 in. total) is the effective loading area for the MMLS3 tires. The MMLS3 testing procedure and equipment can be seen in Figure 11.

The one departure from the picture shown in Figure 11 (d) during actual testing is that the top of the MMLS3 temperature chamber was covered to prevent the escape of heat through the top of the chamber.

The MMLS3 testing procedure involves a two-hour aggregate loss test conducted at 25°C. Prior to the test, the specimen is weighed to determine its weight prior to loading (i.e., at zero loading time). After mounting the samples and allowing the temperature chamber to reach the desired temperature, testing can begin, and the MMLS3 loading is applied for 15 minutes. Then, the test is stopped, and the specimens are removed from underneath the MMLS3 and weighed. This process is repeated at the cumulative testing times of 45 and 120 minutes. Thus, at the end of the two-hour test, specimen weights are available at 0, 15, 45, and 120 minutes. These weights are used to determine the aggregate loss for each specimen under MMLS3 traffic loading.

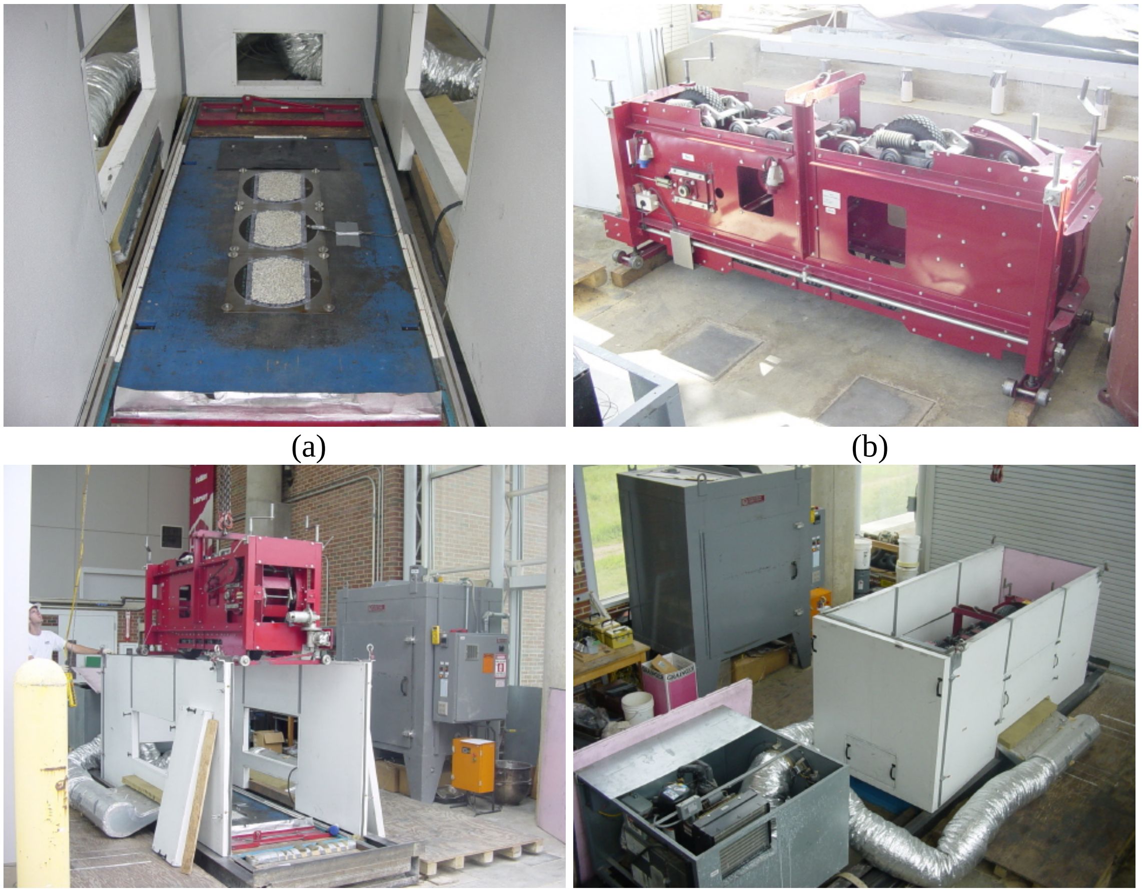

(a) (b)

(c) (d)

Figure 11 MMLS3 test preparation: (a) installation of specimens on a steel base, (b) side view of MMLS3, (c) positioning the MMLS3 in the temperature chamber, and (d) complete MMLS3 test setup for testing

3.4 MMLS3 Bleeding Test Procedure

The bleeding test is conducted after the completion of the two-hour aggregate loss test, and involves four hours of MMLS3 loading at a temperature of 50°C inside the temperature chamber. Prior to the four hours of nonstop MMLS3 loading, the samples are temperature-conditioned for three hours at 50°C. This process simulates the bleeding of chip seal surface treatments during the summer months in the field. During this testing, the goal is to determine the rates at which bleeding will, or will not, occur. The outcome is a function of the AARs and EARs used in the design, as well as the aggregate gradation.

Following the bleeding test, the percentage of the sample that exhibits bleeding can be determined. For this project, this determination was made using the transparency method whereby a transparency is placed over the sample, and the areas of the sample that have bled are shaded on the transparency. Once the bled area for that particular sample is marked, the transparency is scanned using a digital scanner, and the percentage of the sample that exhibits bleeding is determined (i.e., the percentage of sample area bled/total sample area). Various digital imaging software programs exist that can perform this simple analysis. Essentially, within the 7 in. x 12 in. sample area, the analysis seeks to determine the percentage that is black versus white. A threshold value to identify the bled area can easily be determined manually, because the image area is only black or white. This method is used later in the project to determine the percentage of bleeding for the lab-fabricated specimens that are tested during the performance testing part of the project.

The bleeding test thus determines if bleeding will occur, depending on whether the EAR is too high for the aggregate structure in the design. Likewise, bleeding will occur if the amount of aggregate is insufficient for a specific EAR. Bleeding can also occur if the aggregate is not retained and large amounts of aggregate are whipped off during traffic loading.

4. MEAN PROFILE DEPTH ANALYSIS AND TESTING EQUIPMENT

4.1 Mean Profile Depth (MPD) Definition

The mean profile depth (MPD) is a parameter that represents the exposed texture depth of a chip seal surface treatment and is inversely related to the embedment depth. Hypothetically speaking, as the EAR increases (as applied on a given single aggregate layer), the MPD will decrease, and where the EAR (or embedment depth) is decreased for a given aggregate structure, the MPD will increase. Transit New Zealand (2005) defines the MPD as:

$$MPD = \frac{Peak\,level\,(1st) + Peak\,level\,(2nd)}{2} - Average\,level \qquad (1)$$

The various chip seal parameters that make up Equation (1) are shown schematically in Figure 12. In the diagram, the MPD clearly indicates the roughness (i.e., macro-surface texture) and aggregate exposure depth of the chip seal. Roughness is important, because it provides the skid resistance and friction needed for vehicles to brake adequately. The aggregate exposure depth is important because it is a function of the aggregate embedment depth, which is the most important factor that controls the aggregate loss and bleeding performance of chip seals. A small MPD value indicates the likelihood of bleeding and skid resistance problems. A large MPD value after construction indicates the possibility of excessive aggregate loss and, therefore, bleeding due to aggregate loss.

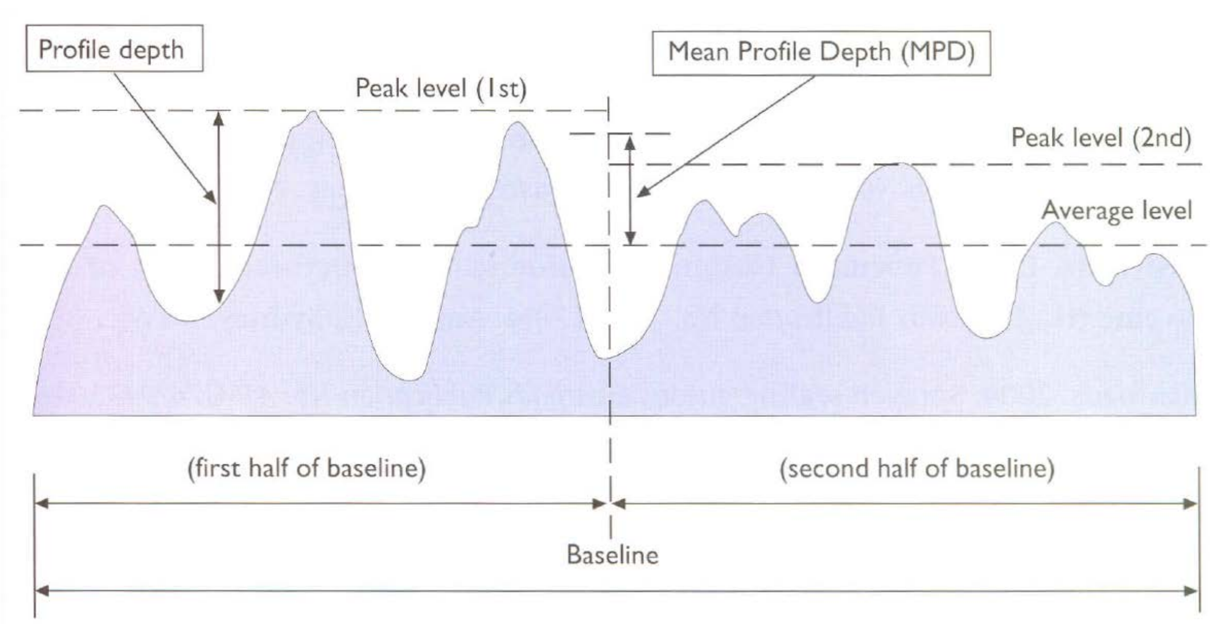

Figure 12 Schematic diagram of the mean profile depth determination

4.2 MPD Determination Method and Three-Dimensional Laser Profiler

The three-dimensional (3-D) laser profiler is shown in Figure 13. This profiler employs the innovative RoLine line laser, produced by LMI Selcom. This laser has been used successfully in developing RoboTex, a 3-D laser sensor technique for the measurement of the surface texture of concrete pavement, under the sponsorship of the Federal Highway Administration. The laser measures the distance between the laser sensor and the pavement surface in both the longitudinal and transverse directions of the pavement and produces a 3-D map of the pavement surface texture. Specifically, the laser scans a 97 mm line on the pavement surface in the longitudinal direction and obtains one distance measurement per millimeter along that 97 mm line. The resulting data, separated into 1 mm increments along the 97 mm line, provide the research team with an accurate picture of occurrences at the microscopic level of the surface of the field sections and laboratory test specimens. Then, the laser moves in 1 mm increments in the transverse direction, perpendicular to the wheel traffic direction, and takes another 97 mm line scan to the end of the travel length of the field section or specimen. This procedure is displayed in Figure 14.

Figure 13 Photo of the 3-D laser profiler scanning a chip seal field section

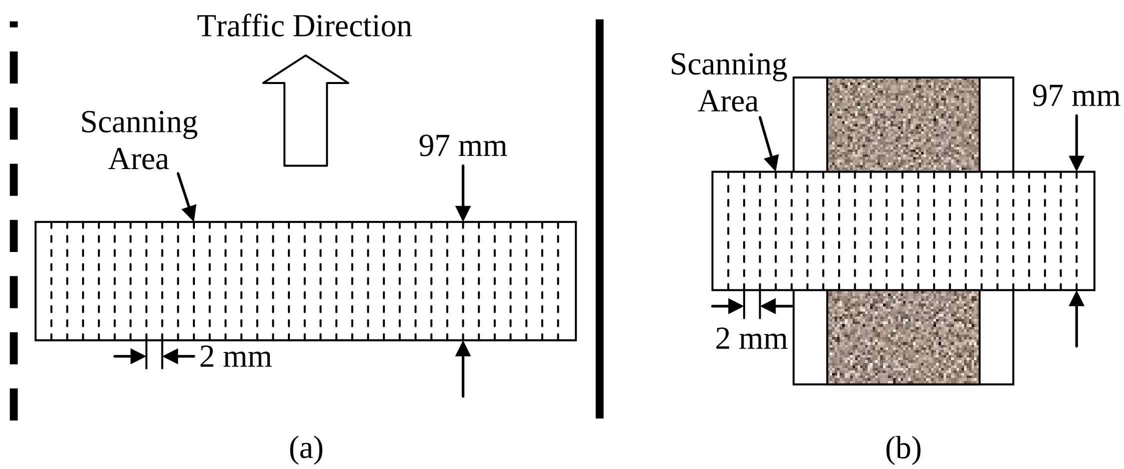

Figure 14 Schematic diagram of the laser scanning procedure: (a) for the field section and (b) for the MMLS3 sample

From this procedure, 3-D data are obtained that are then manipulated to determine the MPD or any other surface texture related parameters for that particular field section or specimen. This procedure involves taking the raw data from the scan of a particular section or specimen and determining the overall MPD value using Equation (1). That is, the height information collected from each 97 mm line is used to determine the MPD value for that line. This operation is repeated every 1 mm in the transverse direction to determine the MPD values for numerous 97 mm scans along the transverse direction of the pavement. Then, all the 97 mm MPD values are averaged to obtain a final MPD value for that section or specimen.

Figure 15 displays the micro-texture data obtained from scanning a field test section that has been trafficked under real field traffic conditions for two days after the initial construction of the test section. These data are representative of all the data obtained from the scan and have not been processed at all prior to being graphed. Figure 15 illustrates the ability of the 3-D laser to capture the micro-texture of each aggregate particle in addition to that of the overall wheel path; such accuracy is essential in determining the surface texture and the MPD changes that occur under traffic loading over time. Figure 15 is color-coded based on height to depict the wheel path more clearly. The graph shows the two 97 mm-wide scans that were performed on one particular location of Section 3.

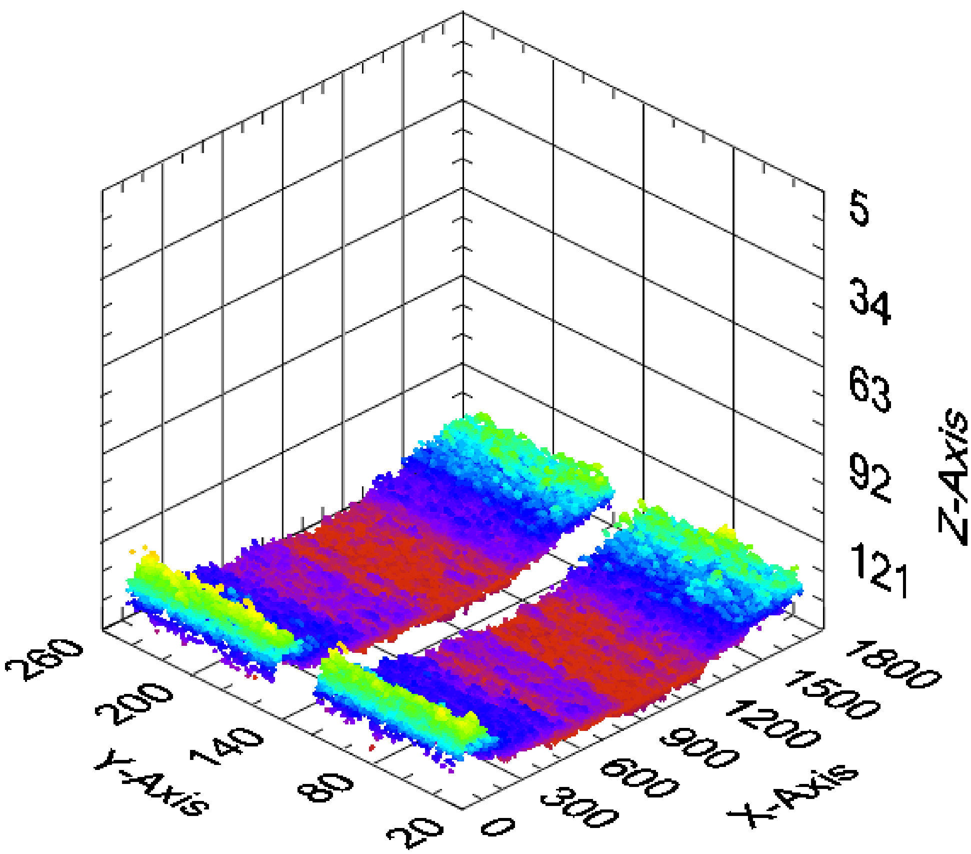

Figure 15 3-D laser profiler graph of a chip seal pavement

Steps involved in the operation of the laser profiler are described below. First, the laser operator must perform setup procedures in order to operate the laser profiler properly. The laser has various components that must be connected prior to the scan. One of the main connections is between the laser profiler and a laptop computer via both USB and ethernet connections. The ethernet connection is used to control the operation of the laser scanner via software specially designed for the laser profiler. The USB connection is used to transfer the data from the laser back to the computer for storage and analysis. Other connections involve the control box that contains all the hardware that powers the x and y-direction motors and encoding aspects of the laser profiler.

With regard to laser positioning for the scan, the laser profiler is first positioned across the roadway so that its 7-foot width is perpendicular to the traveling (longitudinal) direction of the roadway. The laser profiler has two of its wheels positioned as close to the median as possible without extending past the asphalt surface. This positioning is to ensure that the outer wheel path is captured in the laser scan data. Given the current width of the laser profiler (approximately 7 feet), it is impossible to capture both wheel paths in their entirety, though the scan of one wheel path provides sufficient surface texture information. The time required to complete a single scan is dependent upon how high the resolution is for that scan. The laser resolution is a variable user input for the scan. The higher the laser resolution and the larger the area being scanned the longer the scan will take to complete.

Figure 16 shows the scan procedure for each spot in each test section. The laser profiler first scans the area indicated by the yellow bar, marked *SCAN 1* in the diagram, then scans the red area, labeled *SCAN 2*. When scanning, the laser moves from the location shown at the bottom of the diagram to the top, and scans a 4-inch wide scan in the y-direction for every 2 mm it moves in the x-direction. The laser scans every 2 mm until it has scanned the entire 7-foot distance of the profiler. At this point, the laser resets itself in order to make the second scan, shown in red in the diagram. Every 4-inch wide scan contains exactly 100 points of data that include the coordinates (x, y, and z) of each point, with z being the distance from the laser to the road surface. Sufficient laser scan data for analysis in this project were obtained in approximately 5 minutes per scan for a given location. This procedure is performed at three different spots for each test section in order to capture the true void presence for that particular section. The data from the laser are automatically transferred to the laptop via the USB connection between the laser and the laptop.

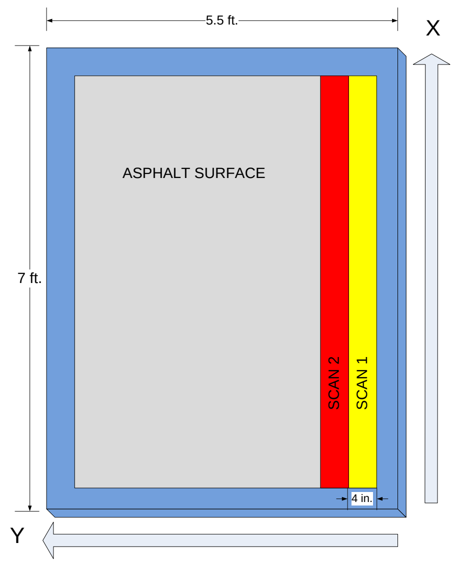

Figure 16 Laser profiler field setup

However, the iteration of the 3-D laser profiler used in this research project is not the best option for the field testing because it is too big for one person to handle and it scans too large an area. Thus, the research team has redesigned the overall size of the 3-D laser profiler to provide a more convenient field test system. (Details of this redesign will be discussed in the final report of the HWY-2009-01 project *Development of a Field Testing System for Asphalt Surface Treatments*.)

4.3 MPD vs. Embedment Depth Verification Analysis

The research team utilized the MPD parameter to quantify the embedment depth parameter of chip seal specimens based on the hypothesized relationship between these two parameters. The research team conducted studies in order to better analyze and validate this relationship.

In order to quantify the embedment depth and analyze its relationship with the MPD, the research team decided to construct chip seal specimens with controlled geometries and dimensions using an aggregate substitute (i.e., one with a known volume) rather than actual aggregate (which is too variable to control). Specifically, the research team used a material called Delrin, which is a plastic sphere that is obtainable in the same sieve sizes that are used for chip seal surface treatments and also has a density similar to lightweight aggregate. With these plastic spheres, the research team knew the exact volume of the aggregate substitute and could determine the true embedment depth using a volumetric method (described later in this report). Then, by scanning the surface texture of the specimen using the 3-D laser profiler, the research team was able to determine the relationship between the MPD and aggregate embedment depth, as well as the relationship between these parameters and other variables.

One note regarding these tests is that, due to the cost of the Delrin sphere material, it was important that the spheres were reusable. Therefore, instead of emulsion, an indoor primer-based paint mixture was used to fabricate the samples. This substitution had no effect on the results because only the initial embedment was under consideration, and no performance tests had to be conducted on the samples. Also, measures were taken to ensure that the final viscosity of the paint mixture was similar to that of actual emulsion. Specifically, 20% water was added to every 80% of paint to obtain a mixture that shows similar viscous characteristics as emulsion. Various materials were tested, and paint was found to be the most effective emulsion substitute for the research. More specifically, the liquid materials were tested not only for their viscosity, but also their ability to be scanned by the laser (which sometimes has problems scanning overly reflective shiny surfaces). In this case, the paint was allowed to dry before scanning to dull the surface for quality scanning. The Delrin aggregate substitute was also tested for its ability to be scanned to ensure that accurate data were being obtained by the laser profiler.

4.4 Volume-Based Embedment Depth Equation (for Delrin Spheres)

In developing a volume-based embedment depth equation, the research team initially defined the variables that would be used to develop the relationships among embedment depth, chip seal material volumes, and the other inputs related to the fabrication of the samples.

The variables used in the volume-based embedment depth equation include: percentage of embedment depth (E_d), number of spheres (S), sample length (L), sample width (W), embedment depth (h), volume of a partial sphere ($V_{partialsphere}$), volume of embedded aggregate ($V_{embedagg}$), total embedded volume ($V_{totalembed}$), volume of emulsion ($V_{emulsion}$), diameter (d), and radius (r).

The equations formulated using the above variables are listed below:

$$E_d = \frac{h}{d}\ x\ 100 \qquad (2)$$

$$V_{totalembed} = L\ x\ W\ x\ h \qquad (3)$$

$$V_{partialsphere} = (\pi h^2 r) - \left(\frac{\pi h^3}{3}\right) \qquad (4)$$

$$V_{embedagg} = \left[(\pi r h^2) - \left(\frac{\pi h^3}{3}\right)\right] X\ S \qquad (5)$$

$$V_{totalembed} = V_{emulsion} + V_{embedagg} \qquad (6)$$

Equation (2) is the equation for embedment depth as a function of emulsion height (h) and the diameter of the Delrin plastic balls used for that particular sample. For this study, the diameter of the aggregate was known, which made determining the embedment depth a simple process. Using Equation (3), the research team determined the total embedded volume, which is the total amount of space that is filled with emulsion and a partial aggregate volume at the specified embedment for each specimen.

After calculating the total embedded volume, the next step was to determine the amount of that available volume that would be filled with aggregate. In order to make this determination, an equation for the spherical cap, or partial sphere volume, was required. Equation (4) is the equation for partial sphere volume used in the analysis. Equation (5) then takes the variables in the partial sphere volume equation and translates them into the corresponding terms for the research team's analysis. The height for this study is the height of the emulsion layer after compaction, and the radius is half of the Delrin sphere diameter. The last step is to multiply that result by the number of spheres used for each sample.

Lastly, knowing both the total embedded volume ($V_{totalembed}$) and volume of embedded aggregate ($V_{embedagg}$), the research team could then use Equation (6) to determine the volume of the emulsion (or, in this case, the paint substitute) required to fill the volume. In order to calculate this volume properly, the density of the paint needed to be determined. Thus, the following relationship was used, where ρ is the density, m is the mass, and V is the paint volume:

$$\rho = \frac{m}{V} \tag{7}$$

The research team used a measuring cup to pour a known volume (determined using the above volumetric embedment depth equations) of the paint mixture, and then weighed that amount using a scale to determine the density. This density was then used to translate the volume of emulsion, calculated using Equation (7) above, into weight (in grams). The reason the research team converted volume into weight (in grams) is to measure the amount of paint mixture that was needed to ensure the designed embedment depth for each specimen. Therefore, using this equation, volumetric calculations could be used in laboratory experiments to determine the embedment depth of a sample.

4.5 MPD vs. Embedment Depth General Testing Procedure

Four steel plates, 200 mm x 200 mm x 25 mm, were fabricated to help create the test specimens. The steel plates were constructed so that the paint could not flow freely in any direction, thus ensuring that the aggregate embedment was uniform throughout the sample, as shown in Figure 17.

Additionally, the modified Kearby board test was conducted to find the appropriate Delrin and aggregate applications rates (Kearby 1953). In effect, this test determines how many Delrin balls could fit inside the steel plate area in a single layer. This test was repeated for each sieve size used in the analysis to ensure a single layer and maximum packing efficiency throughout the samples. The aforementioned details are consistent for all tests completed.

Figure 17 Steel plate example with 12.5 mm Delrin spheres and 70% paint coverage

After completing the modified Kearby board test, the spheres from the board test were then counted and weighed to determine how many spheres would be needed for each test. This information was used to calculate the specific volume of paint needed to provide the embedment percentage necessary for each test (30%, 50%, 70%, and 90%). The amount of paint needed to achieve each embedment depth was found using the volume-based embedment depth equations presented earlier in Section 4.4.

Once the paint was poured onto the plate, and the paint level was even across the sample, the Delrin balls were then embedded into the paint. This process was done by hand to ensure accurate and even aggregate coverage. The balls were aligned as they were in the board test to achieve single layer coverage with a minimal amount of unnecessary free space. The sample was then compacted using a PVC pipe as a roller to ensure that each sphere was compacted sufficiently.

Next, the test specimen was air-dried for 15 to 20 minutes before being scanned by the 3-D laser profiler. This amount of time was short enough to ensure that no water or paint would evaporate between fabrication and scanning, but that the surface would not be too reflective for the laser to scan properly.

Before scanning, the laser was first calibrated specifically for this project. A plate was placed underneath the laser, and the location of all four corners was marked and recorded. The laser location was then set to scan and record 100 data points within a 97 mm line. The laser then moved 1 mm forward and scanned another 97 mm line. This process was repeated until the laser travelled 178 mm, scanning 100 points every 1 mm. The reason the laser scans 178 mm is that this distance is approximately 178 mm out of the 200 mm of the plate that is used to make the samples. The unscanned distance eliminates the end effect by leaving adequate space on both sides of the scan length to ensure the laser does not scan the sample edge. If a 200 mm scan length were used, the laser possibly would have contacted the end of the specimen and the steel plate, which would have caused errors in the laser scan data. This information was stored in a spreadsheet developed by the research team and used to calculate the MPD.

Table 2 summarizes the layout for the testing procedure to determine the MPD versus embedment depth for both the Delrin spheres and the real aggregate. For both sizes of Delrin balls, a target embedment of 30%, 50%, 70% and 90% would be calculated and fabricated based on the volume-based embedment depth equations, i.e., Equation (2) through Equation (7). Table 3 shows the actual measured data from the sample fabrication for the analysis.

Table 2 MPD vs. Embedment Depth Testing Procedure Summary

Material	Sieve Size	Target Embedment
Delrin	6.25 mm	70%
	9.375 mm	30%
		50%
		70%
		90%
	9.375 mm	30%
		50%
		70%
		90%
Aggregate	12.5 mm	50%
		70%
		90%

Table 3 MPD vs. Embedment Test Data

MPD vs. Embedment Test Data					
Sieve Size (mm)	**Plate Weight (g)**	**Paint/H_2O Mix Weight (g)**	**Actual Embedment**	**Delrin Weight (g)**	**Delrin #**
9.375	947.4	79.6	30.50%	295.7	488
9.375	947.3	95.7	50.20%	300	493
9.375	943.9	118.8	70.90%	295.1	483
9.375	947.4	153.5	89.80%	299.9	493
12.5	947.1	104.5	29.99%	401.4	277
12.5	943.9	127.7	50.00%	402	277
12.5	944.1	153.5	70.00%	400.7	274
12.5	944.1	208.3	90.60%	402	277
12.5	944.4	94.2	70.00%	213.54	948

From Table 2 and Table 3, the accuracy of the actual embedment depths in comparison to the target embedment depths can be seen. Because each sample was fabricated so precisely, the research team deemed it unnecessary to make replicates of each condition due to the negligible amount of sample-to-sample variability.

4.6 Theoretical vs. Measured Embedment Depth Test Procedure

In the theoretical versus measured embedment depth testing, new specimens were fabricated in accordance with the procedures listed for the Delrin MPD versus embedment depth test described earlier. In this case, Delrin spheres were also used, but new samples were fabricated because the previous samples had been discarded. The samples used for this testing were fabricated and then scanned using the 3-D laser profiler at a step size of 0.1 mm.

The theoretical embedment depth was determined by taking the diameter of the Delrin spheres minus the part of the Delrin sphere that was exposed to air. The part of the Delrin sphere exposed to air was based on the percentage of embedment for that particular sample.

The measured embedment depth was obtained using the 3-D laser profiler. The specimens were scanned and the data were analyzed to determine the peaks of the Delrin spheres and the minimum level (the paint level), and that difference was found to be the measured embedment depth. Specifically, only the first point of each 97 mm scan was used in the analysis because the resolution in that direction was 0.1 mm, whereas the resolution between each point in the 97 mm scan was 1 mm. Using the 1 mm resolution would raise the probability that the peak of the aggregate could be missed during the scan of the surface, which would lead to erroneous results.

4.7 Delrin MPD vs. Embedment Depth Analysis Results

Figure 18 shows that in a laboratory setting the MPD values obtained from the 3-D laser profiler and subsequent data processing do in fact give a strong representation of the embedment depth for that particular sample. The results show that as the embedment depth increases, the MPD decreases. This phenomenon is consistent with what is expected when the Delrin application rate is kept the same, given the definition of MPD. This graph shows that the three-dimensionality, in combination with the MPD definition, can accurately represent the effect of embedment depth on a chip seal specimen.

Also, as hypothesized, the 12.5 mm Delrin spheres show consistently higher MPD values than the 9.375 mm Delrin spheres. As previously mentioned, the MPD is, effectively, the difference between the peaks and the average overall level of the surface. This difference should be larger for the 12.5 mm Delrin balls, which is shown in the data.

Furthermore, in Figure 18 it can be seen that as the embedment depth falls below 50%, the curve begins to flatten, though it does continue to rise slightly. The reason for this rise is the contact issue shown in Figure 19. Once the embedment drops below 50% of the sphere diameter, the contact area between tightly packed spheres of the same shape will make the 3-D laser assume that the emulsion is at the 50% embedment at all sphere contact points, when it is actually below 50 percent. Despite this assumption, the MPD value continues to rise as the embedment depth decreases below 50%, because areas in between the spheres that have embedment below 50%

can be seen clearly by the laser. The areas that still show embedment below 50% can be seen as the ‘curved diamond’ outline in between the four spheres shown in the plan view of the Delrin model image displayed in Figure 19.

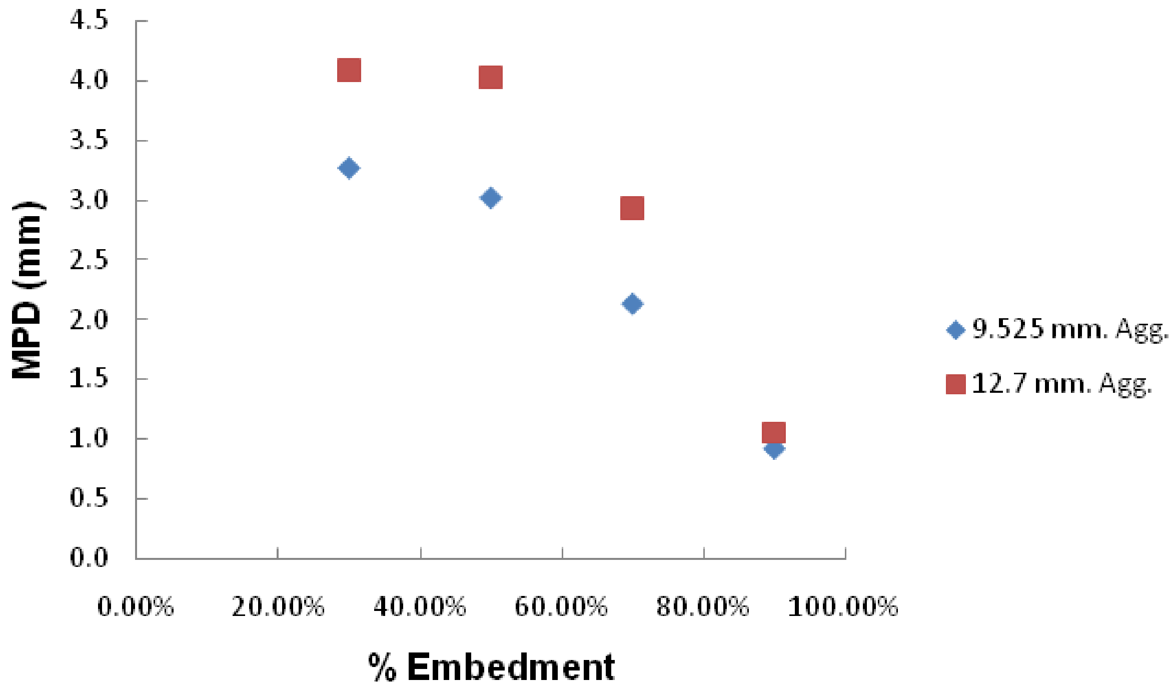

Figure 18 MPD vs. percentage of embedment depth

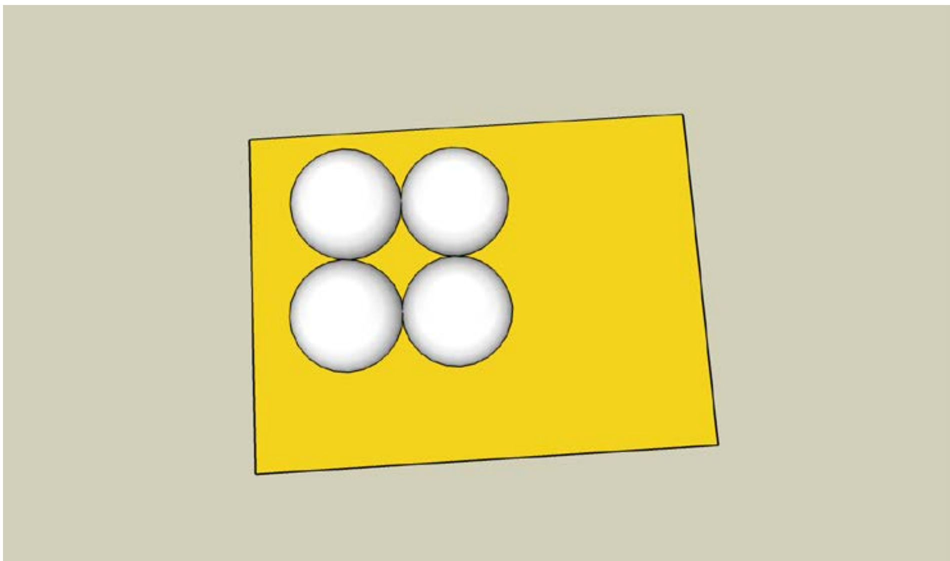

Figure 19 Effect of contact area on MPD

Lastly, it can be seen that as the curves in Figure 18 near 90%, they begin to converge in terms of MPD value. This phenomenon most likely occurs because, based on the definition of MPD, and with such a small amount of the Delrin spheres exposed in both cases, the difference in MPD between the two sizes should become smaller when moving from 50% towards 100 percent. Eventually, as embedment reaches 100%, both the MPD values would be approximately zero for both curves, so the curves should converge as they approach 100% embedment, as shown in Figure 18.

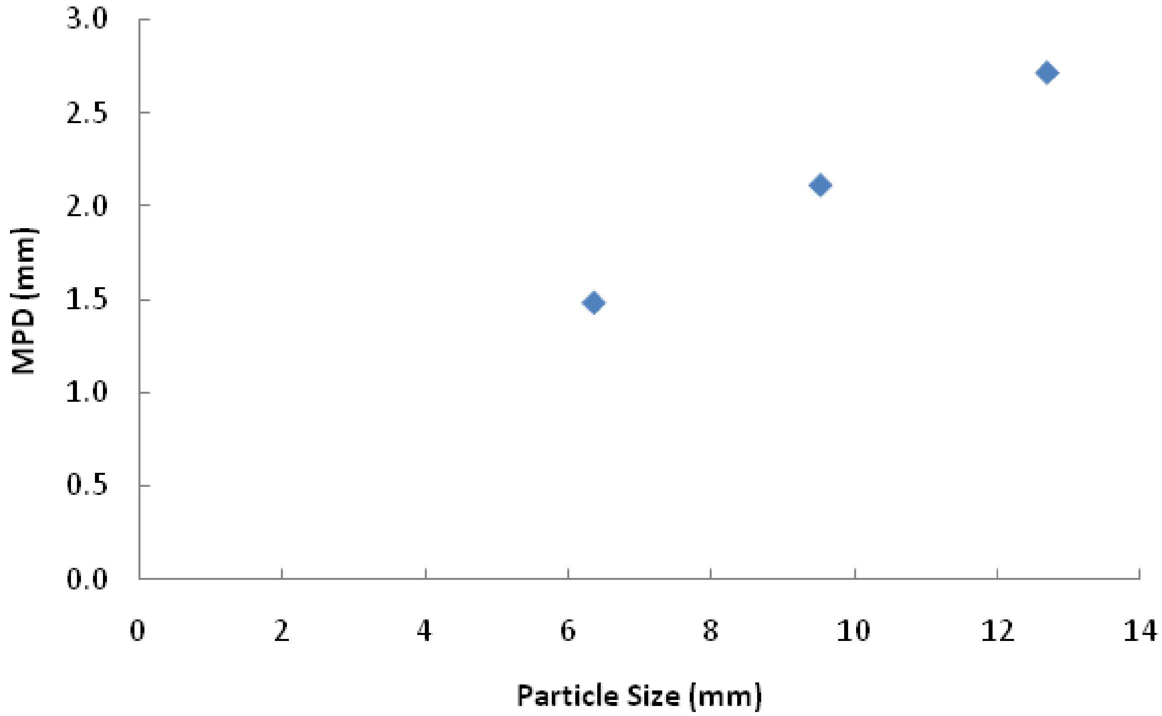

Figure 20 MPD vs. Delrin sphere size at 70% embedment

Figure 20, which shows the MPD as a function of the particle size used, validates the hypothesis that, as the sphere size increases, so does the MPD value at 70% embedment. At sizes smaller than 6.25 mm, the area of contact between the balls is thought to be more problematic; also, working with such a small size proved difficult. The greatest deterrent to the use of a sphere size smaller than 6.25 mm is that it leads the volume-based MPD equation to calculate a low total amount of emulsion. This low amount of emulsion would be difficult to spread evenly over the 200 mm by 200 mm specimen used for testing. Thus, the research team decided that testing small sizes of the Delrin spheres would not be necessary in this analysis.

Thus, the conclusions from the Delrin sphere-based study of MPD vs. embedment depth include that a strong correlation exists between the MPD parameter that is obtained from the 3-D laser profiler and the embedment depth, as shown in Figure 18 and Figure 20. The relevance of this finding is that the embedment of the aggregate into the emulsion is related directly to aggregate loss of the chip seal and, therefore, the MPD should have a correlation to aggregate loss as well.

As the embedment depth (emulsion rate) increases and the MPD decreases, the aggregate loss percentage will also decrease. Furthermore, the findings verify the MPD parameter's ability to represent the amount of available surface voids in chip seal surface treatments. Based on these findings, it is believed that the MPD parameter can be used in analyzing the approximate embedment depth changes in a chip seal surface treatment. Lastly, this study shows that as the emulsion rate increases and the embedment depth increases, the MPD parameter can track the risk of bleeding in the chip seal surface as the MPD value decreases toward approximately 0 (which signifies that all surface voids have been filled by emulsion).

5. NCSU MIX DESIGN PROCEDURE

5.1 Purpose and Need for Mix Design Procedure

The purpose of the NCSU mix design procedure is to provide a systematic analytical method for engineers to design consistent chip seal mixes while ensuring satisfactory performance under field traffic and environmental conditions. The mix design seeks to provide effective quantitative methods and techniques for determining the appropriate AAR and EAR for the chip seal surface treatment to be constructed.

Regarding the need for a design method, Chip Seal Best Practices (Gransberg 2005) provides some insight into the state of chip sealing in North America; see Table 4 that lists the percentage (or lack thereof) of each current design method used in the both the United States and Canada.

Table 4 Design Method Usage in North America (Chip Seal Best Practices, 13)

Chip Seal Design Method	United States (%)	Canada (%)
Kearby/Modified Kearby	7	0
McLeod/Asphalt Institute	11	45
Empirical/Past Experience	37	33
Own Formal Method	19	0
No Formal Method	26	22

Table 4 serves to illustrate that most of the respondents in the Gransberg survey use an empirical/custom method or no method at all. In the United States, this finding represents 82% of the respondents. Thus, a strong need exists for a mix design method that supplies engineers and field personnel with reliable tools and analysis procedures to have at their disposal when designing chip seal mixes. The NCSU non-empirical design method seeks to improve upon the foundation provided by the Hanson, Kearby, and McLeod methods of chip seal mix design.

The techniques and methods described in the NCSU mix design method aim to provide a consistent process for engineers to design chip seal surface treatments regardless of the location, environmental conditions, and expected traffic demand of the chip seal construction site. This method will prove most beneficial to young engineers and inexperienced field personnel who do not have the intuition and experience in designing chip seal surface treatments and need a solid foundation on which to base their designs. The proposed method can also help experienced engineers obtain a quantitative perspective in the mix design phase so they can distinguish between the design components of adequately performing chip seals versus those that do not perform as well in field situations.

5.2 NCSU Mix Design Framework

The chip seal mix design method developed by the NCSU research team incorporates aggregate analysis, volumetric calculations, and detailed 3-D laser profiler scan data in order to determine the AARs and EARs that will ensure quality performance from the constructed chip seal. The flow diagram displayed in Figure 21 shows an overview of steps that are included in the determination of the appropriate chip seal mix design values. These steps are discussed in detail in the subsequent sections of this document.

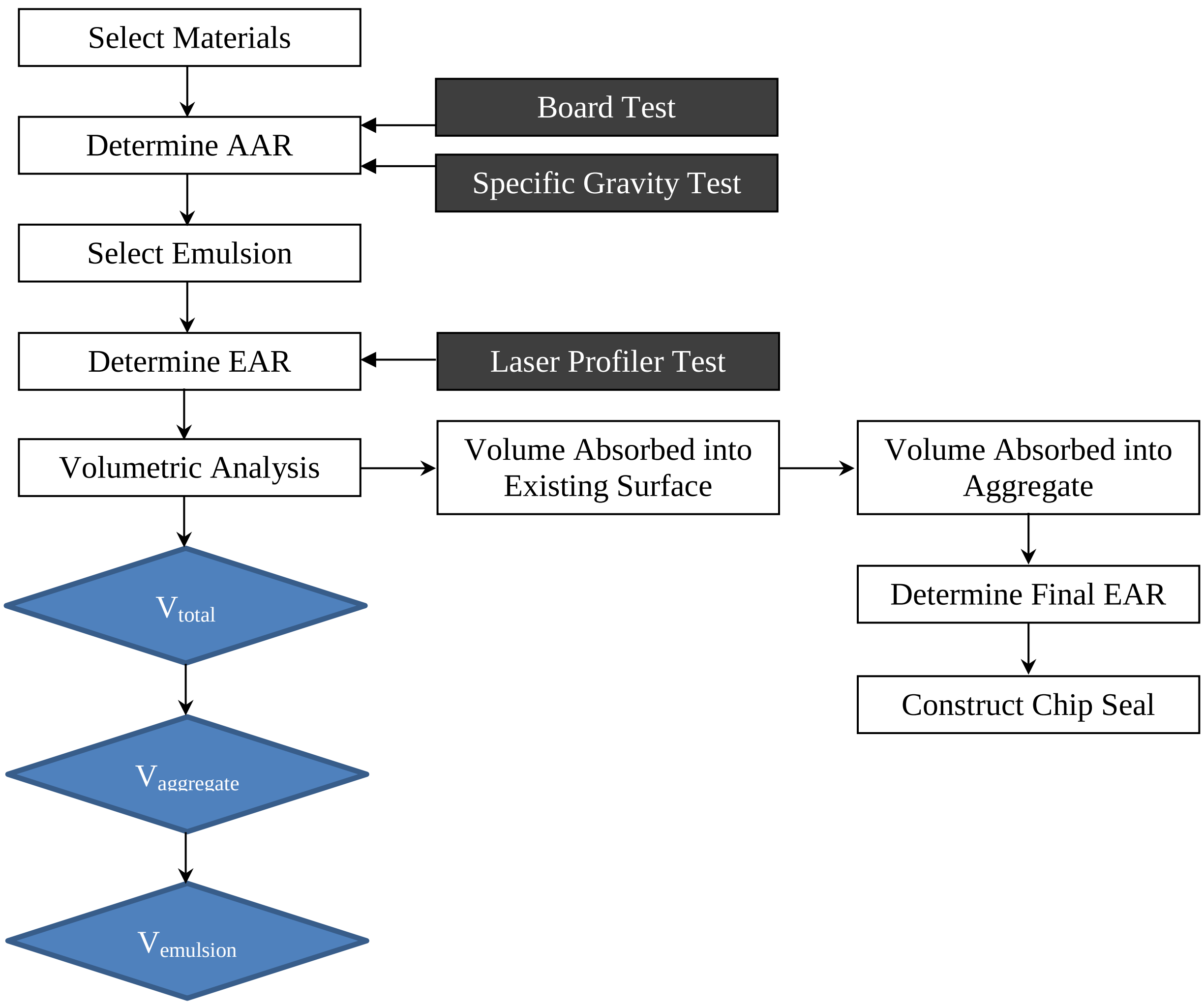

Figure 21 NCSU mix design framework

5.3 Determination of Performance Uniformity Coefficient (PUC)

The first step in the chip seal mix design procedure is the determination of the performance uniformity coefficient (PUC) for the aggregate source being used for the chip seal construction. The chip seal PUC is a performance indicator of aggregate gradation and gives an indication of the uniformity, or lack thereof, of the aggregate source being analyzed. In chip seal surface treatments, gradations that are more uniform perform better than those that are less uniform in terms of the aggregate loss and bleeding failure criteria. Therefore, in the mix design, the PUC of the aggregate source will have an effect on the bleeding and aggregate loss performance of the chip seal surface treatment being constructed. The concept of the PUC is founded on principles that are based on McLeod's chip seal failure criterion. Essentially, McLeod's premise that 70% embedment is the ideal embedment for chip seal surface treatments is implemented in the PUC definition. The PUC is the ratio of the percentage passing at a given embedment depth (P_{EM}) to the percentage passing at twice the embedment depth (P_{2EM}) in a sieve analysis curve, as shown in Equation (8).

$$PUC = \frac{P_{EM}}{P_{2EM}} \tag{8}$$

The P_{EM} value represents the bleeding failure criterion, and the P_{2EM} value represents the aggregate loss failure criterion with regard to the gradation. The P_{EM} value is defined as the percentage passing that corresponds to 70% of the median particle size on the gradation curve. The P_{2EM} value is defined as the percentage passing that corresponds to 1.4 times the median particle size, with the median particle size defined as the particle size of which 50% of the gradation passes through the sieve. In the case of a chip seal, the P_{EM} value should be low, because a low percentage of the gradation passing at the bleeding failure criterion indicates that the aggregate particles in that range of the gradation are larger and less susceptible to bleeding than smaller particles would be. Conversely, for the P_{2EM} criterion, if the value is high, the percentage of aggregate particles that do not meet the aggregate loss criterion is low, and therefore less aggregate loss is expected.

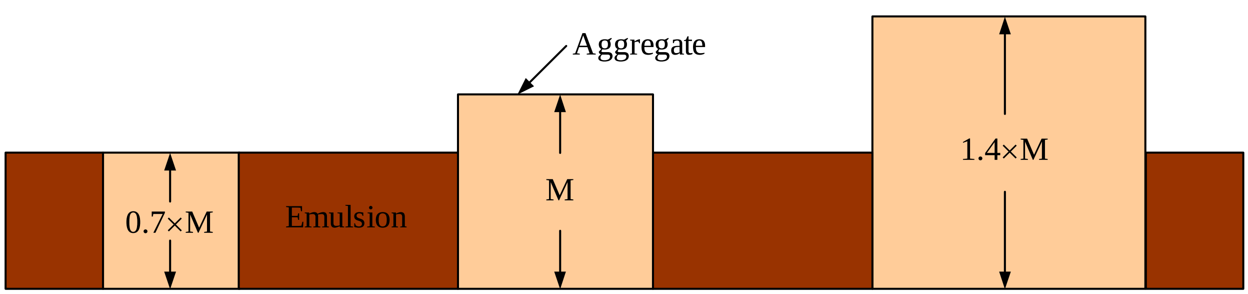

Figure 22 Explanation of PUC parameter

Figure 22 visually displays the concept behind the PUC. In theory, if the aggregate is embedded in emulsion up to 70% of its median (M) particle size, the particles that are smaller than 0.7M will be submerged completely in the emulsion and, therefore, will experience bleeding. Ideally, then, the smaller particles should be larger than 0.7M to avoid bleeding. Conversely, the particles that are bigger than 1.4M are likely to be lost when trafficked because they will be less than 50% embedded after trafficking. In this case, the larger the coarse aggregate particles, the more likely aggregate loss will occur.

Thus, the closer the PUC value is to zero for a particular aggregate gradation, the more uniformly the aggregate is graded. In other words, the P_{EM} value that is closer to 0% and the P_{2EM} value that is closer to 100% indicate a uniform gradation that corresponds to improved chip seal performance; that is, these values indicate less bleeding and a smaller amount of aggregate loss, respectively.

Figure 23 shows graphically how the PUC is determined using the natural granite 78M aggregate gradation employed by the research team.

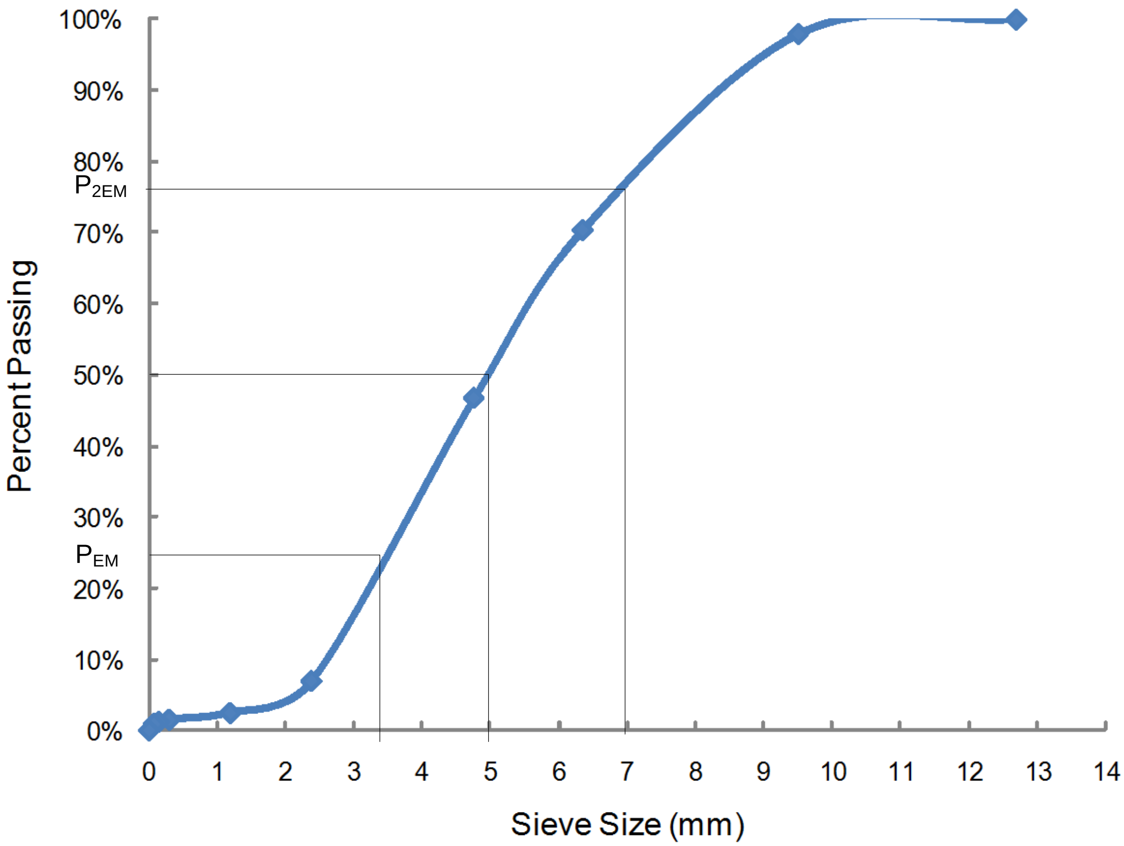

Figure 23 Method of PUC determination

Essentially, once the median particle size (point of 50% passing) is determined, it is used to determine the 0.7M and 1.4M values. As illustrated in the Figure 23 graph, a vertical line is drawn from both the 0.7M and 1.4M particle sizes towards the gradation curve. Once each vertical line intersects the curve, the corresponding percentage passing to the left denotes the critical failure criterion for bleeding (0.7M) and aggregate loss (1.4M), respectively.

The PUC analysis for the 78M gradation shown in Figure 23 is as follows:

$$M = 5 \text{ mm};\ 0.7M = 3.5 \text{ mm};\ 1.4\,M = 7 \text{ mm}$$
$$PUC = P_{EM}/P_{2EM}$$
$$P_{EM} = 25$$
$$P_{2EM} = 75$$
$$PUC = 33.3\%$$

A P_{EM} value of 25 means that 25% of the aggregate passes at the bleeding criterion. The lower this value, the larger the aggregate in the bleeding region of the PUC analysis, which makes the chip seal more resistant to bleeding. A P_{2EM} value of 75 means that 75% of the gradation passes at the aggregate loss failure criterion. The higher the P_{2EM} value, the more resistant the gradation is to aggregate loss, because the coarse aggregates are small enough to allow adequate embedment. Again, if the part of the gradation that is above the median particle size is too large, the aggregate will not be embedded adequately, and aggregate loss will increase.

5.4 Aggregate Gradations Used in Performance Testing

The research team used the PUC parameter for the systematic gradation variation of the aggregate sources in the performance testing aspect of the research. Figure 24 and Figure 25 display the gradations of granite 78M aggregate and lightweight aggregate respectively. Gradation B is the natural gradation in each of the two aggregate sources.

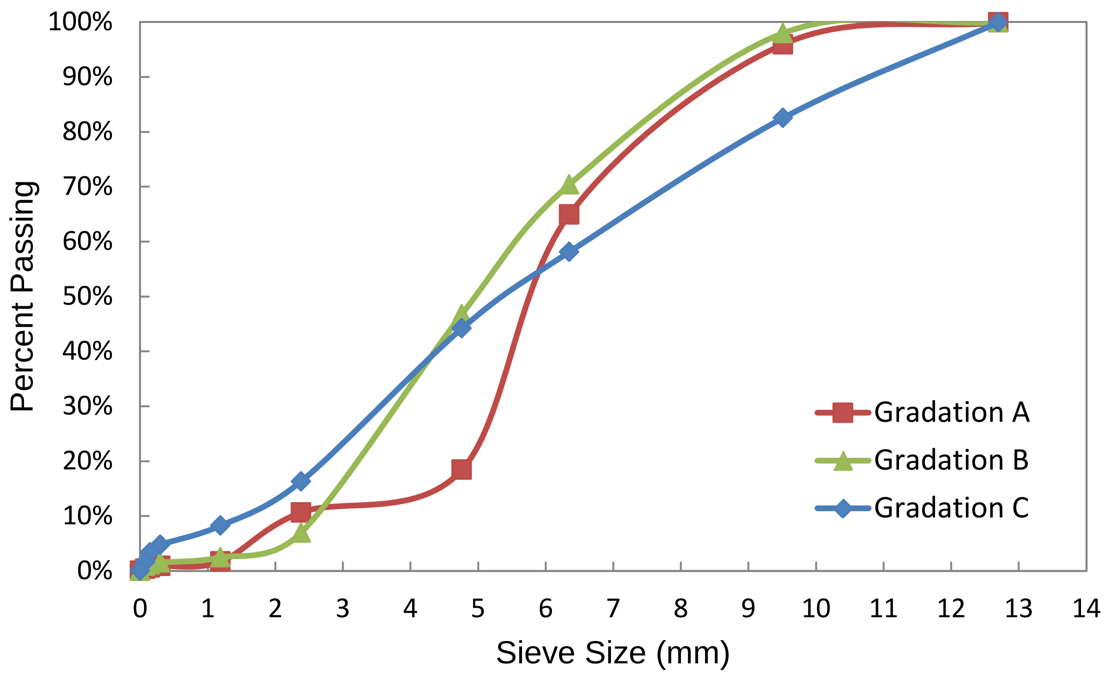

Figure 24 Comparison of granite 78M aggregate gradations

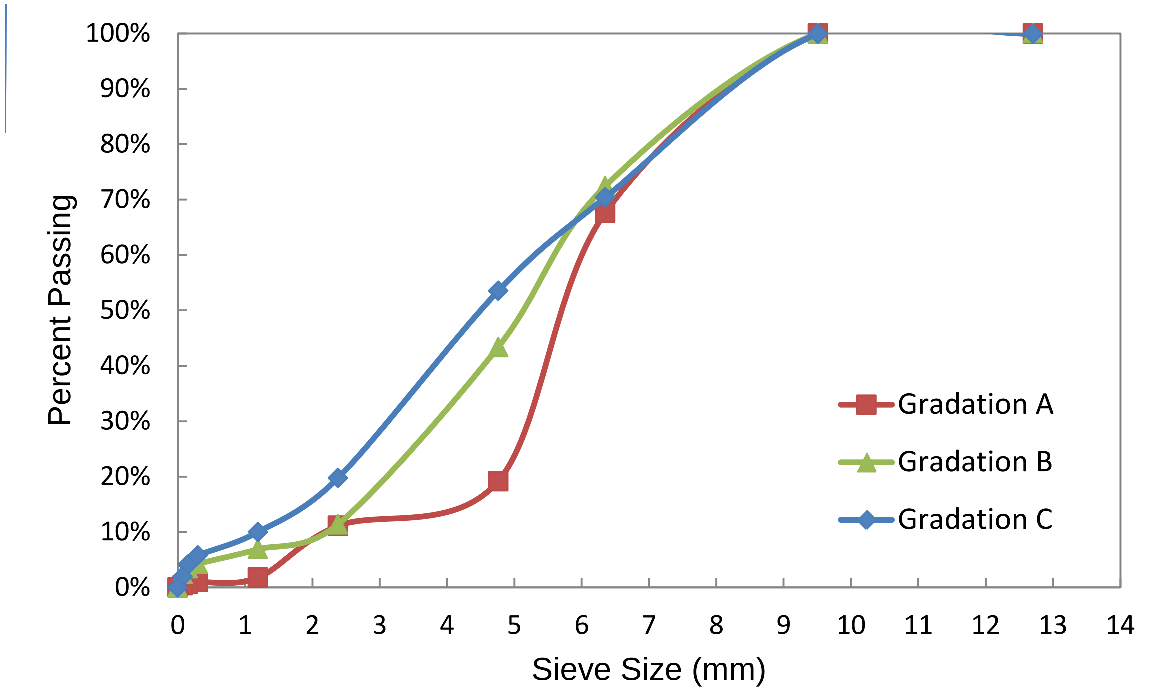

Figure 25 Comparison of lightweight aggregate gradations

Table 5 shows a summary of the PUC of each gradation for both lightweight and granite 78M aggregate. The PUCs for both aggregate types were varied enough to capture the gradation effect in the performance testing. They were not pushed to unreasonable extremes (such as 0% or 100%), because PUCs at those extremes would not be used in realistic chip seal construction situations. Hypothetically, the expectation is that the A gradations for both lightweight and granite 78M aggregate sources will perform best with regard to aggregate loss and bleeding performance, and that the C gradations will perform the least favorably. Recall that gradation A is the most uniform gradation because it has the lowest PUC, with uniformity being a desirable aggregate characteristic with regard to chip seal surface treatment performance.

Table 5 PUC Summary

Gradation	**PUC**	
	Granite 78M	**Lightweight**
A	17.1%	15.9%
B	33.3%	31.3%
C	50.8%	45.5%

5.5 Modified Board Test Background and Procedure

The AAR to be used for the construction of chip seal surface treatments in the mix design procedure is determined by a modified board test analysis. The origins of the board test come from the modified Kearby method that recommends using one square yard (in the field, and a ½ square yard in the laboratory) board to determine the amount of aggregate required to fill a specific area with one stone coverage of that particular aggregate. The person conducting the board test must be sure to fill the board completely with aggregate while avoiding allowing a second layer of aggregate to form, as shown by the grey blocks in Figure 26. In order to perform this task, the aggregate should be spread evenly and in a well-lit area to ensure that a second layer aggregate is avoided or, if detected, removed. It is important to fill up all the empty spaces of the board to ensure that the proper AAR is determined and that the aggregate particles are packed tightly together as they would be in a chip seal surface treatment.

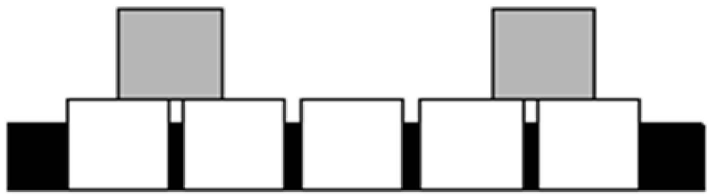

Figure 26 Example of second layer aggregate coverage

Once these tasks are completed and a single stone coverage of aggregate is present, the aggregate is then weighed to determine the AAR for that particular aggregate. Equation (9) is used to find the AAR from the weight of the aggregate. The weight should be converted into pounds (lbs), and the board test size should be converted into square yards.

$$Aggregate\ Application\ Rate = \frac{weight\ of\ agg.(in\ lbs)}{board\ test\ size\ (in\ sq\ yd)} \tag{9}$$

The research team decided to conduct further analysis to determine the board size that is appropriate to properly determine the AAR for a chip seal surface treatment. This analysis was undertaken to ensure that the size of the board would not have an effect on the AAR found during testing. The research team used four different sizes of board: 900 mm by 900 mm, 660 mm by 508 mm, 508 mm by 305 mm, and 305 mm by 127 mm. The team examined the AAR obtained from each board test as a function of the size of the board used. Eighteen board tests were conducted for each board size to ensure that the sample size was large enough that an appropriate final AAR could be determined for each board test area. A single gradation of granite 78M aggregate was used for all the board testing to ensure that there was no gradation effect. The results of this study are shown below in Figure 27.

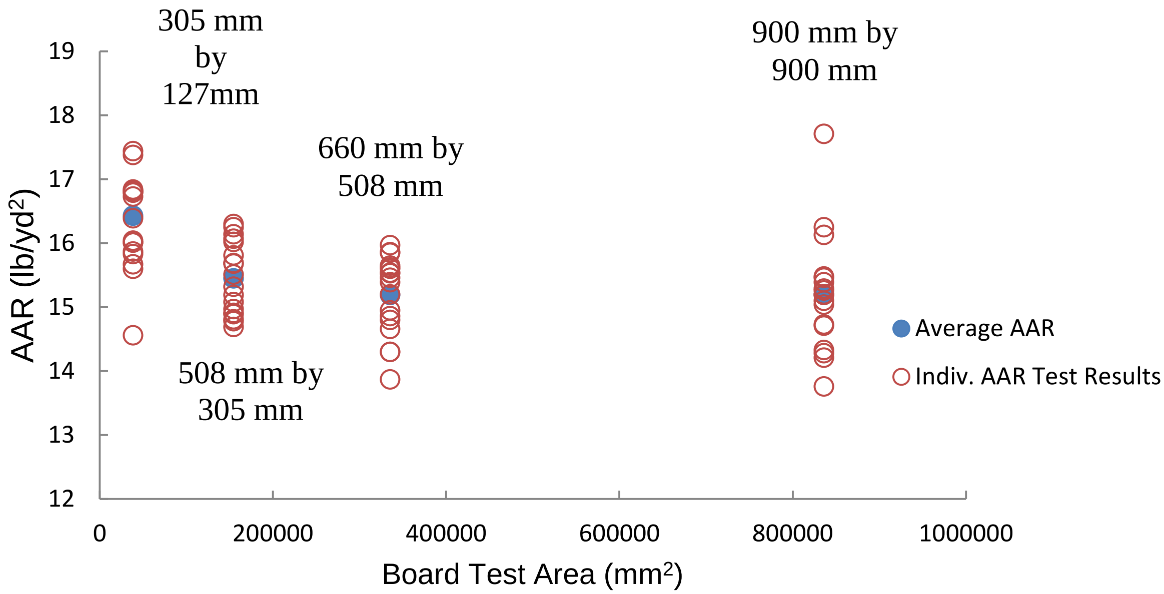

Figure 27 Board test area vs. AAR

The results shown in Figure 27 show all the AAR replicates for each board size as well as the average AAR of those board test replicates (blue filled circles). From the figure, it can be seen that for the granite 78M the asymptotic optimal AAR is around 15.5 lbs/ yd^2 for the aggregate (dry aggregate) used in this study. From the data, it can be seen that the smallest board (305 mm by 127 mm) shows large amounts of variation in the AAR. Therefore, even with a large number of replicates, the resultant average AAR for any given board size is significantly different from the asymptotic AAR found using large board test areas. Essentially, using a board that is too small could lead to an overestimation of the optimal AAR and aggregate loss due to second-layer aggregate that is not embedded properly in the emulsion layer. It can be seen from Figure 28 that the AAR decreases as the board test area increases up to a certain point, and that the AARs from the three largest boards are essentially the same. Conversely, for 18 replicates, the 900 mm by 900 mm board (the largest board) properly identifies the optimal AAR, but it does show a significant amount of variation. This finding raises the possibility that if fewer replicates are used, the optimal AAR cannot be identified properly by the board test analysis. This possibility is problematic, because conducting 18 board test replicates is not practical for field personnel for board test analyses, and is only realistic in research situations. Therefore, an additional study into the variance of each board size was performed to help decide if the large boards are necessary to obtain the optimal AAR. Figure 28 shows the standard deviation of the 18 replicates for the respective board sizes.

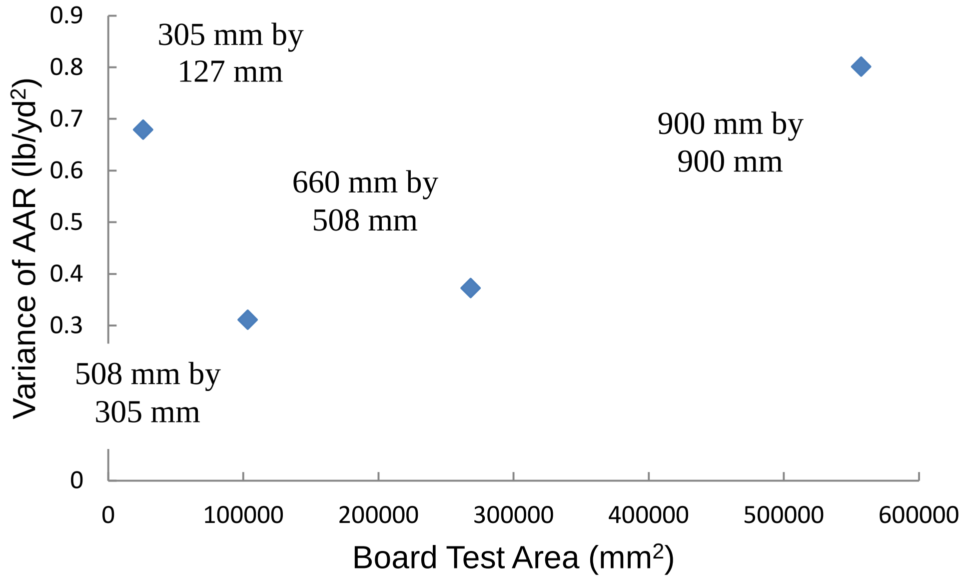

Figure 28 Variance vs. area, based on 18 board test replicates per size

From Figure 28 it can be seen that the second smallest board (508 mm by 305 mm) shows the lowest variance among the 18 samples. Therefore, for that size, the optimal AAR could be found using significantly fewer replicates while still providing the appropriate asymptotic AAR. The reason the largest board size shows the largest amount of variation is that it is more difficult to ensure a single stone coverage over a large area than over a small area. It takes a meticulous approach for such a large area, an approach that would vary from user to user. Therefore, a significantly large number of replicates is necessary to obtain the correct optimal AAR at the largest size. In conjunction with the information shown in Figure 28, the results of the variance analysis show that the 508 mm by 305 mm board is the optimal size to use to determine the optimal AAR while minimizing the variation among the samples.

Next, further analysis was performed for the 508 mm by 305 mm board to determine the minimum number of replicates that is necessary to determine the optimal AAR. The running average was calculated for each board test AAR replicate to accomplish this task.

From Figure 29 it can be seen that after only three board tests the asymptotic 78M AAR value (15.5 lbs/yd^2) is reached. Therefore, this board test size is ideal for performing the board test a minimum number of times with accuracy.

In the NCSU chip seal mix design method, the board test results are scanned and analyzed in order to determine the mix design EAR for the chip seal surface treatment to be constructed. Therefore, in addition to a small board test size that exhibits accuracy from test to test, it is also useful for the time required to scan the chip seal surface after the board test is minimized. This efficiency improves the practicality of the test in field situations by minimizing the time requirement.

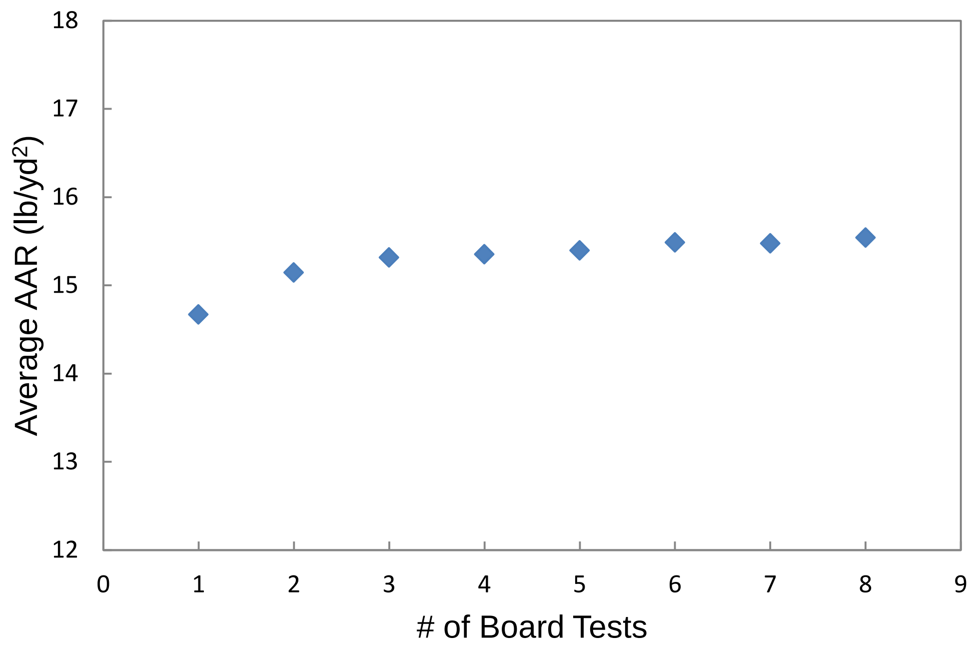

Figure 29 508 mm by 305 mm board test replicates

5.6 Mix Design AAR Summary

Table 6 and Table 7 show a summary of the modified board test results for both granite 78M and lightweight aggregate. The design optimal AARs were used in the laboratory performance testing.

Table 6 Granite 78M Board Test AAR Summary

Sample	**Area (in^2)**	**Aggregate Rate (psy)**	**Running Avg. AAR (psy)**
12X20-1	240	14.67	14.67
12X20-2	240	15.62	15.15
12X20-3	240	15.65	15.31
12X20-4	240	15.47	15.35
12X20-5	240	15.56	15.39
12X20-6	240	15.93	15.48
12X20-7	240	15.42	15.47
12X20-8	240	16	15.54
Design Optimum AAR = 15.54 lb/yd^2			

Table 7 Lightweight Board Test AAR Summary

Sample	Area (in^2)	Aggregate Rate (psy)	Running Avg AAR (psy)
12X20-1	240	6.62	6.62
12X20-2	240	6.4	6.51
12X20-3	240	6.81	6.61
12X20-4	240	6.85	6.67
12X20-5	240	6.59	6.65
12X20-6	240	6.48	6.63
12X20-7	240	6.73	6.64
12X20-8	240	6.68	6.65
Design Optimum AAR = 6.65 lb/yd^2			

5.7 Mix Design Algorithm – Determination of Design Emulsion Application Rate

5.7.1 Volumetric Calculations for Determining Design EAR

The method of determining the optimal EAR for chip seal surface treatments involves a volumetric mix design procedure used in conjunction with 3-D laser profiler board test analysis. Essentially, the goal of this analysis is to determine the amount of emulsion required to ensure satisfactory chip seal surface treatment performance in conjunction with the design optimal AAR, as determined by the board test.

The first step in determining the EAR is to determine all the volumes associated with each phase, as illustrated in the phase diagram for chip seals without emulsion, shown in Figure 30. The phase diagram represents the aggregate from the board test (with air voids, not emulsion, in between the aggregate particles).

The Figure 30 diagram is composed of two phases, aggregate and air; that is, the diagram indicates the aggregate particles and voids within the chip seal surface treatment. On the mass (right) side of the phase diagram, the weight is completely that of the aggregate. This weight of the aggregate (W_{agg}) is found from the weight determined by the modified board test that is performed in the initial step of the mix design procedure. On the volume (left) side of the phase diagram, the three variables that must be determined are the total volume (V_{total}), volume of air (V_{air}), and the volume of aggregate (V_{agg}). The relationship of the three volume terms is displayed as the volume of air in Equation (10).

$$V_{air} = V_{total} - V_{agg} \tag{10}$$

With the weight of the aggregate already found, the density of the aggregate must now be found in order to determine the volume of aggregate based on the board test's optimal AAR for the chip seal surface treatment. The density of the aggregate can be found using the procedure detailed in ASTM C127 -07, which provides the standard test method for density, specific gravity, and absorption of coarse aggregate, as well as in ASTM C 128-07, which gives the standard test method for density, specific gravity, and absorption of fine aggregate. This density value will then be inserted into the volume of aggregate equation (11), to find the volume of aggregate for the mix design.

$$V_{agg} = \frac{W_{agg}}{\gamma_{agg}} \tag{11}$$

where γ_{agg} = density of aggregate.

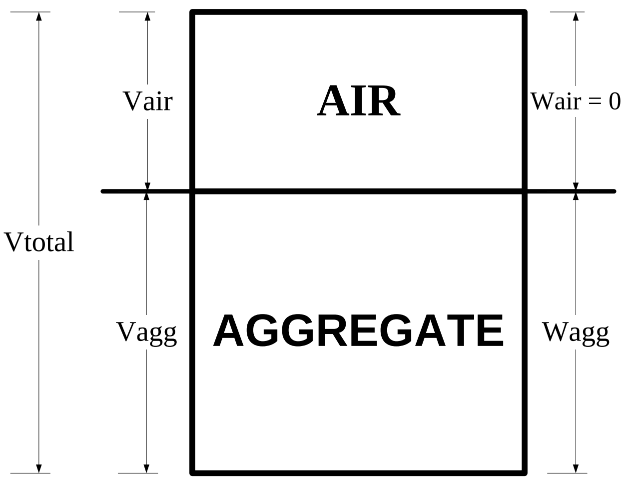

Figure 30 Phase diagram for the board test

5.7.2 Determination of Density of Granite 78M and Lightweight Aggregate

As mentioned in the previous section, the specific gravity/density of the aggregate was found for the granite 78M aggregate in accordance with the procedure described in ASTM C127-07 and C128-07. Because the volume of aggregate in the mix design is sensitive to the specific gravity, the procedure was repeated multiple times to ensure that the correct specific gravity was used to represent the granite 78M aggregate. The results of the testing are summarized in Table 8.

Table 8 Granite 78M Specific Gravity Test Results

Replicate Test #	**Specific Gravity**
1	2.48
2	2.56
3	2.41
Average Specific Gravity	2.48

From these results, the specific gravity of 2.48 was used in the mix design for the granite 78M aggregate to determine the volume of aggregate. It is important that this number is correct because if this value is inaccurate, it will lead to miscalculation of the true volume of aggregate. That is, a misrepresentation of the volume of the aggregate in the mix design calculations will cause the volume of emulsion necessary to fill the subsurface voids to be calculated incorrectly, thus jeopardizing the effectiveness of the mix design.

For the lightweight aggregate a different method was used to determine the specific gravity. The original manufacturer, Carolina Stalite, of the 5/16 in. lightweight aggregate used in the project had extensive specific gravity testing data available. The specific gravity test results obtained from Carolina Stalite are provided below in Table 9.

Table 9 5/16" Lightweight Aggregate Specific Gravity Test Results by Carolina Stalite in Gold Hill (August 2010)

Date	Sample #	1/2"	3/8"	# 4	# 8	SG	Unit Weight	Moisture (%)
		100.0	**80.0-100.0**	**5.0-40.0**	**0.0-20.0**			
2-Aug	QC-358	100.0	100.0	32.0	6.0	1.76	53.8	2.3
3-Aug	QC-359	100.0	100.0	29.0	6.0	1.73	52.4	3.2
4-Aug	QC-360	100.0	100.0	21.0	5.0	1.62	50.4	4.6
5-Aug	QC-361	100.0	100.0	22.0	4.0	1.65	48.2	3.1
6-Aug	QC-362	100.0	100.0	19.0	5.0	1.53	44.0	4.0
9-Aug	QC-363	100.0	100.0	19.0	3.0	1.54	50.3	2.1
9-Aug	QC-364	100.0	100.0	32.0	7.0	1.69	52.7	4.5
10-Aug	QC-365	100.0	100.0	20.0	3.0	1.62	46.7	2.8
11-Aug	QC-366	100.0	100.0	18.0	3.0	1.67	49.3	2.8
12-Aug	QC-367	100.0	100.0	22.0	5.0	1.63	47.9	4.7
13-Aug	QC-368	100.0	100.0	33.0	5.0	1.67	51.8	3.7
16-Aug	QC-369	100.0	100.0	26.0	4.0	1.70	50.1	2.2
17-Aug	QC-370	100.0	100.0	26.0	5.0	1.71	53.5	2.3
18-Aug	QC-371	100.0	100.0	22.0	4.0	1.70	52.0	3.9
19-Aug	QC-372	100.0	100.0	19.0	3.0	1.60	48.2	10.3
20-Aug	QC-373	100.0	100.0	18.0	3.0	1.77	53.3	4.3
23-Aug	QC-374	100.0	100.0	26.0	5.0	1.59	48.4	2.8
24-Aug	QC-375	100.0	100.0	34.0	7.0	1.57	49.1	3.7
25-Aug	QC-376	100.0	100.0	19.0	4.0	1.56	49.4	3.1
26-Aug	QC-377	100.0	100.0	24.0	6.0	1.60	50.5	5.1
27-Aug	QC-378	100.0	100.0	25.0	5.0	1.66	53.0	2.7
30-Aug	QC-379	100.0	100.0	14.0	2.0	1.67	46.6	0.1
31-Aug	QC-380	100.0	100.0	32.0	7.0	1.53	51.3	2.5
1-Sep	QC-381	100.0	100.0	15.0	3.0	1.54	47.3	2.1
2-Sep	QC-382	100.0	100.0	19.0	1.0	1.59	47.3	0.9
3-Sep	QC-383	100.0	100.0	33.0	6.0	1.57	48.0	2.4
7-Sep	QC-384	100.0	100.0	11.0	2.0	1.63	47.7	2.0
8-Sep	QC-385	100.0	100.0	13.0	2.0	1.65	50.6	2.5
9-Sep	QC-386	100.0	100.0	18.0	3.0	1.57	47.5	2.6
10-Sep	QC-387	100.0	100.0	13.0	3.0	1.60	46.3	1.6
13-Sep	QC-388	100.0	100.0	23.0	3.0	1.58	47.9	2.6
14-Sep	QC-389	100.0	100.0	23.0	4.0	1.58	46.9	2.3
15-Sep	QC-390	100.0	100.0	40.0	13.0	1.64	47.5	3.4
16-Sep	QC-391	100.0	100.0	27.0	5.0	1.63	52.0	3.5
17-Sep	QC-392	100.0	100.0	21.0	3.0	1.63	46.3	2.5
20-Sep	QC-393	100.0	100.0	30.0	4.0	1.71	50.2	2.5
21-Sep	QC-394	100.0	100.0	21.0	4.0	1.66	56.3	3.3
22-Sep	QC-395	100.0	100.0	35.0	6.0	1.63	48.2	2.0
23-Sep	QC-396	100.0	100.0	26.0	4.0	1.74	55.7	2.0
24-Sep	QC-397	100.0	100.0	18.0	3.0	1.58	47.6	3.7
Average		**100.0**	**100.0**	**23.5**	**4.4**	**1.63**	**49.7**	**3.1**
STD Deviation		**0.00**	**0.00**	**6.84**	**2.04**	**0.06**	**2.78**	**1.55**

As with the granite 78M aggregate specific gravity results, the average specific gravity of 1.63 for lightweight aggregate, as determined by Carolina Stalite, was used throughout the mix design.

5.7.3 Determination of Mix Design Total Volume

The next step is to determine the total volume (V_{total}) of the chip seal surface treatment. This volume can be determined by using the 3-D laser profiler to perform a laser scan on the aggregate during the board test. Multiple scans of multiple board tests were performed for research purposes just to ensure that the proper V_{total} was captured and that the variance from test to test was not an issue.

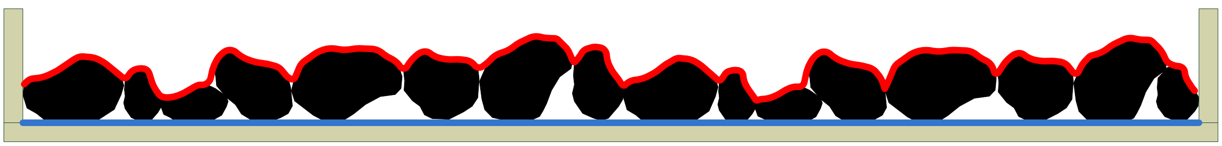

Figure 31 Aggregate board test (profile view)

Figure 31 shows the profile view of the aggregate structure during the board test analysis phase of the mix design. During the board test, a one stone coverage is maintained across the aggregate layer, and the aggregate is lightly compacted so as to be oriented in a realistic and natural post-construction state. Scanning the aggregate in this state using the 3-D laser profiler gave the research team a representative profile of the aggregate surface. The surface profile obtained is shown in red on Figure 31. The laser profiler provides a precise representation of the surface profile of the aggregate to an accuracy of 0.1 mm. This accuracy is fine enough to capture even the intricacies of the complex aggregate structure adequately. This accuracy is pivotal because the aggregate surface heights are used in the determination of the total volume. With regard to the scan procedure, the board (shown in grey) is scanned prior to the aggregate being placed on the board in order to provide the bottom baseline profile (horizontal line in blue) for analysis. Using these two profiles, the various heights along the aggregate profile can be found by finding the difference between the two scans. From these height measurements, the area of the aggregate can be found by using the trapezoidal rule detailed in Figure 36.

The trapezoidal rule allows for an accurate approximation of the area under the curve of any function f(x) or, in this case, a dataset. The smaller the interval between the t values, the more accurate the estimation of the area under the curve will be. In the case of the research team's analysis, the interval between the t values is 0.1 mm, which is small enough to accurately approximate the area under the aggregate profile, as obtained using the 3-D laser profiler. Thus, the trapezoidal area formula is applied to find the area of each trapezoid from t = 0 to t = b, the end of the existing aggregate profile data shown in Figure 32. The formula used to find the area of the shaded trapezoid between t_1 and t_2 in Figure 32 is shown in Equation (12):

$$Area = (t_2 - t_1)\left[\frac{f(t_1)+f(t_2)}{2}\right] \quad (12)$$

Figure 32 Trapezoidal rule example schematic

The areas of the respective trapezoids are then summed to find the total area under the curve of the function or dataset. Once the area of the aggregate structure has been found, the total volume can be determined using the formula for calculating total volume in Equation (13).

$$V_{total} = \sum_{i=1}^{n} Area\ from\ bottom\ profile\ to\ surface\ profile\ x\ Distance\ between\ scans \quad (13)$$

where *n* is the number of scans performed on the board test aggregate structure, and the distance between scans (1 mm) represents the scan resolution of the laser as it moves across the board test aggregate. It should be noted that the total volume includes the aggregate and air voids that are present between the board and the surface profile, as shown in Figure 31. Essentially, one complete scan of a board test aggregate structure includes a large number of scans. The number of scans depends on the size of the board test area.

Figure 33 shows the laser profile over the board test area. The board size used for the aggregate analysis is 508 mm by 305 mm based on the analysis discussed in Section 5.6. The 3-D laser profiler can obtain a scan every 0.1 mm for the complete length of the board in the x-direction (with each scan being 97 mm wide in the y-direction); then it moves in the y-direction without overlapping the previously scanned area. Then, the laser profiler scans the length of the board again (shown as scan 2 in Figure 33), moving in the x-direction for the complete length of the board. This process is repeated until the entire area of the board is scanned. Each scan is exactly 97 mm wide and collects 97 data points (1 mm apart) along that scan width. For the analysis of the scans, the profile view (from left to right) shown in Figure 31 is the same as the scan x-direction (shown in Figure 33) with a resolution of 0.1 mm between points. In Figure 31, the y-direction (as seen in Figure 33) is the direction going into the page and represents the distance between each 97 mm scan (1 mm). Therefore, the "distance between scans" parameter in Equation (13) is 1 mm for the 3-D laser profiler used in this study. This distance is the smallest allowable between each of the 97 data points on the line laser of the profiler. Thus, the line laser can achieve 0.1 mm resolution in the x-direction, and 1 mm resolution in the y-direction, as indicated in Figure 33. Future models of the laser will include a point laser instead of a line laser so that a resolution of 0.1 mm can be obtained in both the x and y directions.

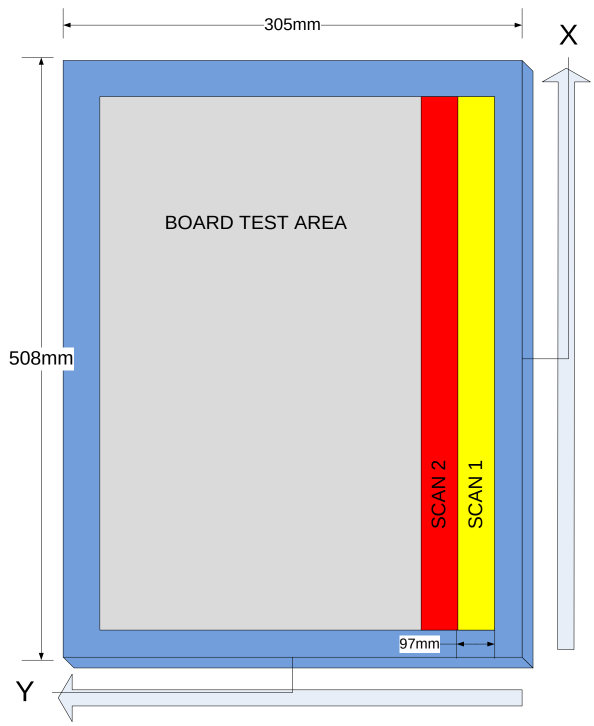

Figure 33 3-D laser scan of aggregate in the board test

At this point in the mix design, the total volume (V_{total}) and the volume of aggregate (V_{agg}) have been found. Therefore, the volume of air (V_{air}) can be calculated using Equation (10).

5.7.4 Handling of Zero Laser Data in the Scan Analysis

Occasionally data points are lost and read as zero data points in the resulting Excel output after laser scanning. This occurrence is normal and does not happen often enough to negate the accuracy of the laser scan data. The zero (lost) data points that do occur, however, are not left as zero data points in the analysis in order to ensure maximum accuracy. In some analyses (such as the MPD analysis), these zero points are completely excluded from the analysis because to exclude them is the most efficient way of dealing with the lost data points without affecting the MPD parameter obtained. However, in the case of the determination of the total volume using the scan data for the mix design procedure, removing these data points or allowing them to be read as zero is not acceptable. Allowing these data points to be read as zero would cause an underestimation of the total volume in the aggregate structure during the analysis of the scan of the board test. Therefore, in the data analysis of the scans used to determine the volume, the zero data points were converted using conditional if/then statements for each zero data point to the nearest non-zero data point in the dataset. The research team concluded that using these conditional statements in Excel was an accurate way to ensure that the zero data points are not allowed to underestimate the total volume or ultimately lead to an incorrect assessment of the volume of emulsion required from the volumetric calculations.

Figure 34 gives a visual description of the way the Excel macro handles lost laser scan data points. The solid outlined arrows represent data points (heights) that are properly recorded by the laser. The dash outlined arrow represents a lost data point that the laser read as a zero data point (or a height of 0 mm). Essentially, Excel Macro coding includes a conditional statement that checks every data point to ensure that the data point height is not 0 mm. If a data point is zero, the program will automatically take the height of the nearest non-zero data point. This nearest non-zero (non-lost) data point is represented by the dotted arrow to the immediate left of the dashed arrow in Figure 34. So, in the figure, the dashed arrow would assume the height of the green arrow. Figure 38 is not to scale for clarity purposes, so the distance between points appears larger than the realistic distance between data points. In reality, the distance between the data points is 0.1 mm, so the difference in the heights between the lost data point and the last non-zero data point is extremely small. In fact, even in the event of a few consecutive lost data points (which occurs occasionally in the dataset), all the lost data points defaulting to the last non-zero data point still allow for an accurate estimation of the height at that point, and thus an accurate representation of the volume for that small slice of the scan profile. An extremely small percentage of the data points are lost, but the research team has accounted for this phenomenon to ensure the analysis is as accurate and consistent as possible.

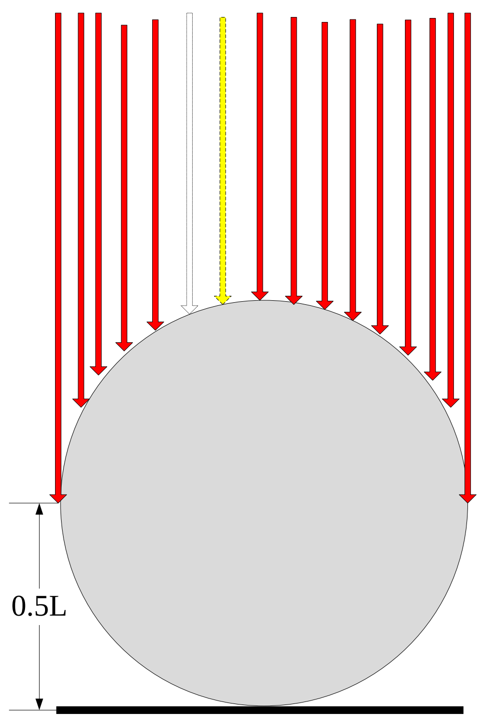

Figure 34 Lost laser data point conversion graphic representation

The Excel algorithm that accounts for lost data points also serves another important function in the laser scan volumetric analysis. This other function of the algorithm helps to ensure that the total volume is not underestimated when analyzing the board test scans. This function is best explained using a graphic representation, as shown in Figure 35.

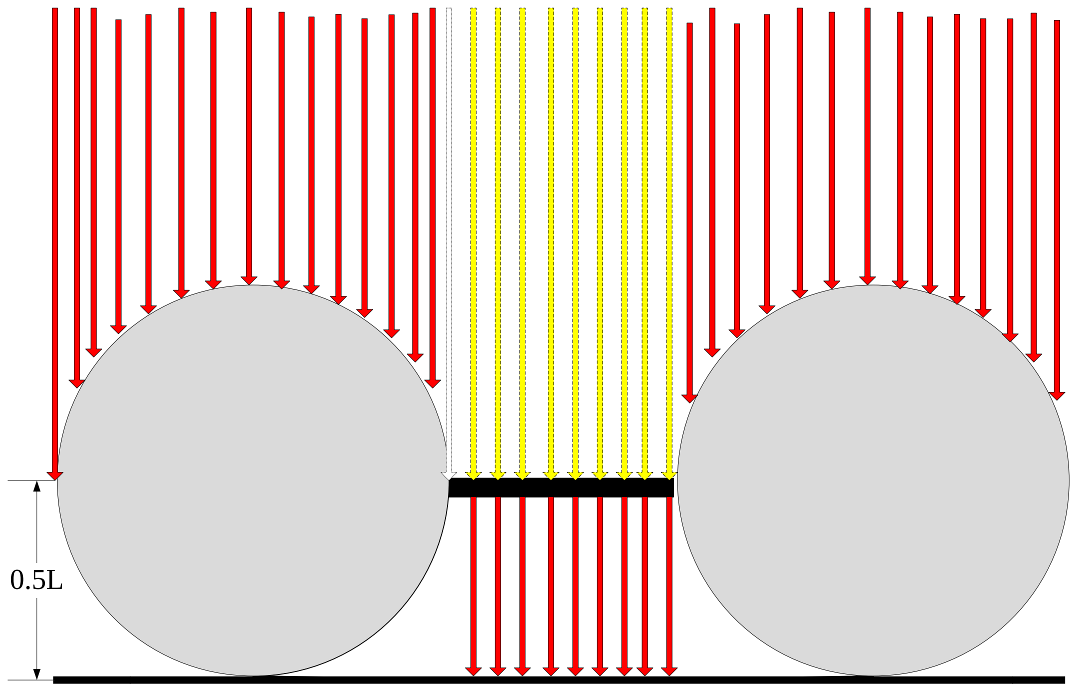

Figure 35 Visual description of 50% embedment assumption

Figure 35 shows two aggregate particles (two circles) separated by an empty space, thus representing the potential space between any two aggregate particles in the aggregate board test. The red arrows represent the laser scan as it crosses the aggregate and records height data at each position. At each position the laser reaches the tip of the solid outlined arrow, which is in between the two aggregate particles, and reaches all the way down to the empty board itself, as seen in the figure.

Without the aforementioned algorithm, the data from the laser scan at each position in between the aggregate particles would read zero (recorded as the height from the board). The problem with this measurement is that, although it calculates the total volume for this profile underneath the aggregate profile (as seen by the red line in Figure 31), the space between the aggregate particles should be added to the total volume amount (and, therefore, would later be filled with emulsion). Thus, an algorithm is needed that can account for this occurrence. The conditional Excel statement utilized earlier to handle the lost (zero) laser data points also serves this purpose. In Figure 35, all of the laser points in between the two aggregate particles (designated by the short solid outlined arrows underneath the horizontal solid bar) would be converted from zero height data points (or points where the laser hits the board because no aggregate is present) to the height of the last non-zero data point, which is denoted by the clear dotted arrow to the immediate right of the aggregate in Figure 35. Each of the solid outlined arrows would then be analyzed as if they were the dash outlined arrows that take on the height of the last non-zero data point on the aggregate. Therefore, whenever there is blank space between the aggregate particles, the side (about midway on the particle, depending on the aggregate shape) of the aggregate particle where the last data point was scanned will be the height of the emulsion in between the two aggregate particles that the analysis assumes. Thus, the volume in between the aggregate particles is not underestimated and seen as empty space, but rather is seen as additional total volume that is not filled with aggregate, which later will be filled with emulsion in the volumetric analysis.

5.7.5 Explanation of 50% Embedment by Filling Subsurface Voids

With the volume of air known, the research team was able to calculate the total amount of emulsion needed to fill the available air voids, as needed. The research team assumed that by filling the available voids in the chip seal, the estimated embedment depth is about 50 percent. More importantly, using this method that determines all the voids between the aggregates, the mix design procedure will adjust accordingly in the event that the board test operator in the field overestimates or underestimates the optimal AAR. For example, an overestimation would lead to some additional second layer aggregate, which in turn would lead to a higher aggregate surface profile obtained by the laser. This scenario would cause a higher volume of air in the aggregate structure. Therefore, if the research team were to fill 100% of the available voids in this case, additional emulsion would be used that would help retain the excess aggregate above the optimal AAR, and vice versa for underestimation.

Figure 36 further explain the way that filling the subsurface voids attains 50% embedment of the aggregate. Whereas Figure 35 and its discussion describes the way that the empty space between aggregate particles is filled to 50% embedment, Figure 36 clarifies the way that filling the subsurface air voids, as described earlier, results in an approximate 50% embedment.

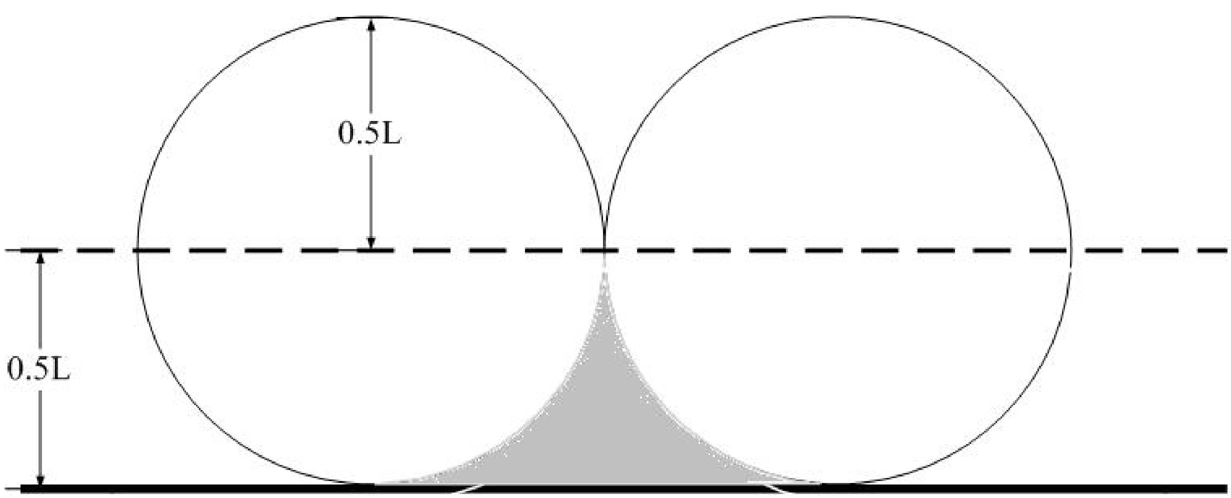

Figure 36 Explanation of 50% embedment concept

If the two circles shown in Figure 6 are assumed to be two uniform aggregate particles, and the grey in between them is assumed to be emulsion, it can be seen that if all the available subsurface voids are filled, 50% embedment of the aggregate is attained, with embedment being defined as the emulsion height divided by the aggregate height. In the realistic case where aggregate particles vary in size, this example becomes an approximation. Nonetheless, the research team believes that this concept serves as an adequate method to approximate embedment, because the mix design method accounts for the changing heights of the aggregate particles in the laser scan and subsequent analysis of the aggregate structure.

Furthermore, the research team conducted large-scale performance testing (discussed in a later section) using various EARs to account for varying embedment depths. Therefore, this assumption that filling the available subsurface voids translates to a 50% embedment depth does not affect the recommendation of the research team with regard to an optimal EAR that ensures low aggregate loss/bleeding performance in field situations.

5.7.6 Determination of the Optimal Mix Design EAR

The equation for the final emulsion volume ($V_{emulsion}$) to be used in the construction of chip seal surface treatments is shown in Equation (14).

$$V_{emulsion} = V_{air} + V_{agg-abs} + V_{pvmt-abs} \tag{14}$$

Equation (14) includes the volume of air (V_{air}), the volume of emulsion absorbed into the aggregate ($V_{agg\text{-}abs}$), and the volume of emulsion absorbed into the existing pavement surface itself ($V_{pvmt\text{-}abs}$). By adding the $V_{agg\text{-}abs}$ and $V_{pvmt\text{-}abs}$ terms, the emulsion absorption that would lead to an underestimation of the EAR is taken into account, which avoids unnecessary aggregate loss in the performance of the AST. The method of finding both the $V_{agg\text{-}abs}$ and $V_{pvmt\text{-}abs}$ is discussed in detail later.

The $V_{agg\text{-}abs}$ is based on the absorption values for the various aggregates used in chip seal construction. Therefore, during the mix design phase, the absorptive capabilities of the aggregate that is to be used for a specific project should be determined, and the appropriate adjustment should be made for the amount of emulsion that the particular type of aggregate absorbs. The McLeod method suggests a correction factor of 0.02 gal/yd^2 if the aggregate absorption is at or above 2%, as determined by ASTM C-127 and C-128 (alternatively, Tex 403-A can be used to find absorption as well). If the aggregate absorption is below 2%, then no adjustment is made. The South Dakota DOT chip seal specifications make an adjustment of 0.02 gal/yd^2 if the aggregate absorption is at or above 1.5 percent. For the purposes of this mix design, this method was determined to be adequate for determining if an adjustment is needed.

The 78M and lightweight aggregates used for determining the performance of the NCSU chip seal mix design procedure were found to have an absorption percentage below 2%, so no adjustment was made for aggregate absorption ($V_{agg\text{-}abs}$), and $V_{agg\text{-}abs}$was set to zero in Equation (14).

5.7.7 Determining the Emulsion Volume Absorbed into Pavement

The $V_{pav\text{-}abs}$ is defined as the volume of emulsion that is absorbed into the existing pavement surface during chip seal construction. Determining this volume is important because during the first phase of chip seal construction, if the amount of sprayed emulsion that is absorbed into the existing pavement is not taken into account, an underestimation of the optimal EAR could occur, depending on the nature of the existing pavement surface. By adding into the mix design the amount of emulsion that the existing surface will absorb, the EAR is likely to be appropriate, and the emulsion will adequately embed and retain the aggregate when trafficked. For the NCSU chip seal mix design, this parameter is found using the laser profiler and the analysis of the laser scan data. This method determines the available voids in the existing surface beneath a certain reference level, and the amount of emulsion needed to fill those spaces can then be determined. The following figures describe the ways the research team determined the amount of absorbed emulsion into the existing pavement surface.

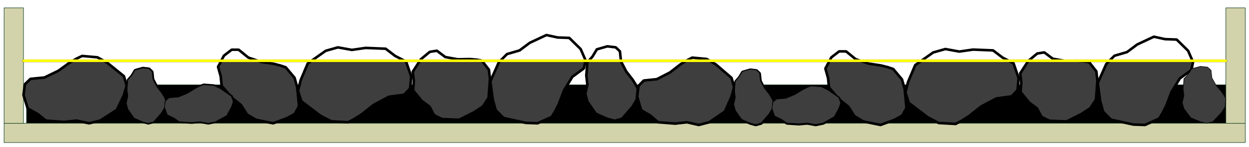

Figure 37 Profile of existing asphalt surface

The process of determining the existing pavement surface absorption begins with a 3-D laser scan of the surface of a chip seal, as shown in Figure 37. A chip seal surface is used in the example although this absorption method is applicable also to hot mix asphalt, etc. Essentially, the concept behind this method is to determine the amount of surface voids beneath a certain reference line in the chip seal surface. The appropriate reference line determined by the research team is the average of all of the peaks of the existing surface. If the highest peak is used to set the reference, the existing surface will be overestimated in most places and the EAR will likely be too high. Conversely, if just an overall average of the data is used, the reference line could be too low and, therefore, might not be high enough to fill the existing surface voids. Therefore, the research team decided to use the average of the peaks of the existing surface to determine the reference level. This reference level is symbolized by the horizontal line in Figure 37. From the figure, it can be seen that the voids (white space below the horizontal reference line) above the existing surface, but below the reference line, are to be filled while excluding the surface voids above the reference line.

In order to find this reference, the first step is to find all of the peaks for the existing surface. After scanning the surface using the 3-D laser, height information, such as that which forms the profile view shown in Figure 37, is known. From there, a three-point slope technique is used to find the peaks, such as those displayed in Figure 38.

The three-point slope technique involves taking a running slope of the data for every consecutive three points in order to use the change in slope to determine when a true peak has occurred. The three-point slope technique is used to avoid the addition of overly localized peaks in the peak analysis. The analysis is concerned with only the true peaks, which are captured when the running three-point slope changes from positive to negative in the dataset (when analyzing from left to right). Using this method, all the peaks, as shown by the small circles in Figure 38, are identified and averaged to determine the peak average reference line (displayed in yellow in Figure 38).

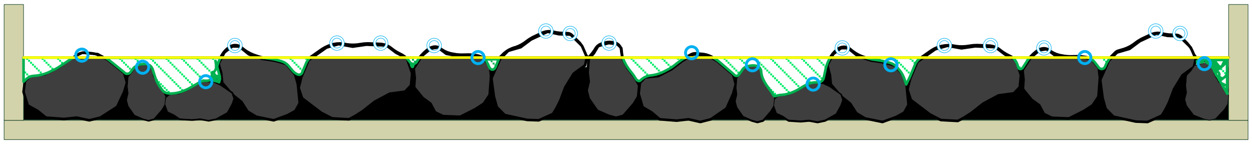

Figure 38 Visual analysis of surface absorption technique

With the overall peak average determined, the difference between the overall peak average and each individual height in the dataset is then found using the formula shown in Equation (15).

$$\textit{New data point } i = \textit{overall peak average} - \textit{old data point } i \qquad (15)$$

where i = 1……n and n = the number of data points in the whole dataset.

The data set now has both negative and positive values for each data point along the profile view of the existing surface, depending on its relative location to the overall peak average reference level. With the new reference established, the analysis seeks to determine the area (and ultimately the volume) associated with the dashed area below the reference line in Figure 38 while omitting the white outlined aggregate area from the analysis. This part of the analysis uses a conditional statement that excludes the white outlined aggregate area from the total volume calculation.

At this point in the analysis, the trapezoidal rule is used to determine the area of all the dashed absorbed areas in Figure 38 throughout the whole scan. This area is then converted to a volume by assuming that each scan profile is 1 mm thick (into the page), because this thickness is the space between each line scan using the 3-D laser profiler, and the sum of all the absorbed volumes is found. This number, in mm^3, is then converted into gal/yd^2, which is the standard unit for EARs, so that the appropriate adjustment can be made.

It should be noted that for the performance testing aspect of the research, to be discussed later, the existing surface absorption adjustment factor is not added to the mix design optimal EAR because the chip seal specimens used for the testing were fabricated on felt disks with no significant surface absorption.

Alternatively, in situations where the laser profiler is not available for determining the existing surface absorption, a qualitative visual method can be applied to determine the correction factor that can account for surface absorption in the field. For this method, the engineer or field construction supervisor visually observes the condition of the existing pavement surface texture prior to construction and categorizes it into one of the five categories in the McLeod method listed in Table 10. Depending on the category in which the existing surface is placed upon inspection, the appropriate correction factor from the McLeod method is then applied to the final design EAR.

Table 10 McLeod Method's Qualitative Existing Pavement Surface Correction Factor

Existing Pavement Surface Texture	**Correction (in gal/yd^2)**
Black, flushed asphalt surface	-0.06
Smooth, nonporous surface	-0.03
Slightly porous, oxidized surface	0.00
Slightly pocked, porous, oxidized surface	+0.03
Badly pocked, porous, oxidized surface	+0.06

5.8 Determining Final Mix Design EAR

Once all the values for the terms in Equation (14) have been found, the $V_{emulsion}$ to be used in the chip seal construction can be determined from Equation (14). This volume should be converted to gallons per square yard (the unit of measure most commonly used for emulsion application in chip seal construction) by taking into account the size of the chip seal surface to be constructed. For field construction purposes, this process requires multiplying the lane width by the length of the chip seal to be constructed. In order to simplify this process, all the volumes in Equation (14) should be considered based on the area for which they were determined.

Using granite 78M aggregate gradation B (with a PUC of 33.33%) for explanation purposes, Table 11 and Figure 39 show the way that the final mix design EAR is found for each gradation and aggregate source. First, for each scan, a mix design EAR is determined using the analysis procedure discussed previously, and the resultant EARs are listed in Table 11. Table 11 details the final mix design EARs determined for each board test scan analysis as well as the overall final mix design EAR of 0.18 lbs/yd^2 for this particular 78M aggregate gradation that is found from averaging all the EARs for each replicate scan.

Table 11 78M Aggregate Gradation B Design EAR Determination

Scan	**Mix Design EAR (lbs/yd^2)**
1	0.149
2	0.155
3	0.198
4	0.134
5	0.238
6	0.157
7	0.235
8	0.132
9	0.201
10	0.179
11	0.166
Final Mix Design EAR: 0.18 lbs/yd^2	

Performing this number of tests and analyses is not practical in non-research situations, so Figure 39 plots the running average as the scan number increases in order to determine the approximate number of scans that are needed to determine the asymptotic true final design EAR.

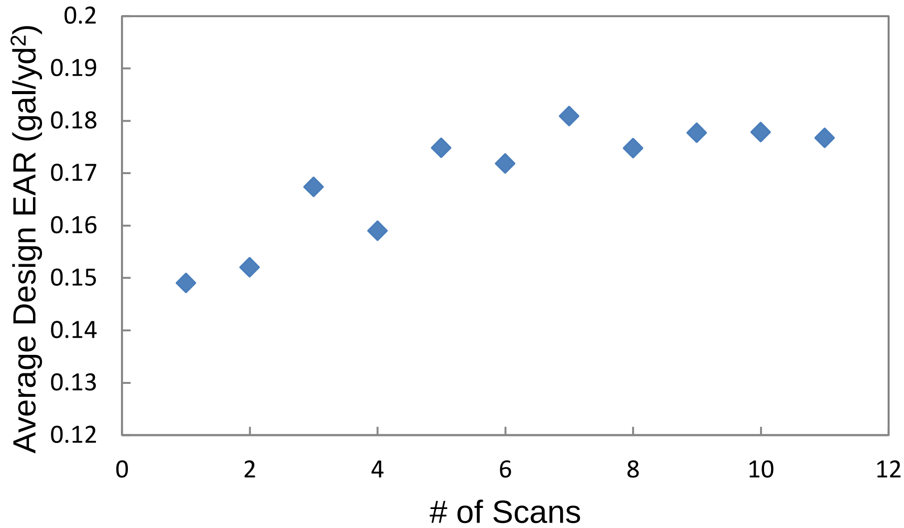

Figure 39 Average design EAR vs. number of scans analyzed

Figure 39 shows that it takes about six scans to properly determine the asymptotic value for the mix design EAR for a particular aggregate gradation. However, this does not mean that five or six board test scans must be performed and fully analyzed using the full mix design procedure described previously in order to find the final mix design EAR for a particular gradation and aggregate source. The scans shown in Figure 39 come from different board tests with a full analysis of each board test, and therefore, the design EAR determined for one particular board test will be different than the next board test, depending upon the aggregate weight differences from one board test to the next. So, the variability shown in Figure 39 is due inherently to the variation among the board tests. Alternatively, in order to simplify the analysis and improve the time efficiency, three board tests could be performed in order to determine first the representative AAR value for the given aggregate, and then the scan data could be analyzed for only the board test with a weight closest to the representative AAR in order to determine the final design EAR. In this way, the design EAR is determined in field situations where it is not practical to perform full analysis on five to ten different board test results, as was performed by the research team.

Table 12 and Table 13 present the final design EAR values as a function of the PUC for the granite 78M and lightweight aggregate sources, respectively. The trend shows that as the PUC increases, the design EAR decreases. Thus, gradation A should allow for the highest EAR without bleeding, which also maximizes its ability to retain aggregate. Therefore, as expected, gradation A is the best gradation for chip seal construction followed by gradation B, then C. This finding will be confirmed in the performance testing aspect of the research that is discussed later in this document.

Table 12 Final Mix Design EAR vs. Gradation for Granite 78M Aggregate

Gradation	% PUC	Design EAR (gal/yd^2)
A	17.1	0.21
B	33.3	0.18
C	50.8	0.17

Table 13 Final Mix Design EAR vs. Gradation for Lightweight Aggregate

Gradation	% PUC	Design EAR (gal/yd^2)
A	15.9	0.23
B	31.3	0.21
C	45.5	0.18

5.9 Verification of Mix Design Algorithm

The verification of the mix design algorithm involves using an object of known volume and dimensions (such as the Delrin spheres used previously) and verifying the accuracy of the mix design algorithm developed by the NCSU research team. For this task, 9.525 mm diameter Delrin spheres (with the same NMAS as that of the granite 78M aggregate used in this study) were placed in a fixed board 508 by 102 mm (20 in. x 4 in.). The 20 inches represents the length of the NCSU-developed modified board test size, and the 4 inches represents the scan width of the 3-D line laser used to scan the surface of the board.

For this test, the board was scanned when empty to obtain a reference for the laser for data manipulation purposes. Following the empty board scan, the board was packed with the maximum number of Delrin spheres that could fit inside the board test area while maintaining single layer coverage. The Delrin board test used for verification can be seen in Figure 40.

Figure 40 Delrin mix design algorithm verification board test

Following this scan, the difference between each point in the full Delrin board scan and the corresponding point in the empty board scan was determined in order to obtain the correct height information for the board test. Following this step, the calculations were performed just as they were for the normal NCSU mix design board test, and the volume of emulsion required to obtain an initial embedment of 50% was determined. This value was then compared to the theoretical value of emulsion required to achieve 50% embedment, and the percentage of error was found.

For the theoretical calculation, the Delrin sphere density of 1.41, provided by the Delrin manufacturer, was used. Additionally, the weight of the Delrin balls that were contained inside the board test area at the time of scanning was known, so the volume of the Delrin spheres could be calculated easily using the density = mass/volume relationship. The calculation of the volume of emulsion required to achieve 50% embedment involved using half the height of the Delrin spheres to calculate the total volume of air to be filled (1/2 Delrin diameter x board length x board width), and subtracting half of the previously calculated Delrin volume (only half in order to attain 50% embedment of the total Delrin amount). The remainder is the volume of subsurface voids required to embed the Delrin spheres up to 50 percent. This theoretical value was found to be 0.377 gal/yd^2. This amount was then compared with the volume of emulsion required to achieve 50% embedment using the mix design algorithm, and the percentage of error was calculated. The results of this analysis are summarized in Table 14.

Table 14 Verification of Mix Design Algorithm

Delrin Replicate Test	**Laser EAR**	**Theor. EAR**	**% Error**	**Avg. % Error**
Replicate 1	0.34	0.377	-9.8%	
Replicate 2	0.336	0.377	-10.9%	-8.6%
Replicate 3	0.358	0.377	-5.0%	

The results presented in Table 14 show that the mix design laser scan and volumetric calculations determine an EAR that is close to the theoretical EAR. All the replicate tests show percentage of error values below 11%, with an average error of 8.6 percent. The research team deemed this value of error to be acceptable, because 10% of a typical EAR such as 0.25 would yield an EAR of approximately 0.23, which would perform similarly well to the 0.25 EAR that is based on the performance testing results provided in this report.

5.10 Additional Location-Specific Adjustments

5.10.1 Aggregate Penetration

As discussed in the literature review, aggregate penetration is an issue when the existing pavement substrate surface is soft. Constructing a chip seal on a substrate surface that is too soft can lead to premature flushing of the chip seal surface. Aggregate penetration can be tested using the aforementioned ball penetration test that is specified by TNZ P/17: 2002 (New Zealand specification for bituminous reseals). As recommended by the New Zealand specification, chip seals should not be constructed on a surface with a ball penetration test value greater than 5 mm for the aforementioned reasons. Currently, the mix design does not adjust for ball penetration values between 0 and 5 mm, although a decrease in binder, as suggested in cases where the ball penetration value is around 3 to 4 mm, should be considered based on engineering experience (New Zealand 2005).

5.10.2 Steep Grades

The engineer should be cautious when constructing chip seals on a steep grade (especially an uphill grade), because slow moving heavy vehicles can cause premature flushing on the surface treatment as the truck tires pick up binder from the chip seal surface (New Zealand 2005). A slight reduction in the binder application rate would help remedy this problem at sites with steep grades. Currently, the mix design does not include an adjustment factor for steep grades. This adjustment should be made based on engineering experience.

6. VALIDATION OF NCSU MIX DESIGN METHOD VIA PERFORMANCE TESTING

6.1 Experimental Design

The purpose of performance testing is to determine if the mix design procedure, as presented by the research team, designs a chip seal that performs well with regard to aggregate loss and bleeding performance criteria, based on the design emulsion and AAR. Thus, the performance testing results provide verification of the NCSU mix design model and its determined rates for the respective material combinations. Table 15 gives an overview of the material combinations used in this study to assess the performance of the chip seal mix design method.

Table 15 Full Factorial Combinations of Aggregate and Emulsion

		Granite 78M (AAR = 15.5 lbs/yd^2)			Lightweight (AAR = 6 lbs/yd^2)		
		Grad. A	Grad. B	Grad. C	Grad. A	Grad. B	Grad. C
CRS-2L	0.1 gsy	x	x	x	x	x	X
	0.15 gsy	x	x	x	x	x	X
	0.2 gsy	x	x	x	x	x	X
	0.25 gsy	x	x	x	x	x	X
	0.3 gsy	x	x	x	x	x	X

The first step in the experimental design involves the use of optimal AARs for both the lightweight and granite 78M aggregates used in the research. As previously mentioned, the optimal AARs were found using the modified board test described earlier in this document. These rates are 15.5 lbs/yd^2 and 6 lbs/yd^2 for the granite 78M and lightweight aggregate types, respectively. For each aggregate type, the gradation was varied using the PUC as the representative measure of the gradation. During the sample fabrication process, each sample was made using batched aggregate to control the gradation for that particular sample set. For both types of aggregate, the B gradation is the natural gradation of the aggregate. Gradations A and C are both reasonable gradation intervals from the original. The same PUC was not used for the lightweight and granite aggregate because the natural gradation of the two types is slightly different. In addition, the 78M aggregate gradation has a larger sieve size than the lightweight aggregate gradation. Nonetheless, the PUCs of both types of aggregate are close and show similar variation between gradations. Therefore, a reasonable comparison can be made between the lightweight and 78M aggregate in terms of performance, despite the slight gradation differences between the respective A, B, and C gradation of each aggregate type.

The emulsion type used for these experiments is CRS-2L, which is cationic rapid setting (CRS) latex-modified emulsion. Time constraints did not allow full experimental designs to be performed for both the CRS-2L and CRS-2 emulsions. All replicates were made using the CRS-2L emulsion at varying rates. The EARs were varied from 0.1 to 0.3 gal/yd^2 at increments of 0.05 gal/yd^2. These rates needed to vary enough to capture the differences in performance as the emulsion rates changed from dry (of optimum 0.1) to wet (of optimum 0.3) conditions. For each particular aggregate type/gradation/emulsion rate combination, a minimum of six replicates were fabricated to ensure that each condition was properly captured in the performance analysis. If too few samples were fabricated and tested, it is possible that the correct trend would not be captured with confidence. All samples were tested for aggregate loss and bleeding performance using the MMLS3 testing procedures discussed in Section 3. Also, the samples were laser scanned in order to determine the changes in MPD (and therefore the embedment depth) as a function of traffic load as the emulsion rate and gradation changed.

6.2 MMLS3 Aggregate Loss Performance Test Results

The first performance characteristic measured by the MMLS3 is aggregate loss. MMLS3 aggregate loss testing was performed as described in Section 3 of this report. Figure 41 and Figure 42 show the results of the testing for granite 78M and lightweight aggregate, respectively. Each data point represents six or more replicate samples for each condition to ensure that true, representative aggregate loss is captured for each condition (i.e., for each emulsion rate/aggregate type/gradation combination). Each data point represents the final average cumulative aggregate loss for each sample condition after being tested for two hours under MMLS3 traffic loading. In addition to testing samples with varying EARs, the gradation was varied in the experimental design to capture that effect as well (gradations A, B, C are shown).

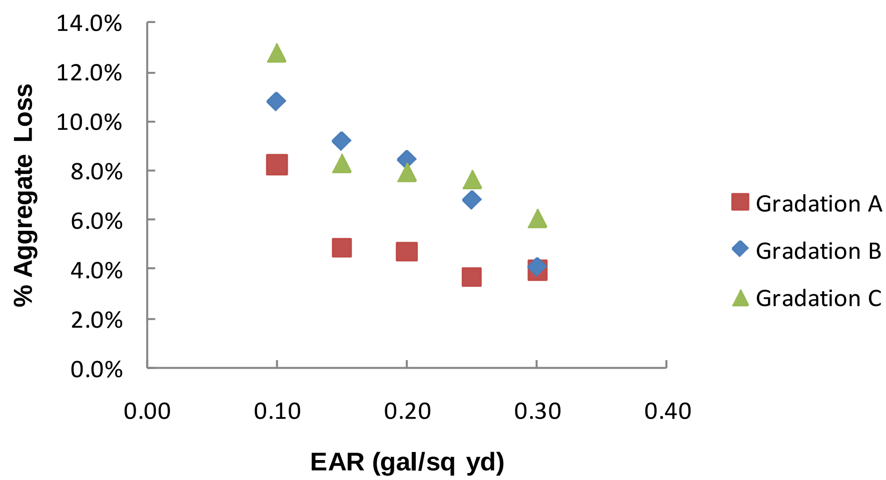

Figure 41 Aggregate loss performance of granite 78M aggregate

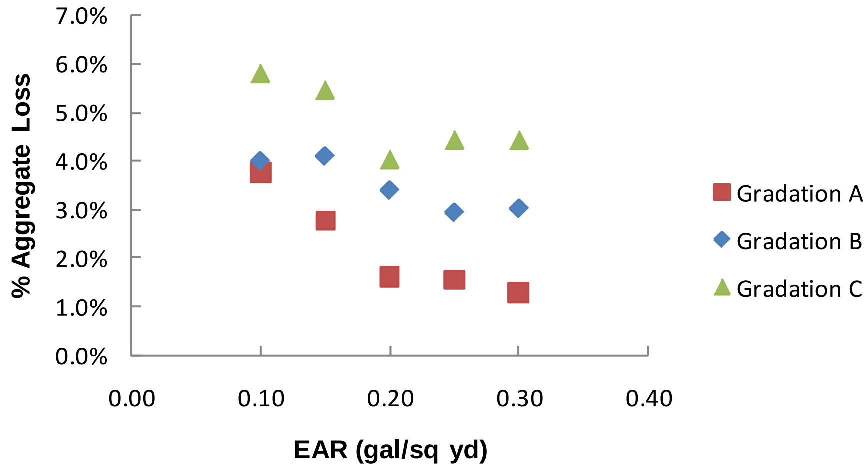

Figure 42 Aggregate loss performance of lightweight aggregate

The aggregate loss versus EAR relationship is plotted separately for each gradation in Figure 43 and Figure 44 for the granite 78M aggregate and the lightweight aggregate, respectively. The horizontal dashed line in each graph indicates the maximum allowable aggregate loss (10%) criterion established by the Alaska Department of Transportation. Figure 43 and Figure 44 show that, for all three gradations, as the EAR increases the aggregate loss decreases, which is the expected outcome. The more emulsion in the chip seal specimen, the better the aggregate retention performance, and the lower the aggregate loss percentage. The second observation to be made from these two figures is that the lightweight aggregate shows better aggregate retention performance than the granite 78M aggregate for all three gradations. As a matter of fact, the percentage of aggregate loss from the lightweight aggregate chip seals does not exceed 6% even at the lowest EAR of 0.1 gal/yd^2. The superior aggregate loss performance of the lightweight aggregate has been found from the HWY-2004-04 project, *Optimizing Gradations for Surface Treatments*, and is probably due to its more uniform natural aggregate gradation as well as the enhanced ability of the latex-modified emulsion to hold lighter weight aggregate than the granite aggregate.

Another finding from Figure 43 and Figure 44 is that the aggregate retention performance is the best with gradation A and the worst with gradation C. The reason for these findings is that gradation A is the most uniform gradation (which improves chip seal aggregate loss performance), and gradation C is the least uniform (i.e., has the highest PUC). Thus, a strong relationship exists between the aggregate gradation (captured by the PUC parameter) and the aggregate loss performance of the chip seal surface treatment. This finding validates the use of the PUC as an indicator for chip seal performance.

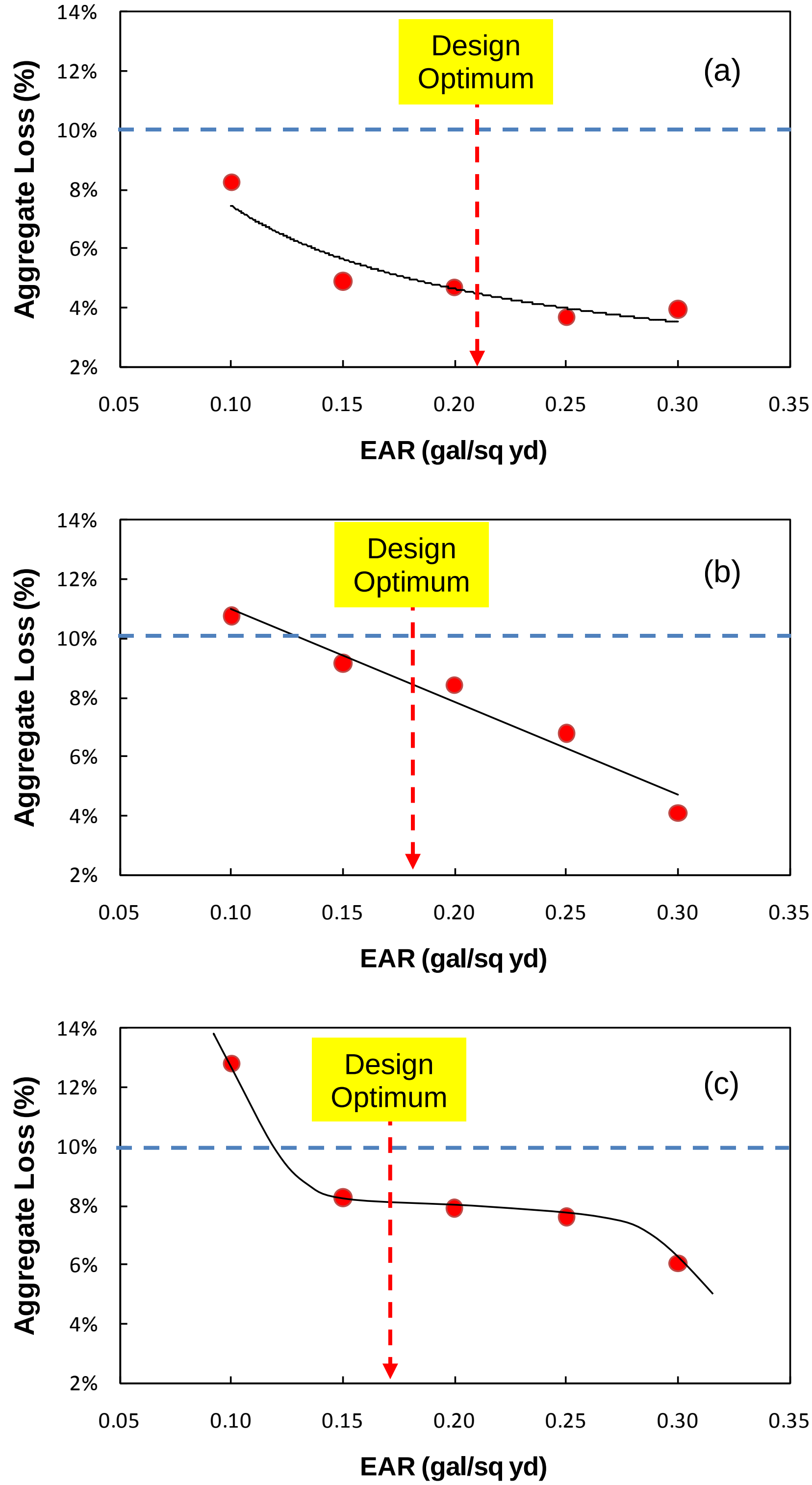

Figure 43 Aggregate loss performance of granite 78M aggregate: (a) Gradation A, (b) Gradation B, and (c) Gradation C

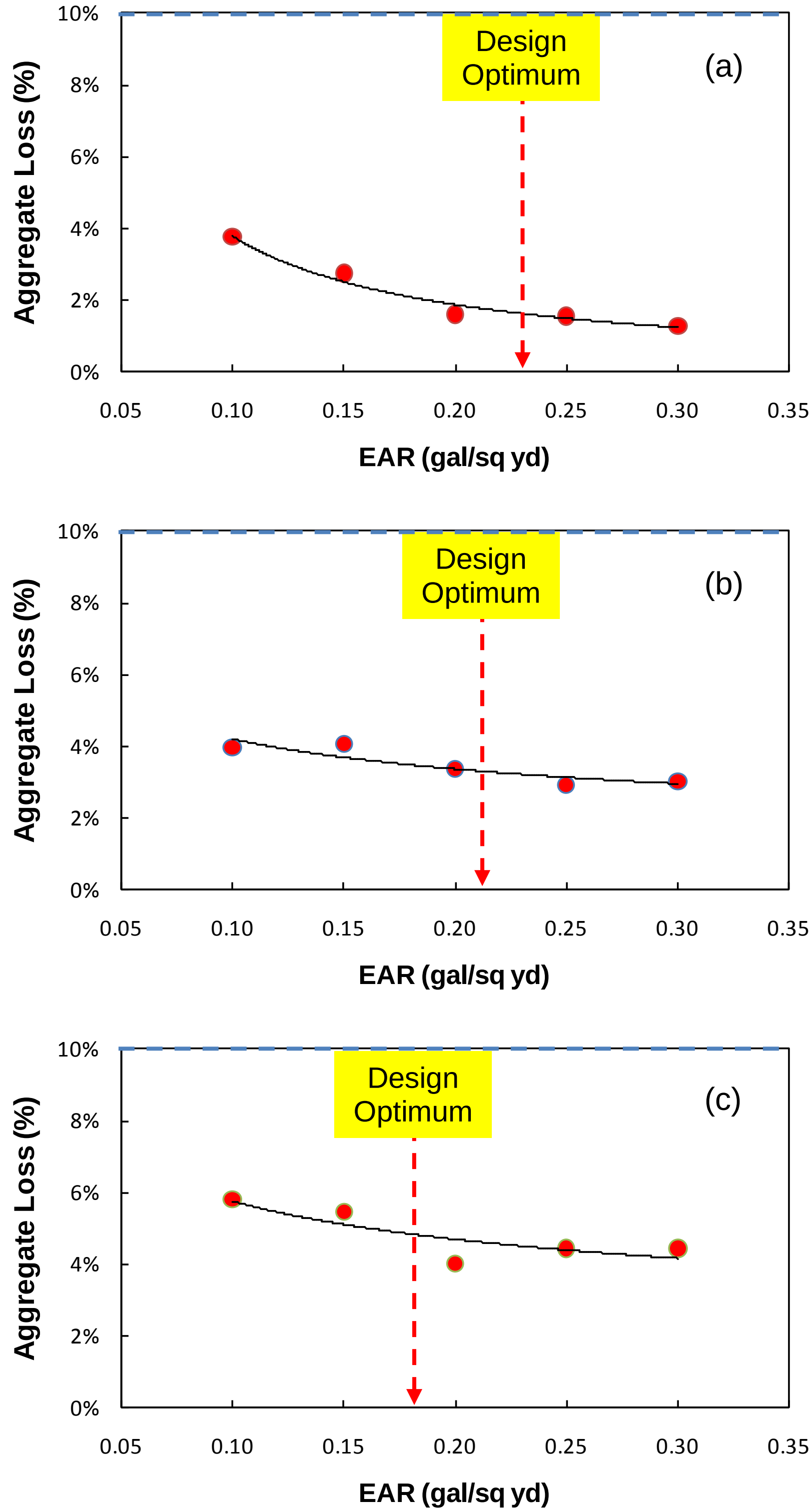

Figure 44 Aggregate loss performance of lightweight aggregate: (a) Gradation A, (b) Gradation B, and (c) Gradation C

For the 78M aggregate loss performance, at an EAR of 0.3 gal/yd^2, gradations A and B converge to the same point at approximately 4%, whereas gradation C shows higher average aggregate loss at around 6 percent. A possible explanation for this occurrence, and an additional reason that gradation C shows the highest aggregate loss of the three gradations, is found when analyzing gradations A, B, and C, displayed together in Figure 24. The figure shows that gradation C has the largest amount of large coarse aggregate retained on the 9.5 mm sieve (about 10% to15% more than the other gradations that are similar in terms of the large sieve size). As discussed in Section 5.3 with regard to the PUC definition, the more coarse aggregate, the more susceptible the gradation is to aggregate loss. Gradations A and B have less large coarse aggregate in their gradations and, therefore, are less susceptible to aggregate loss.

6.3 MMLS3 Bleeding Performance Results

The next performance measure used to validate the mix design is the bleeding performance obtained from the MMLS3 bleeding test, discussed in detail in Section 3. In the performance-related chip seal mix design method, the optimal EAR is determined by the maximum allowable amount of emulsion that does not cause bleeding. The results of the bleeding tests for granite 78M and lightweight aggregate are displayed in Figure 45 and Figure 46, respectively. Then, the same results are plotted separately for each gradation in Figure 47 and Figure 48 for the granite 78M and lightweight aggregate, respectively. Each data point is replicated to ensure that the true asymptotic average bleeding performance is captured for each EAR condition. In Figure 47 and Figure 48, the optimal EARs determined by the NCSU mix design method are shown as “Design Optimum”. These values are summarized in Table 12 and Table 13 for the granite 78M and the lightweight aggregate, respectively.

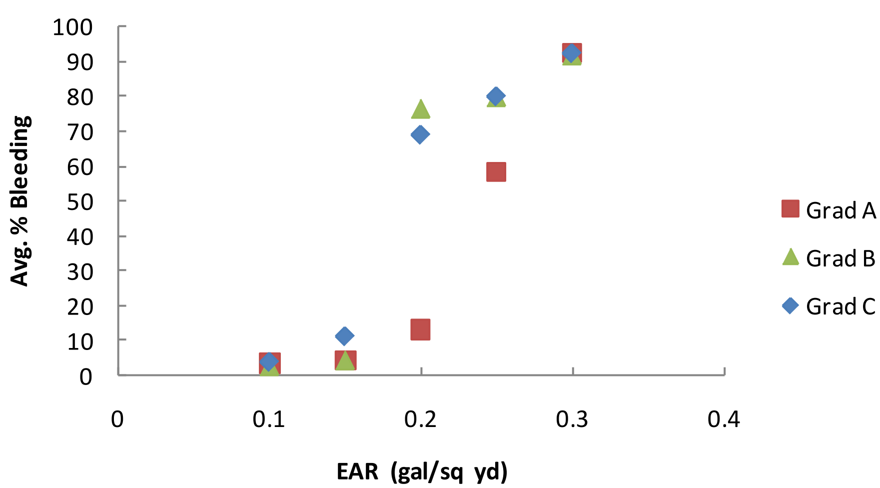

Figure 45 Granite 78M aggregate bleeding performance

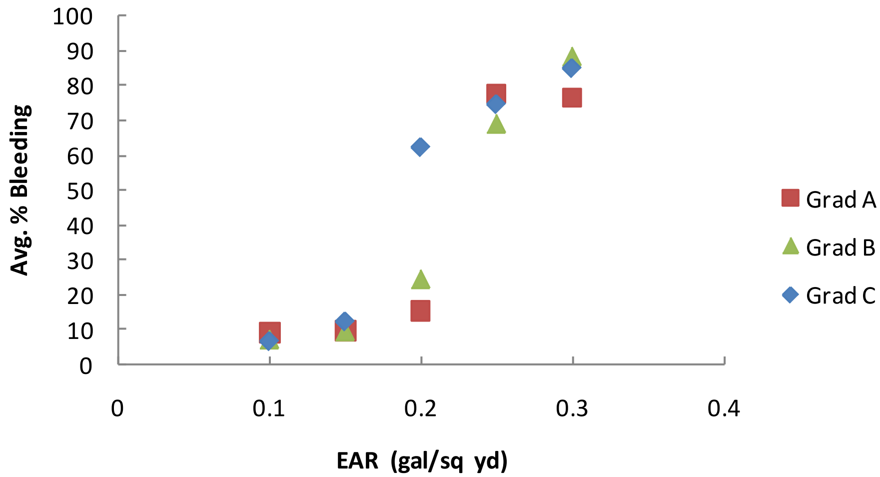

Figure 46 Lightweight aggregate bleeding performance

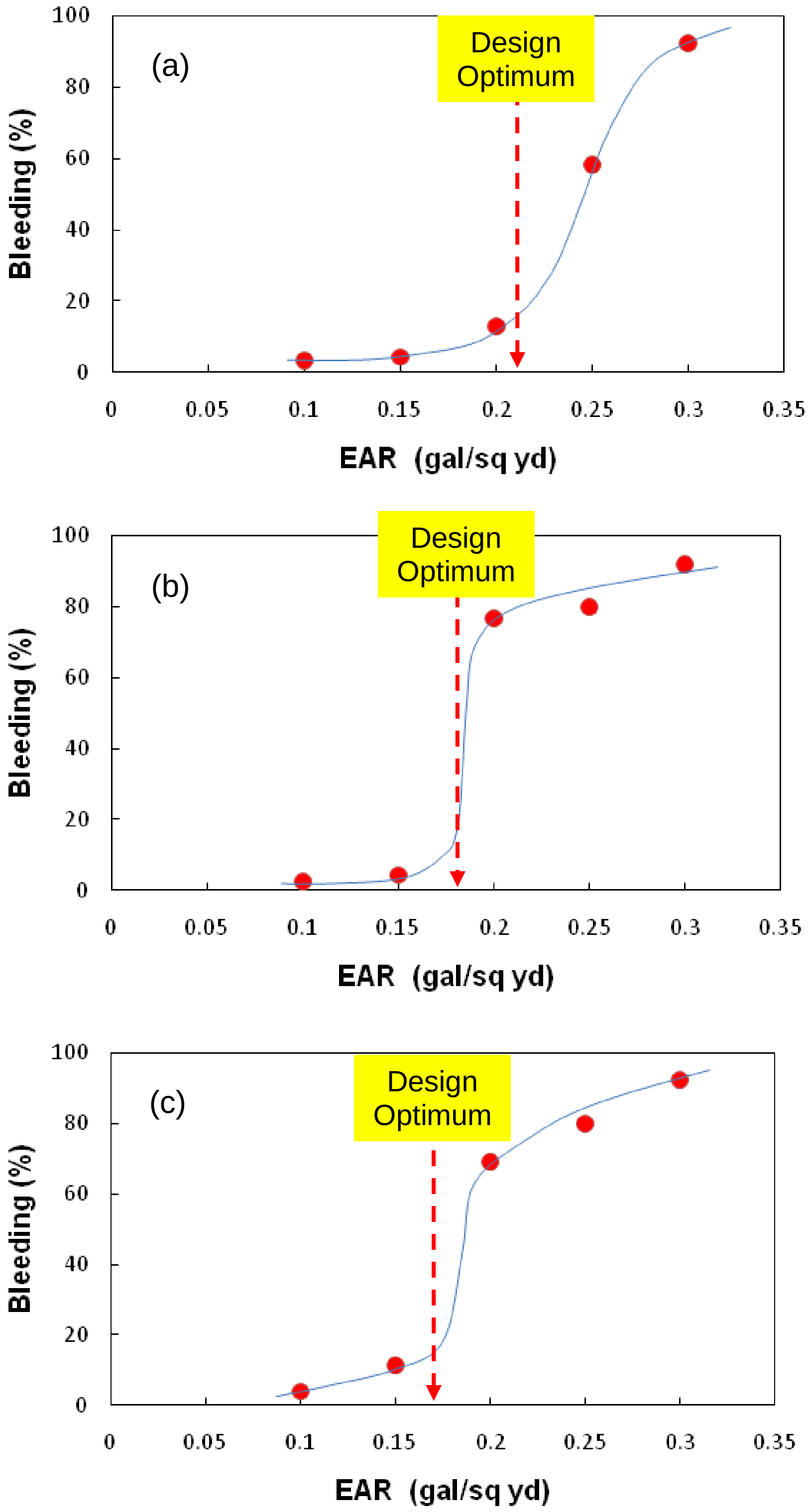

Figure 47 Verification of optimum EAR for granite 78M aggregate: (a) Gradation A, (b) Gradation B, and (c) Gradation C

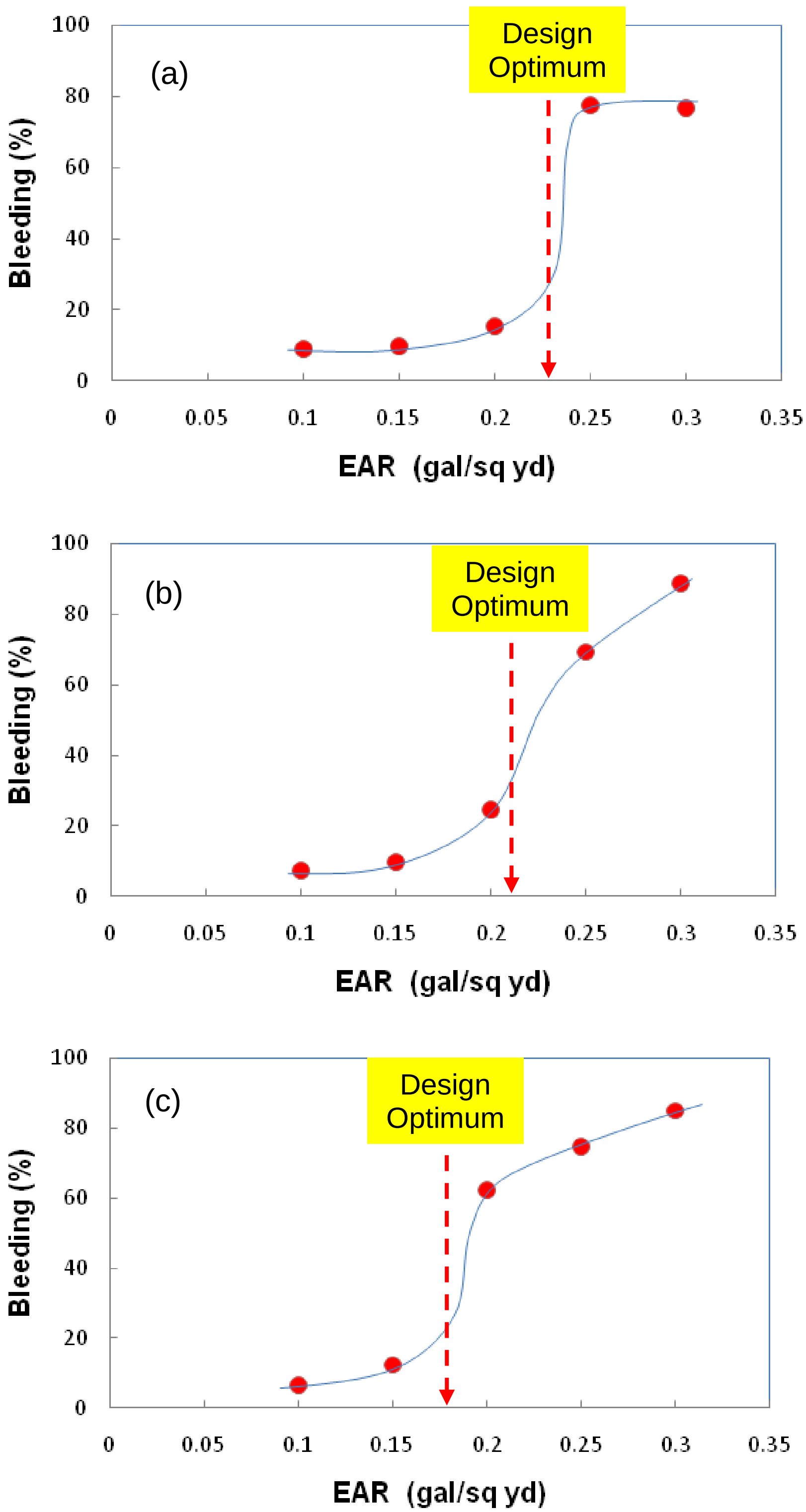

Figure 48 Verification of optimum EAR for lightweight aggregate: (a) Gradation A, (b) Gradation B, and (c) Gradation C

From the bleeding performance tests it can be seen that, as expected, as the emulsion rate increases, the likelihood of the sample bleeding increases as well. Further, it can be seen that each gradation has an EAR level above which the percentage of bleeding increases dramatically, as signified by the spike in bleeding seen in each curve. For example, in the case of gradation A in Figure 47, the EAR at which bleeding occurs is between 0.2 and 0.25 gal/yd^2. At 0.2 gal/yd^2, only about 15% bleeding occurs, whereas at 0.25 gal/yd^2 the bleeding spikes to about 60 percent. Therefore, for this gradation, the optimal EAR based on the bleeding performance should be between 0.2 and 0.25 gal/yd^2. The optimal EAR determined by the NCSU mix design method is 0.21 gal/yd^2. The same observation can be made for all the other graphs with different gradations and different aggregate types in Figure 47 and Figure 48, indicating that the NCSU mix design provides an EAR that reflects wet conditions as much as possible, which minimizes the possibility of aggregate loss issues without raising the likelihood of bleeding issues.

Another observation to be made is that the design optimal EAR decreases as the gradation moves from A to B to C. This trend is supported by the bleeding test results, although the trend is not as clear as in the mix design results. For example, the performance-based optimal EAR for gradation A is between 0.2 and 0.25 gal/yd^2 for the granite 78M aggregate, whereas the optimal EAR for gradation B is between 0.15 and 0.2 gal/yd^2, and that for gradation C seems to be lower than that for gradation B, considering the greater slope between 0.1 and 0.15 gal/yd^2 in gradation C than gradation B. This trend is explained by looking at the gradation effect. At lower PUC values (indicating more uniform gradation), the gradation is more resistant to bleeding and, therefore, requires a higher EAR for bleeding to occur. On the other hand, as the PUC increases to gradation B and then C, the amount of emulsion required to induce bleeding decreases. The reason for this phenomenon is explained earlier in the PUC definition.

As expected, at extreme low and high EARs, the bleeding performance is the opposite. At extremely low EARs, bleeding does not occur regardless of the gradation used because not enough emulsion is present to induce bleeding. Conversely, at high EARs, the chip seal will bleed for most gradations, as displayed in Figure 45 and Figure 46. Thus, for all gradations to converge at 0.1 and 0.3 is a logical occurrence. Moreover, it seems that gradations B and C show similar bleeding performance, and both perform worse than gradation A. Because the gradations' PUC values are spaced apart evenly, gradation C would be expected to continue to show worse bleeding performance than B at a magnitude similar to the difference in bleeding performance between gradations B and A. The reason gradation C in fact does not show more bleeding than B in Figure 45 is explained by looking again at the gradation comparison in Figure 24. Once again, recall the PUC definition in Equation 8 wherein the numerator includes the bleeding criterion parameter (P_{EM}) in the numerator of the equation. In this case, the higher this value, the lower the PUC, and the more resistant the gradation is to bleeding. Essentially, the more that aggregate is below the 50% passing mark, the more resistant it is to bleeding. Thus, looking at the gradation comparison in Figure 24, it can be seen that gradation A has significantly less aggregate passing the 4.75 mm sieve size (around 20% to 25% more retained) than gradations B and C. That is, among the smaller aggregate, gradation A has larger, more bleeding-resistant aggregate particles at sieve sizes smaller than the median particle size (50% passing), whereas gradations B and C show similar curves below 50% passing. This occurrence explains the reason that gradations B

and C show similar bleeding performance and worse performance than gradation A in Figure 45. This finding also further validates the importance of aggregate gradation in relation to its effect on chip seal performance. All general trends with regard to the EAR and gradation effects on bleeding performance are the same for both the granite 78M and lightweight aggregate.
A closer look at the lightweight gradations presented in Figure 25 indicates that gradations A, B, and C are similar for each sieve size, except for the low sieve sizes where gradations A, B, and C have different percentages of passing (especially at the 5 mm sieve). Therefore, more aggregate is retained on the smaller sieve sizes, and gradation A has large (or fewer small) aggregate particles below 50% passing, which makes gradation A more resistant to bleeding (in accordance with the PUC definition) than the other gradations. The same can be said for the comparison of gradations B and C. Gradation C has the highest percentage retained (% retained = 100% - % passing) at the low sieve sizes, which makes it less resistant to bleeding because more of the small aggregate particles are likely to be completely submerged in the emulsion. This gradation trend supports the bleeding performance results seen in Figure 46 for the lightweight aggregate.

6.4 MPD Analysis Results

In addition to the performance results listed above, the specimens were scanned using the laser profiler, and the MPD was determined based on the MPD definition discussed earlier in Section 4.1. The MPD vs. loading time results for the granite aggregate are listed in Figure 49, Figure 50, and Figure 51 for the respective gradations as a function of EAR from 0.1 to 0.3 gal/yd^2. The same graphs are made for the lightweight aggregate in Figure 52, Figure 53, and Figure 54.

In Figure 49 to Figure 54, it is clearly demonstrated that the MPD determined by the laser profiler can detect the surface texture change as the MMLS3 loading continues. Also, the MPD results presented here show that most of the change occurs during the initial 15 minutes of MMLS3 loading and asymptotes soon after for the remainder of the loading time. Finally, there is a clear trend of the MPD decreasing as the EAR increases. This finding essentially displays the predictive ability of the MPD with regard to expected performance. This capability is due to the fact that the MPD is inversely related to the embedment depth; therefore, at low MPD values, deeper embedment can be expected (to the point where bleeding will eventually occur). This relationship between the MPD and the embedment depth is studied under the HWY-2009-01 project *Development of a Field Testing System for Asphalt Surface Treatments* and the findings will be documented in the final report of the project.

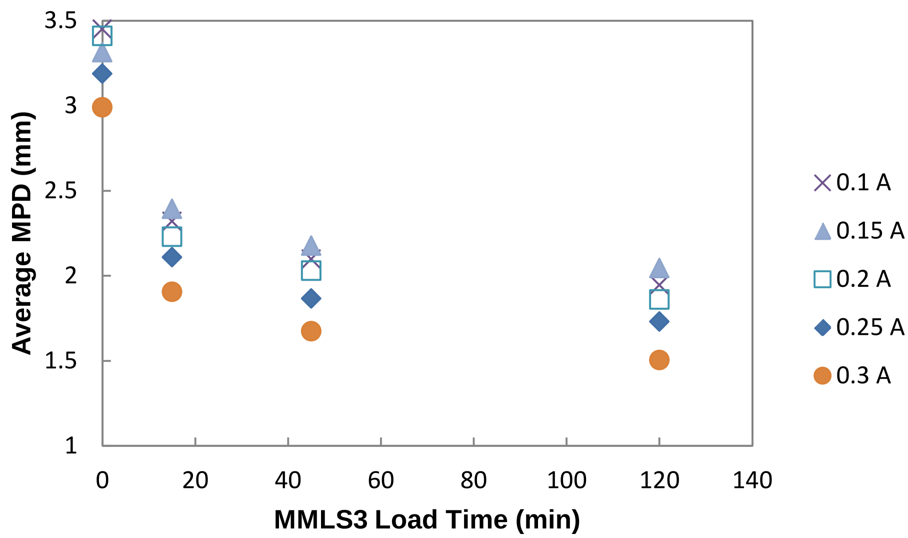

Figure 49 Granite 78M aggregate gradation A: MPD vs. loading time

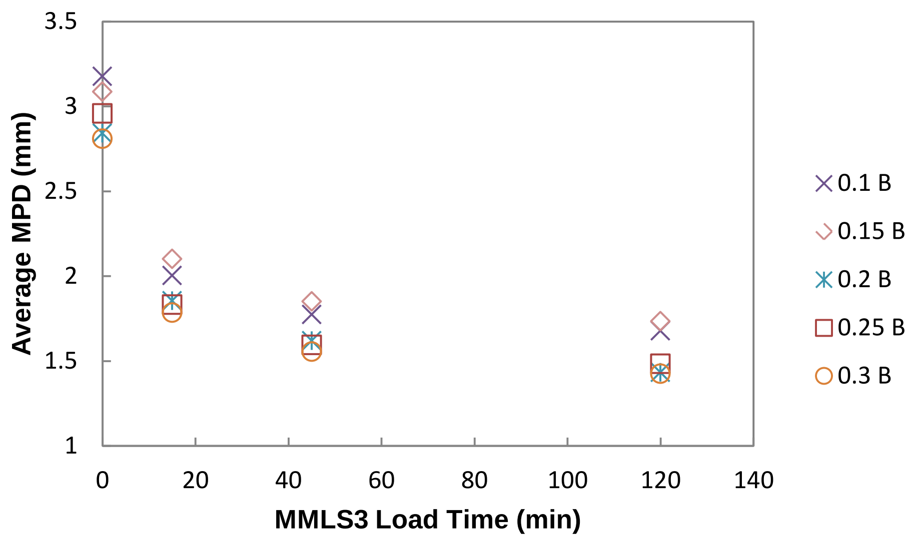

Figure 50 Granite 78M aggregate gradation B: MPD vs. loading time

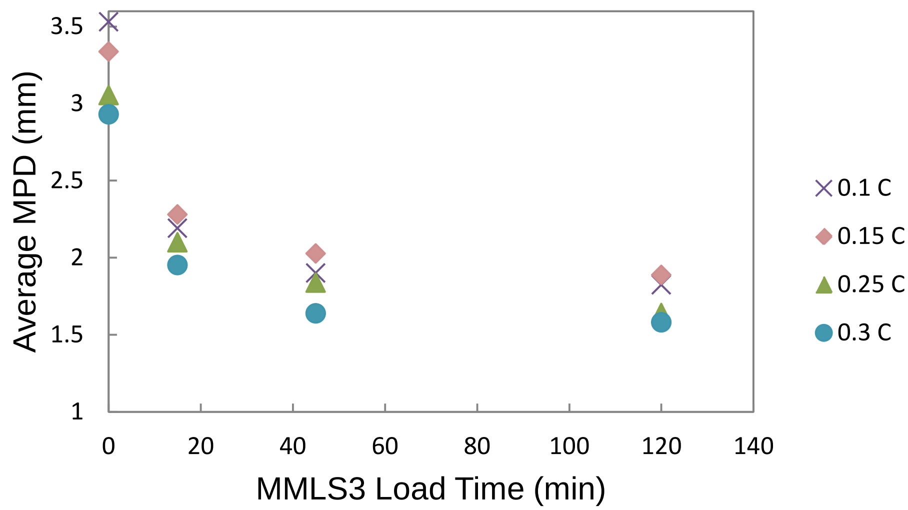

Figure 51 Granite 78M aggregate gradation C: MPD vs. loading time

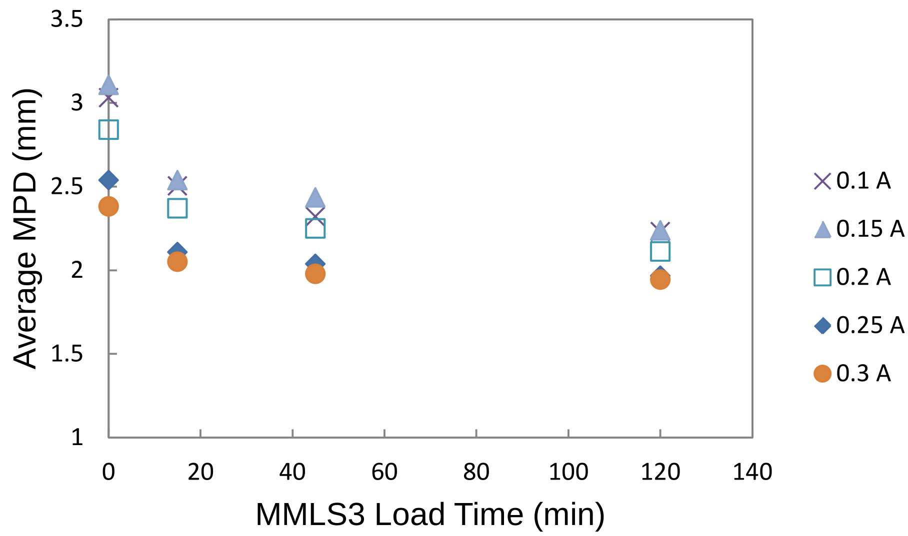

Figure 52 Lightweight aggregate gradation A: MPD vs. loading time

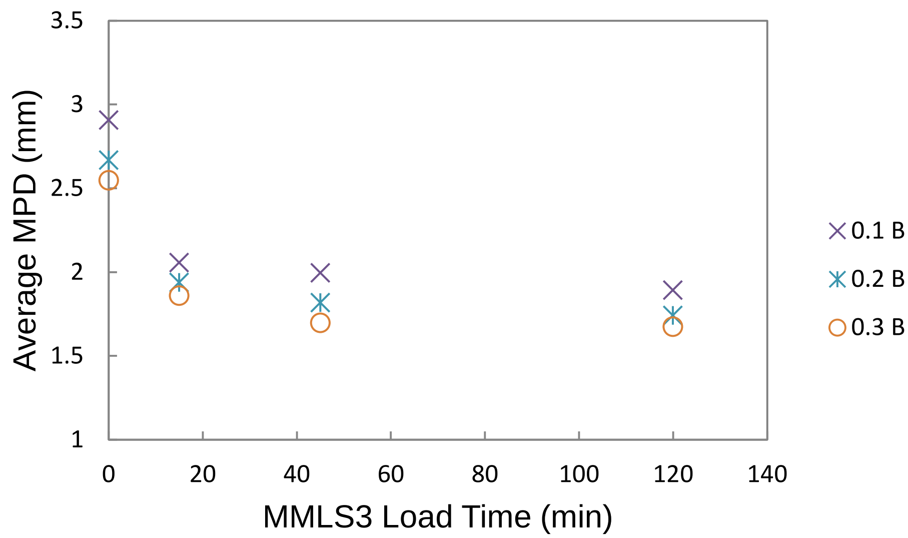

Figure 53 Lightweight aggregate gradation B: MPD vs. loading time

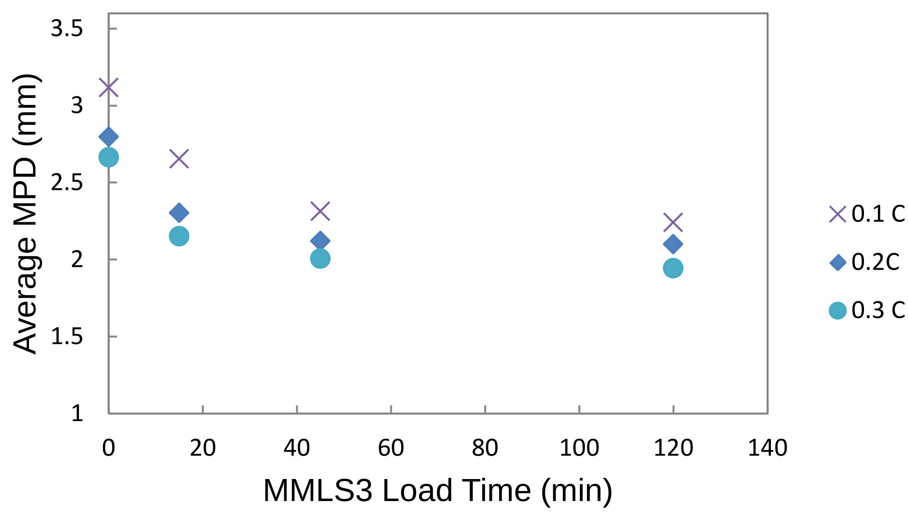

Figure 54 Lightweight aggregate gradation C: MPD vs. loading time

7. FIELD SECTION FABRICATION AND PROCEDURES

7.1 Field Test Section Construction Location

The location of the field construction for the NCSU mix design project is near Franklinton, NC, in a rural area just outside Wake County. This location features all three volume categories that are needed for the test sections and that are in accordance with the NCDOT definitions of low, medium, and high volumes. Also, all three test section locations conveniently fall within the same mile radius. The low volume sections are on a road that features an average daily traffic (ADT) count of less than 500 vehicles. The medium volume section has an ADT count of approximately 4,500 vehicles, which falls within the acceptable medium volume ADT range of 2,000-5,000 vehicles, as determined by the research team and NCDOT officials. The high volume section contains an ADT count of about 5,400 vehicles, which meets the high volume criterion of an ADT count greater than 5,000 vehicles.

Another criterion that each location meets is that none of the sections contains side roads that could possibly disrupt the uniformity and consistency of traffic for each test section. Furthermore, all the sections are relatively flat, which minimizes excess shear forces that could be caused by excessive grade variations.

Another variable that the research team has taken into consideration for the test sections is the consistency of the aggregate source used for each of the three days of test section construction. In order to ensure that no differences exist in the aggregate sources, the aggregate used for the construction of all the sections was stockpiled weeks prior to the field construction. This safeguard ensured that no variation was introduced into the sections due to a possible alternative aggregate source. Ideally, the research team would have preferred to use the same emulsion source on all three days of test section construction, but that desire proved to be unrealistic for various reasons. However, the research team did make accommodations for the same emulsion company to provide all of the emulsion used for the field construction.

7.2 Field Construction Timeline

The first step in the field construction procedure was to hold a meeting between the research team and NCDOT field personnel on the day(s) of construction. In this meeting, the plan for that particular day and the tasks that each person was expected to carry out, were decided. The EARs and AARs were determined prior to the delivery of the emulsion and aggregate to the field location, and the seal types that would be constructed that given day were discussed. The construction timeline for the August 19, 2008 test section construction is displayed in Figure 55.

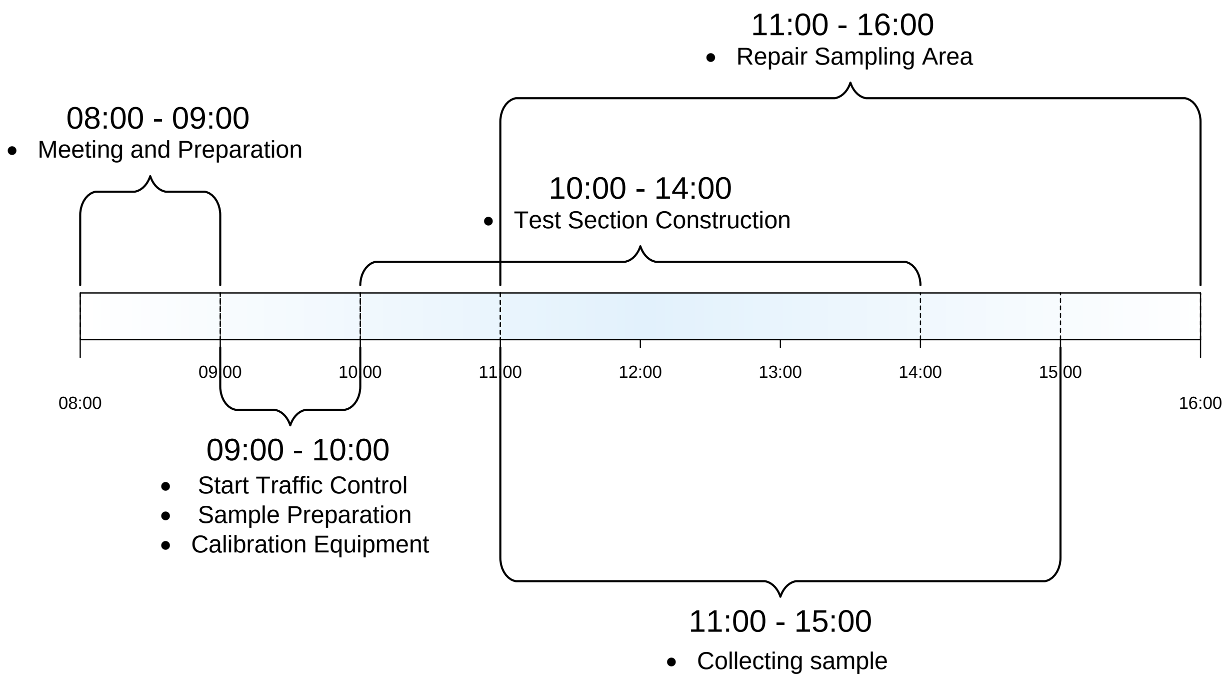

Figure 55 Field construction timeline

7.3 Team Organization

The available workers from the research and construction teams were divided according to responsibility, as diagrammed in the organizational chart shown in Figure 56. While most members of the construction crew were constructing the test sections, the research team members were overseeing the construction process to ensure that all sections were built according to the specifications set forth in the design plan. After the construction procedure was completed and the test sections were adequately rolled, the sample collection and laser scanning began for the sampling and monitoring sections, respectively. The laser scanning team was responsible for scanning the sections in the areas designated for monitoring. The laser setup and operation was handled by the research team, and moving the laser from location to location was performed with the help of the NCDOT research team. Details of the laser scanning procedure are discussed later in this document.

While one group handled the laser scanning of the monitoring area, another group simultaneously collected samples. After all the scanning and sample collection tasks were completed, the final step was for the construction team to repair the sample area.

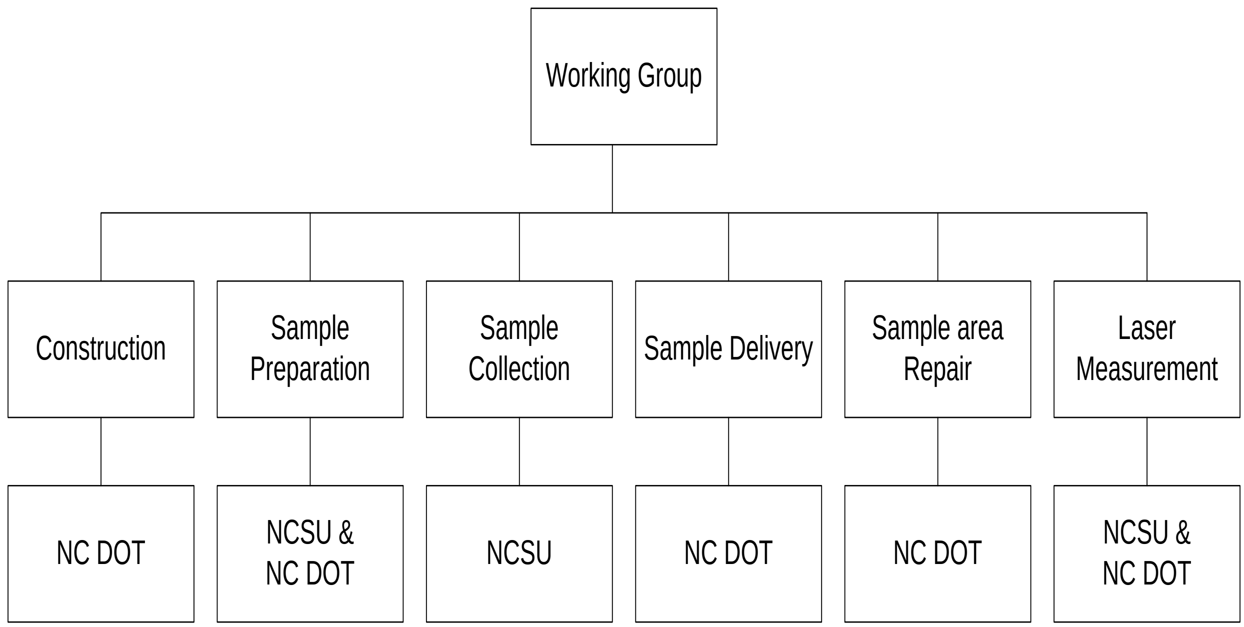

Figure 56 Worker organizational chart

7.4 Sample and Sampling Area Preparation

The procedure for sampling includes preparation of the felt disks, Vialit plates, and wood boards for the respective test sections. This preparation was completed in the days prior to the arrival of the research team at the field location. A team placed high quality ground paper onto the road surface and taped down the felt disks and Vialit plates, as illustrated in Figure 57, to prepare the sample area for the day of construction.

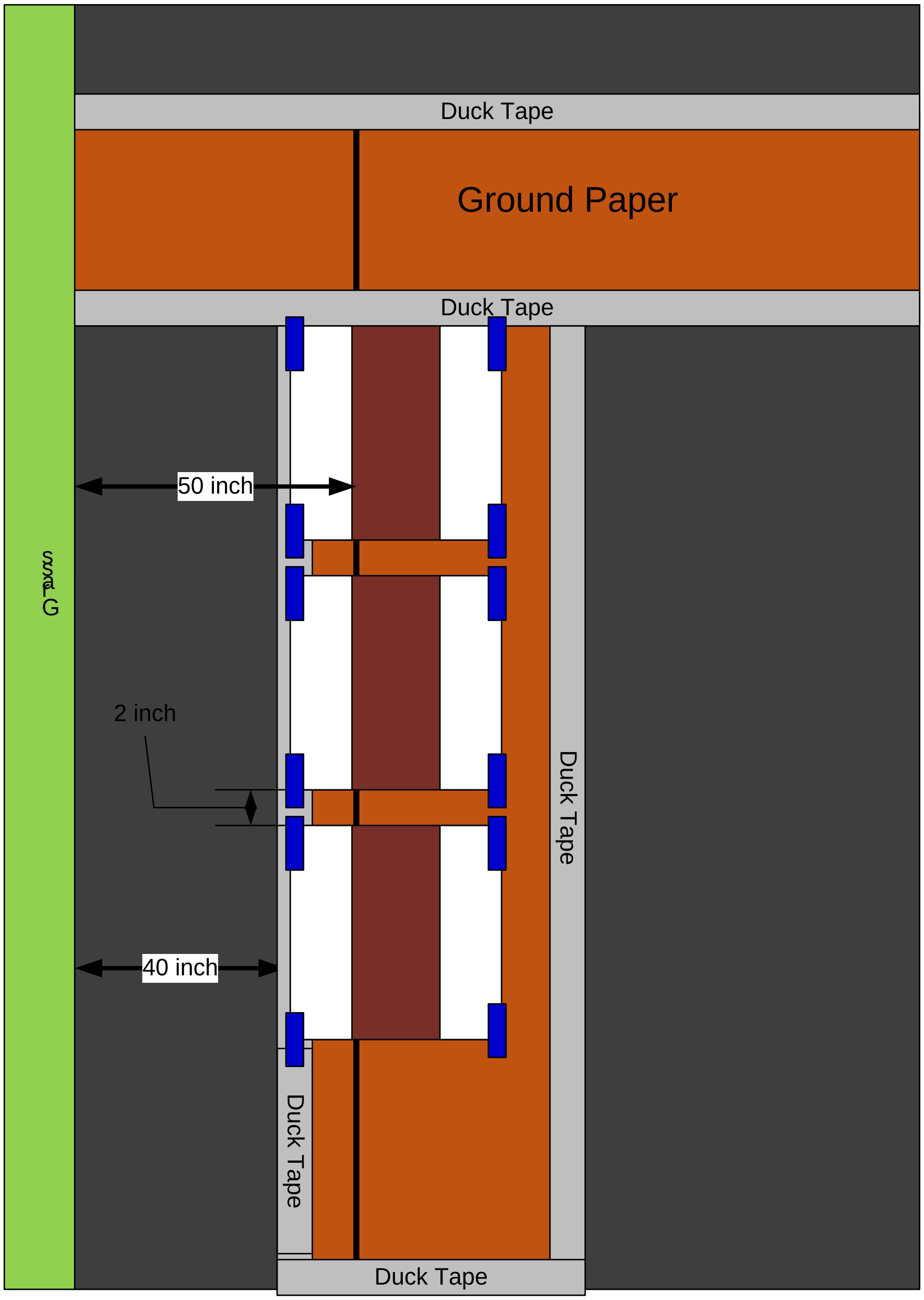

Figure 57 Sample template mounting procedure

The procedure that was used by the sample area preparation team is illustrated in Figure 57 and is as follows:

1. Tape the ground paper onto the existing pavement. The ground paper thus forms a T-shape in each section.

2. Mark a straight line on the ground paper that runs the entire length of the sampling area. This line will be 50 inches (in width) from the edge of the pavement, and will mark the position of the felt samples.
3. Align the sample section of the sample template with the straight line.
4. Affix the template with blue-tape (not duct tape) onto the ground paper.
5. Leave at least 2 inches between each sample.
6. Continue this procedure until all the samples have been affixed to the ground paper in the sampling area of each section

7.5 August 19, 2008 Field Construction

The field construction plan for the first day of construction was to build eight test sections on a high volume road. The specifications for each test section are detailed below in Figure 58, Figure 59, and Figure 60.

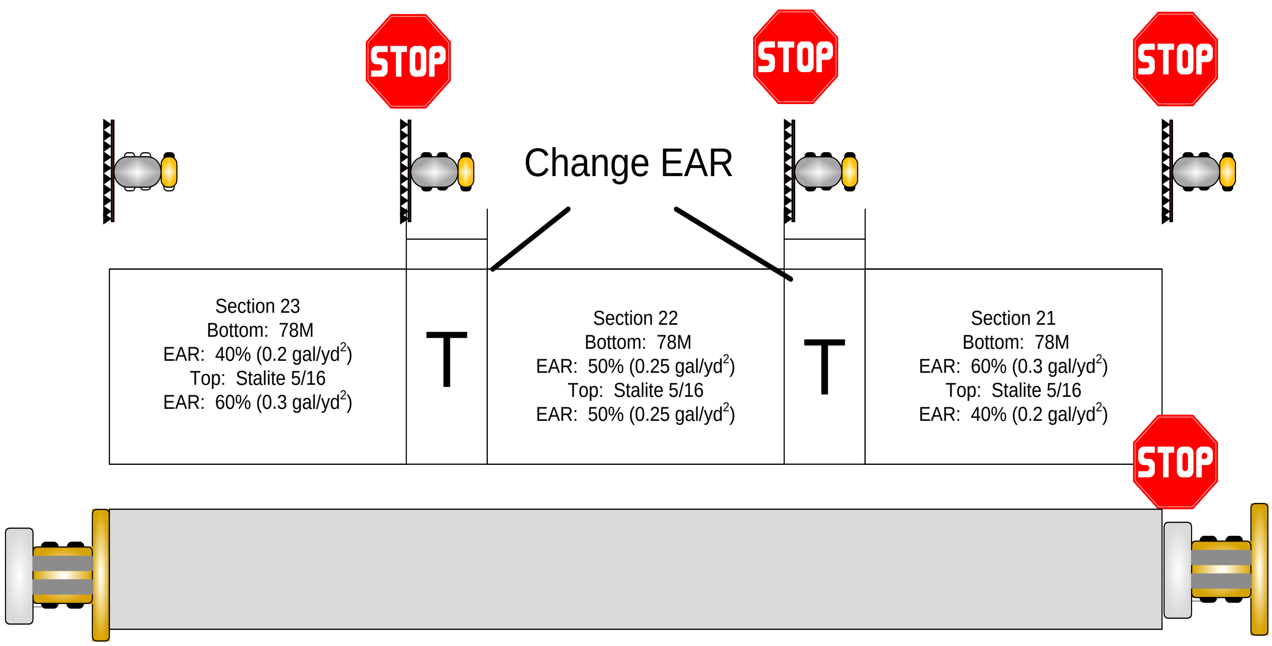

Figure 58 Test section specifications for Sections 23, 22, and 21 (displayed in actual construction order).

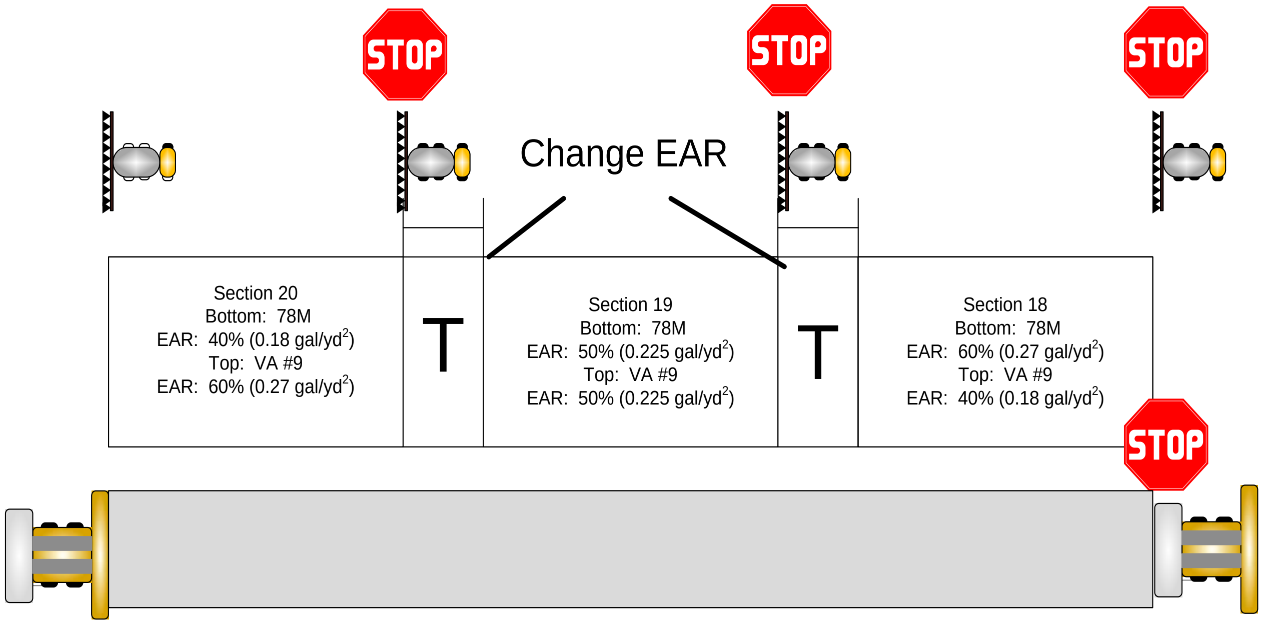

Figure 59 Test section specifications for Sections 20, 19, and 18 (displayed in actual construction order)

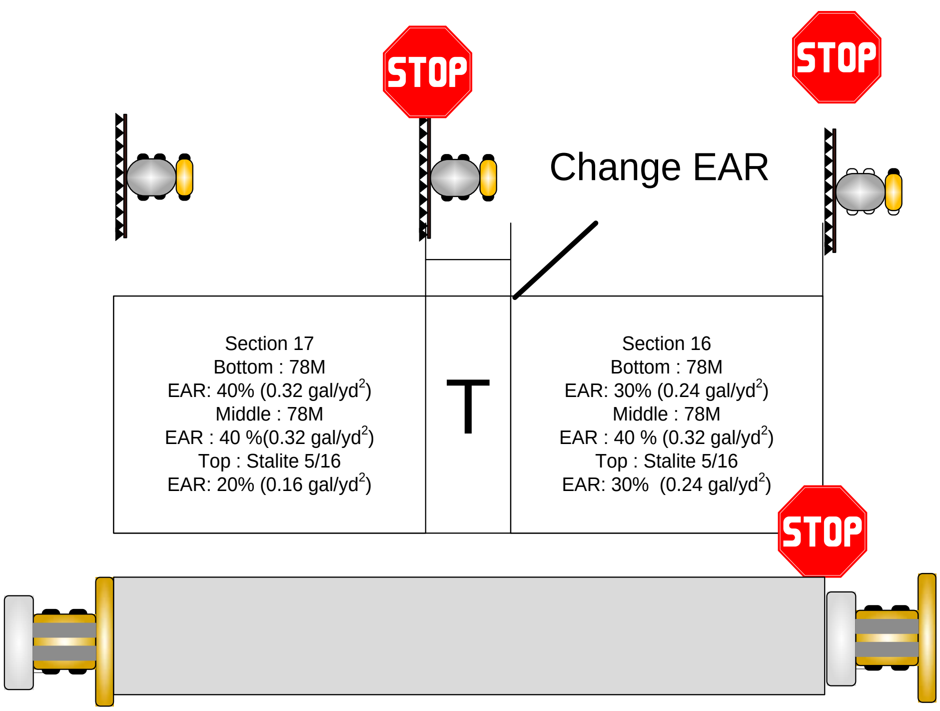

Figure 60 Test section specifications for Sections 17 and 16 (displayed in actual construction order)

Construction Step 1 Section 23 to Section 21 Double Seal with Stalite and 78M	Construction Step 2 Section 20 to Section 18 Double Seal with VA #9 and 78M	Construction Step 3 Section 17 to Section 16 Triple Seal with 78M/78M/Stalite

Figure 61 Construction sequence for Sections 16 - 23

The first three test sections constructed at the high volume location are split seal sections that used granite 78M aggregate on the bottom layer of the seal and lightweight aggregate on the top layer of the seal. All the sections had the same AAR for the granite aggregate (22 lbs/yd^2) and lightweight aggregate (11 lbs/yd^2). The variable for the three sections is the emulsion ratio that was used between the two layers. That is, for all three sections, an optimal total EAR of 0.5 gal/yd^2 for double seals was used, but the percentage of distribution of the total emulsion into the top and bottom layers changed from 40%/60% to 50%/50% to 60%/40% (with the first number representing the top layer).

The next three test sections contained 22 lbs/yd^2 of granite 78M aggregate on the bottom layer of the seal, and Virginia #9 aggregate on the top layer of the seal. Like the first three sections, these sections had emulsion distribution ratios that varied between 40%/60%, 50%/50%, and 60%/40%.

The final two sections constructed on this particular day were triple seal sections. These sections contained the same AAR and type between the seals, but varied the emulsion distribution ratio from 40%/40%/20% to 30%/40%/30%. The emulsion percentages are based on an optimal total EAR of 0.8 gal/yd^2.

7.6 August 25, 2008 Field Construction

The procedure followed on the second day of construction is identical to that of the first day, except the sections were single seals as opposed to the double and triple seals constructed on the first day. The section specifications and construction sequence of the three test sections are displayed in Figure 62, Figure 63, and Figure 64, respectively.

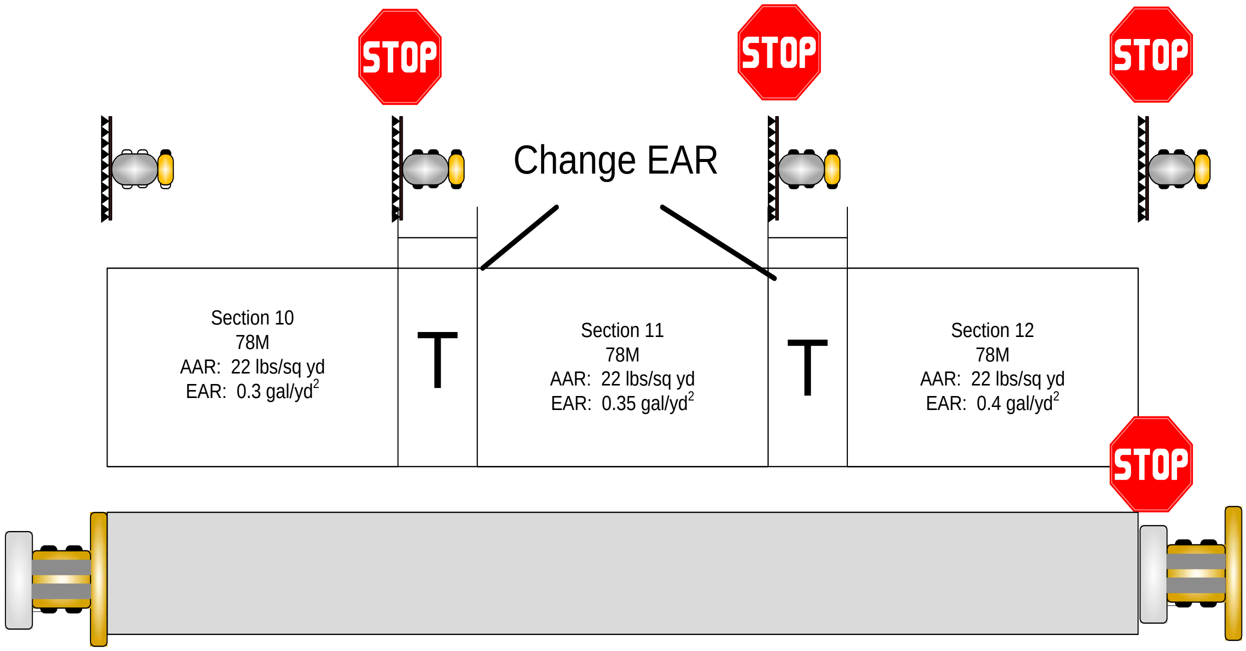

Figure 62 Test section specifications for Sections 10, 11, and 12.

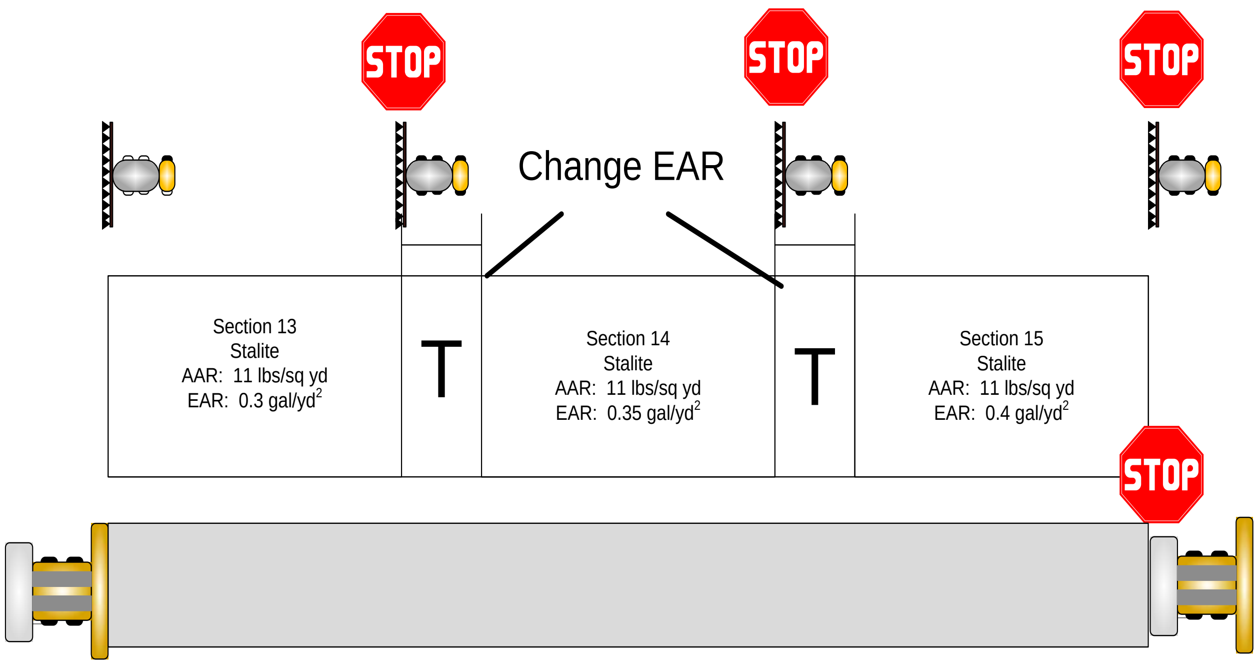

Figure 63 Test section specifications for Sections 13, 14, and 15.

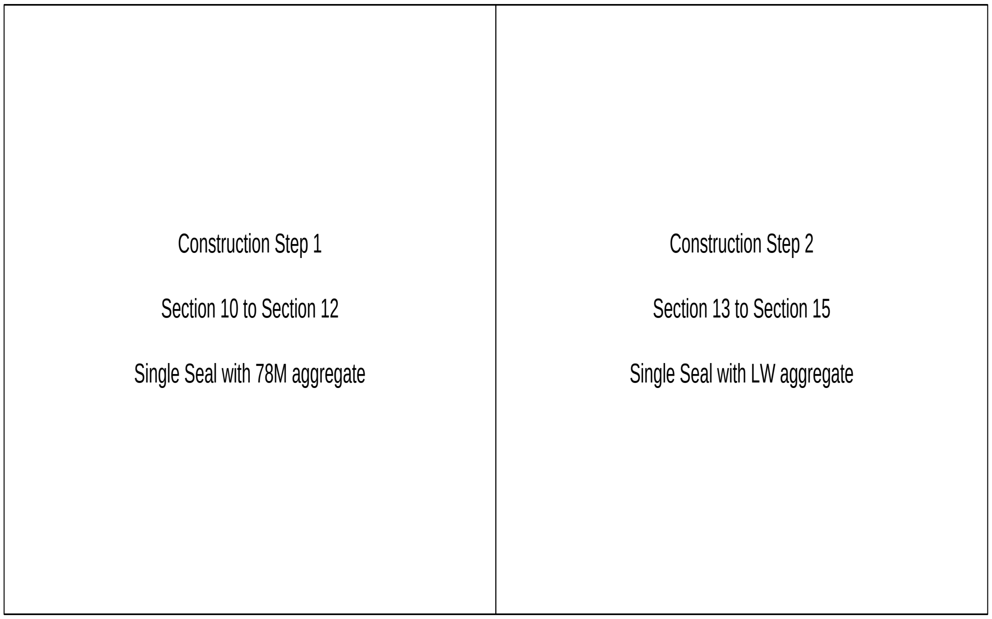

Figure 64 Construction sequence for Sections 10 - 15

The test sections were comprised of three granite 78M aggregate single seal sections and three lightweight aggregate single seal sections. These sections were designed and constructed to provide a valid comparison between the performance of the single seals at low and medium volumes. At a later date, six single seals (of the same specifications) were built on a medium volume road in order to make that comparison and enhance the accuracy of the void reduction model that the research team will create for the project. The construction of these sections, in addition to three double seal sections to be used also for comparison of the volumes, is described below.

7.7 September 22, 2008 Field Construction

The construction procedure for the third and final day of field construction follows that of the first two days, except that these test sections were constructed on a medium volume road with an ADT of approximately 4,500 vehicles. The single and double seal sections constructed on this day are compared to the similar sections that were created on previous days.

Another change from the procedure of the first two days is that the air temperature was 5 to 8 degrees cooler on this date than the previous two construction days. It was important to construct the final test sections on a day when temperatures were similar to that of the first two days of construction. So, although the temperature on the third day of construction was a few degrees lower than that of the first two days, the research team believes that the temperature difference was not significant enough to hinder the analysis and comparison of the sections.

The specific test section specifications for the sections constructed on the third construction day are detailed in Figure 65, Figure 66, and Figure 67.

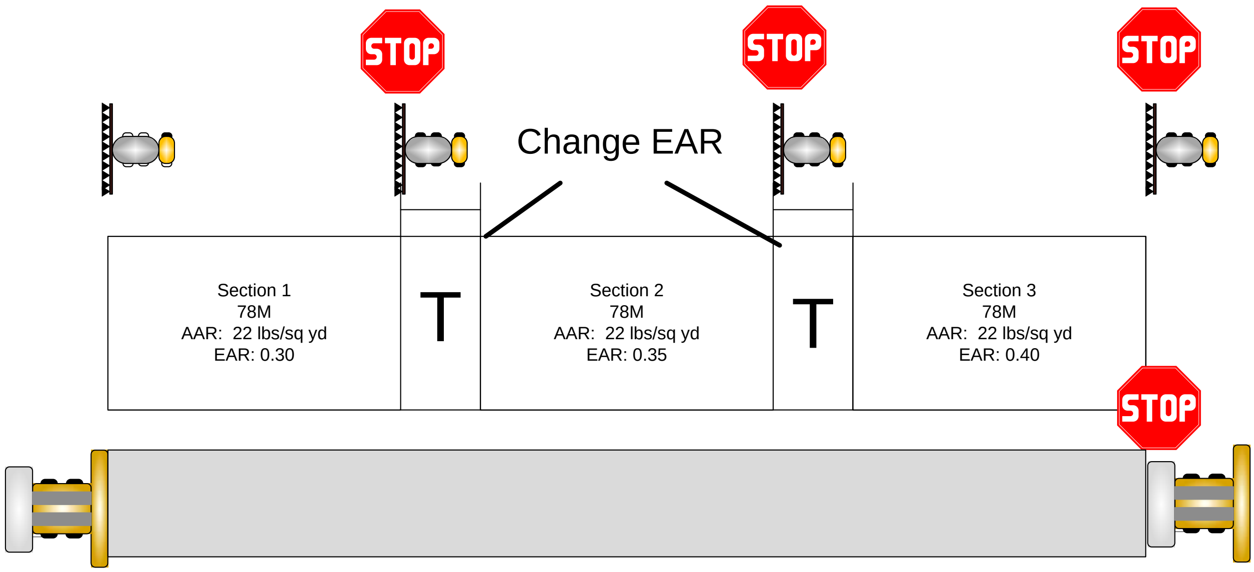

Figure 65 Test section specifications for Sections 1, 2, and 3

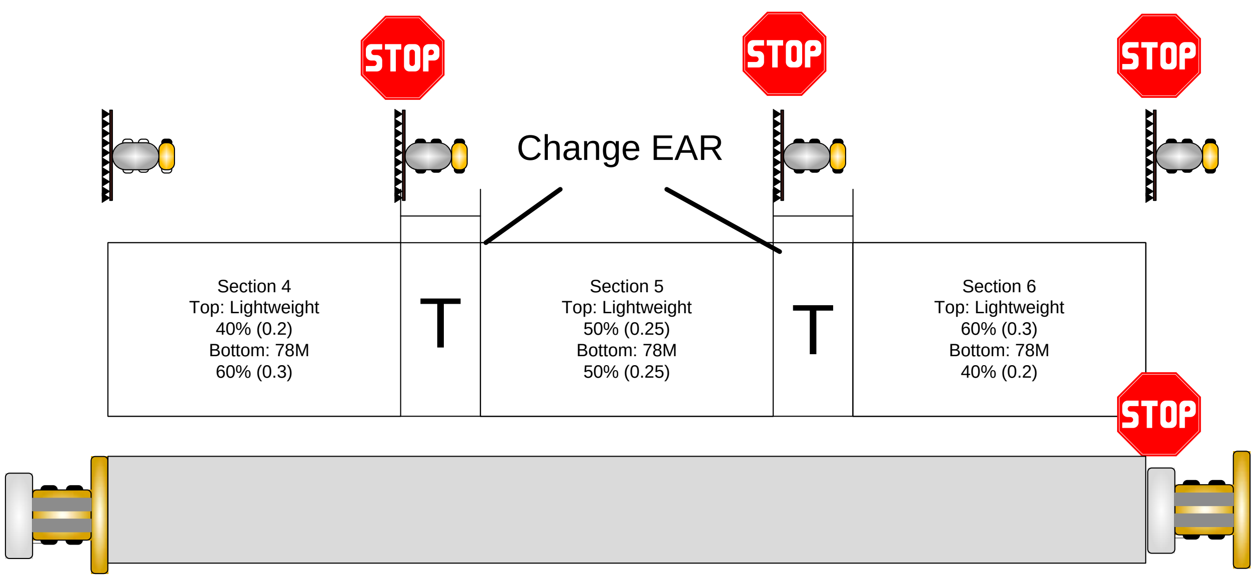

Figure 66 Test section specifications for Sections 4, 5, and 6

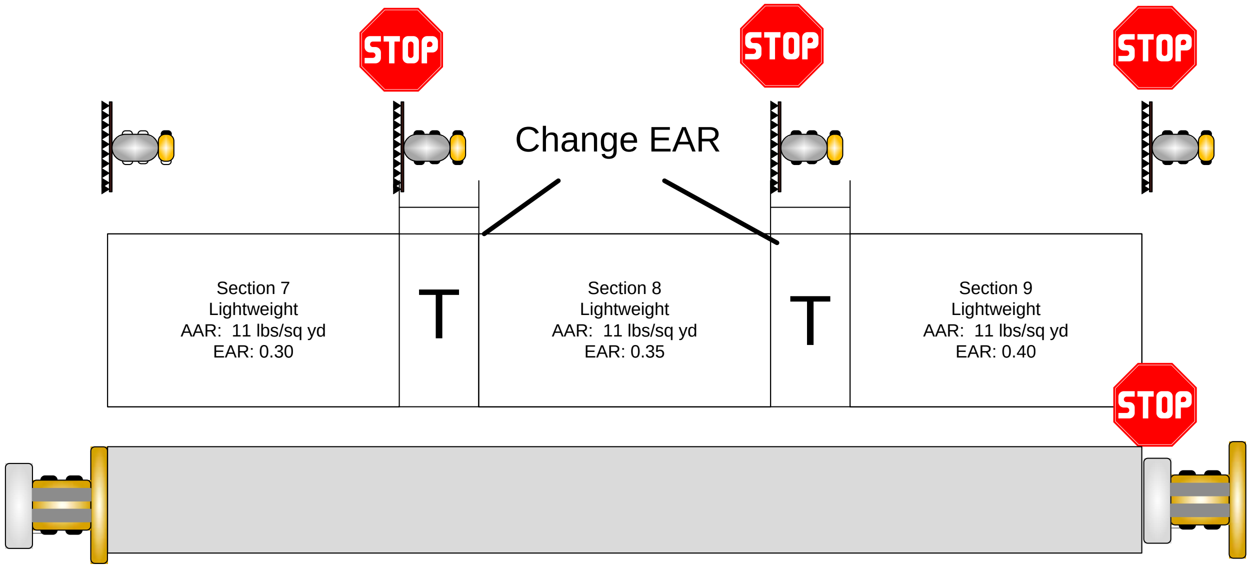

Figure 67 Test section specifications for Sections 7, 8, and 9

The first three test sections constructed are single seal sections with 78M granite as the aggregate type. These sections are followed by three double seal sections with 78M granite as the bottom layer and lightweight aggregate as the top layer. The final three sections are single seals that used lightweight as the aggregate type. The sequence displayed in Figures 68, 69, and 70 allows the aggregate spreader to spread Sections 1 through 6 continuously with 78M granite aggregate, and then spread Sections 3 through 9 continuously with lightweight aggregate. The research team determined this procedure to be the optimal construction sequence for these particular test sections.

The EARs for the single seal sections (Sections 1-3 and 7-9) vary from 0.3 to 0.4 lbs/yd^2. The double seal sections (Sections 4-6) vary between 40/60, 50/50, and 60/40, just like the double seals from the first day of construction. Specific rates for the double seals are displayed in Figure 66.

7.8 Field Sample Collection Procedure

The next step in the timeline is to collect the samples from the sampling section. The task of removing the samples from the ground was performed by the NCSU research team. After removing the samples from the ground, the sides were cleaned, and the samples were placed on wood boards for stable transport. The samples were then transported to racks on a box truck and taken back to the research laboratory for testing.

7.9 Field Laser Scanning Procedure

In order to monitor the voids at the test sections effectively over the course of one year, the laser profiler created by the research team was employed to scan the monitoring area. The information obtained from these scans was analyzed to determine the reduction in voids as a function of traffic load over the course of the year.

8. FIELD PERFORMANCE EVALUATION

8.1 Field Traffic Analysis and Conversion

Traffic data were collected in Franklinton, NC by the NCDOT at the three locations where field test sections were constructed: NC 96 south of SR 1632/Canady Drive, NC 96 south of SR 1705, and SR 1623 east of NC 96. Data were collected using traffic counters for eight twenty-four hour periods each quarter. Wheel path data from the field were obtained specifically in the lane where the test sections were constructed for each location. Field traffic count data for each vehicle class were converted into equivalent wheels based on the FHWA vehicle axle factors shown in Table 16.

Table 16 FHWA Average Axle Configurations

FHWA Class	Count of Class	Sum of Axles	Avg. # of Axles
4	39015	85277	2.186
5	144920	289840	2
6	51154	153462	3
7	3194	12776	4
8	74334	273274	3.676
9	440740	2203700	5
10	5065	30575	6.037
11	17305	86525	5
12	7600	45600	6
13	1049	7343	7

For the traffic counts, the number of vehicles as well as the class of vehicles were recorded. Figure 68 shows the 13 FHWA vehicle classes used in the traffic study and subsequent research analysis.

Vehicle weights were not recorded for the traffic study performed by the NCDOT because such data were deemed unnecessary for chip seal performance analysis. Essentially, because chip seal failure is not based on structural strength, the specific weight of each vehicle was not deemed worth the significant costs associated with collecting that information. However, because aggregate loss is the main performance criterion for chip seals, it is worth considering nonetheless that heavy vehicles serve to further embed aggregate, just as they also contribute to aggregate loss as their wheels pass over the chip seal.

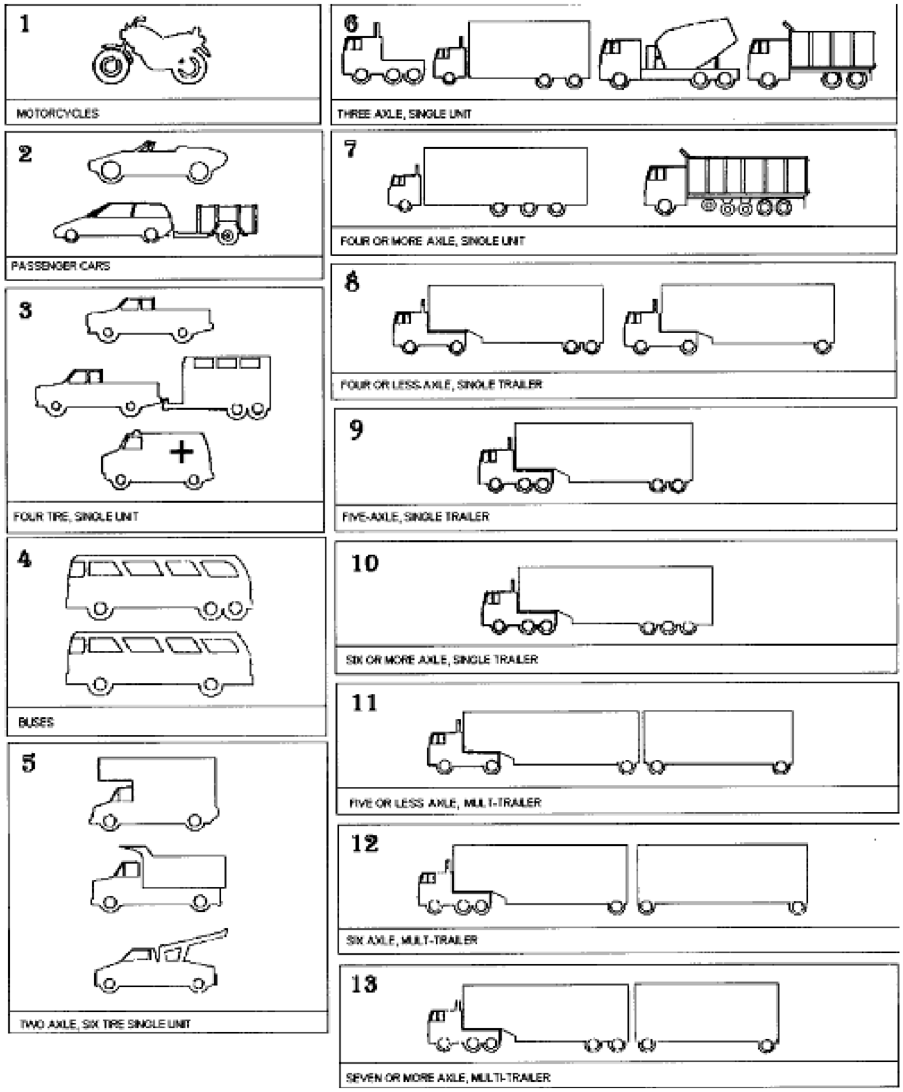

Figure 68 FHWA vehicle class information

8.2 Field vs. MMLS3 Traffic Load MPD Graphs

Adjustments to the field traffic loading information needed to be made in order to compare those data directly to MMLS3 traffic loading information (which involves units of wheel passes). This adjustment was made based on the traffic class axle conversion rates discussed in Section 8.1. Additionally, some field samples were tested using the MMLS3 for time periods longer than normal aggregate loss test in order to ensure that the MPD curves remained near an asymptotic value after two hours of MMLS3 loading.

Therefore, the quarterly traffic count information taken at the test section construction locations for a year were used and converted from vehicles (in separate classes) to equivalent wheel passes. This conversion was made using the average number of axles for each FHWA class, as displayed in Figure 68. For each axle on a vehicle, a single wheel will travel across any spot on the chip seal section. Therefore, each axle equals one equivalent wheel pass when considered from a static location for the purposes of this analysis. Therefore, by multiplying the number of vehicles that pass the traffic counter for each FHWA vehicle class by that class's corresponding average number of axles shown in Table 16, the average number of equivalent wheels that cross the section can be found. The average number of axles per FHWA vehicle class used for the conversion was provided by Kent Taylor of the NCDOT.

Thus, Figure 69 through Figure 79 show the changes in the MPD as a function of the equivalent wheel pass loads for each chip seal field-trafficked section as well as the MMLS3-trafficked samples from those same sections.

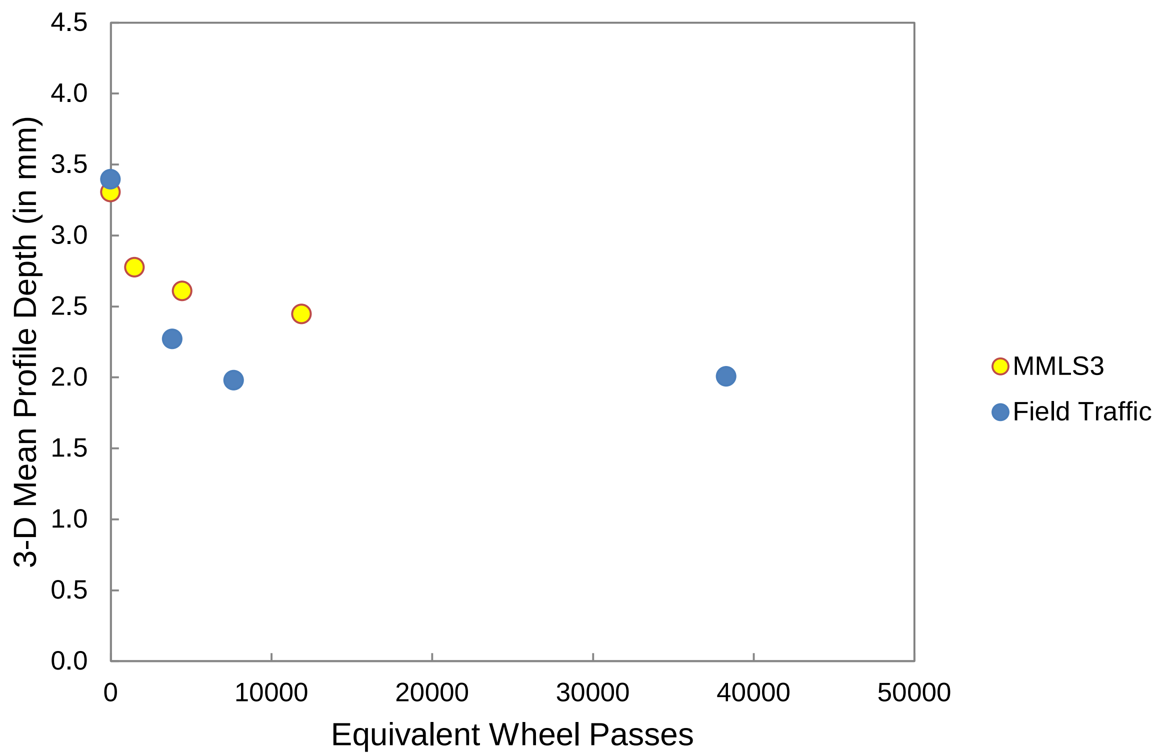

Figure 69 Section 2: granite 78M aggregate

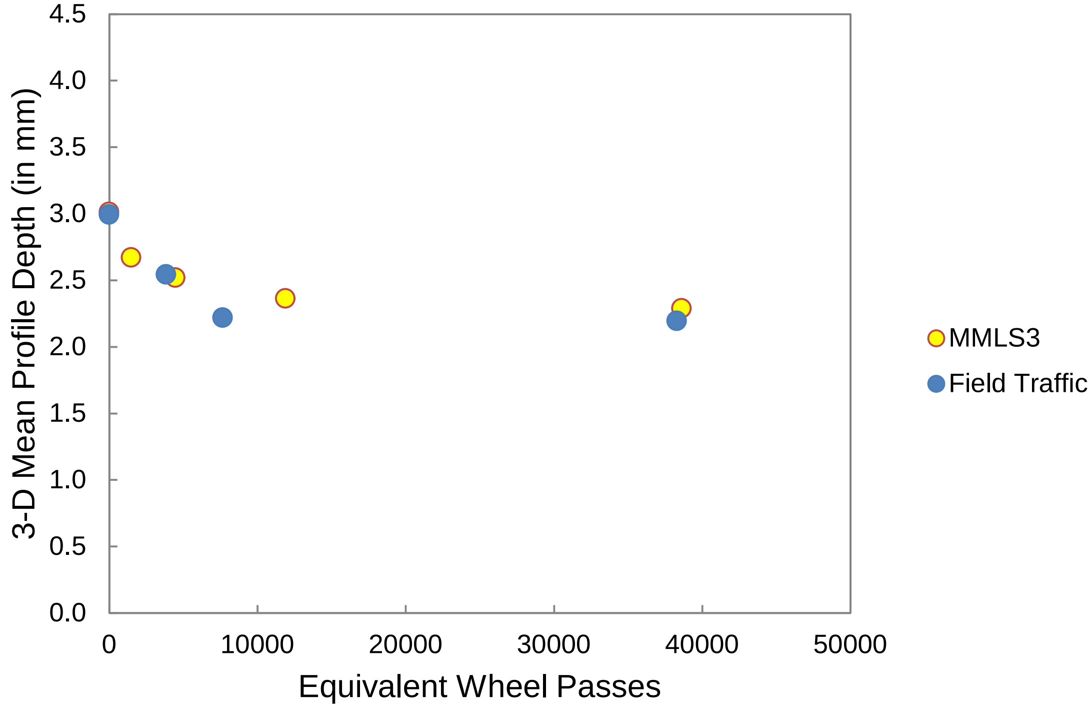

Figure 70 Section 3: granite 78M aggregate

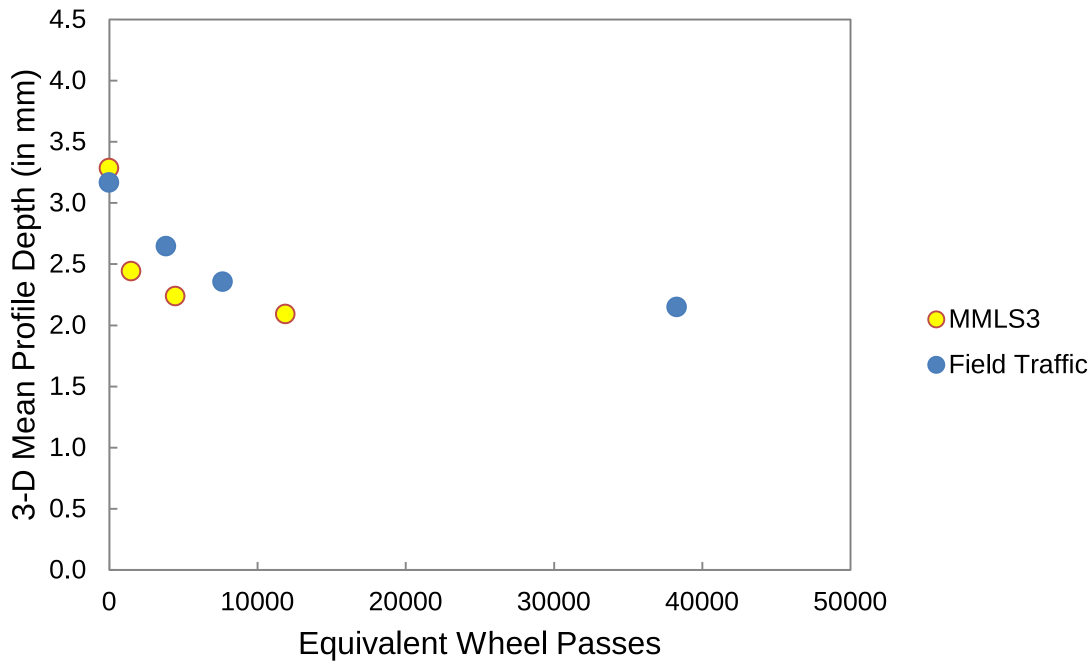

Figure 71 Section 7: lightweight aggregate

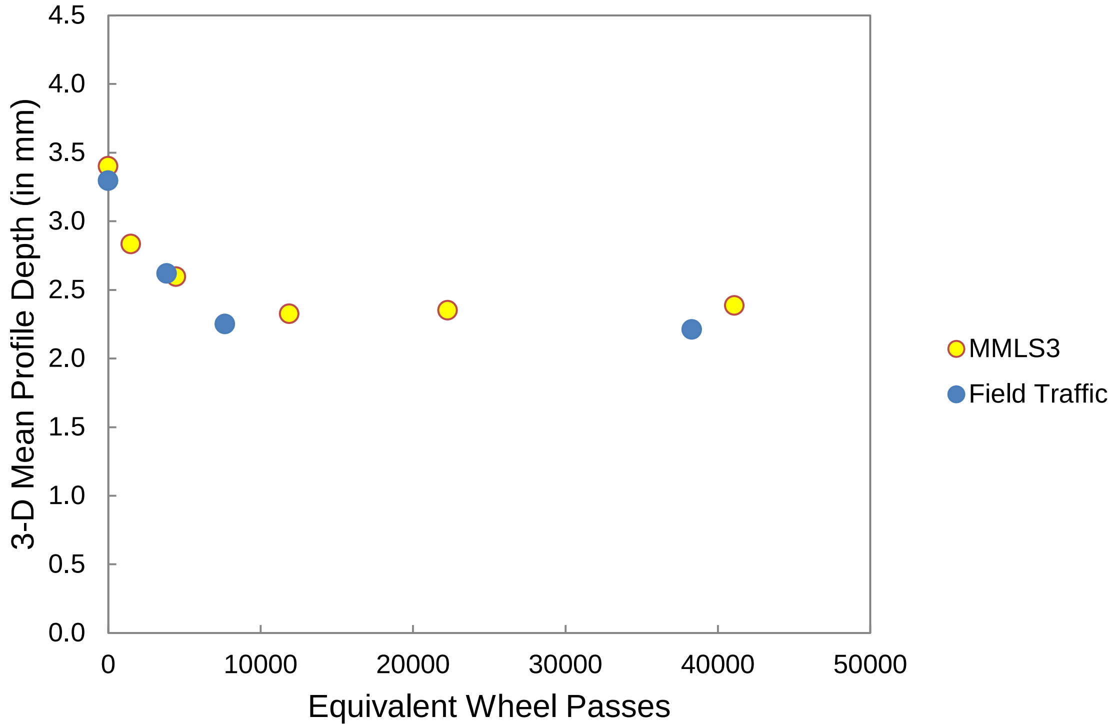

Figure 72 Section 8: lightweight aggregate

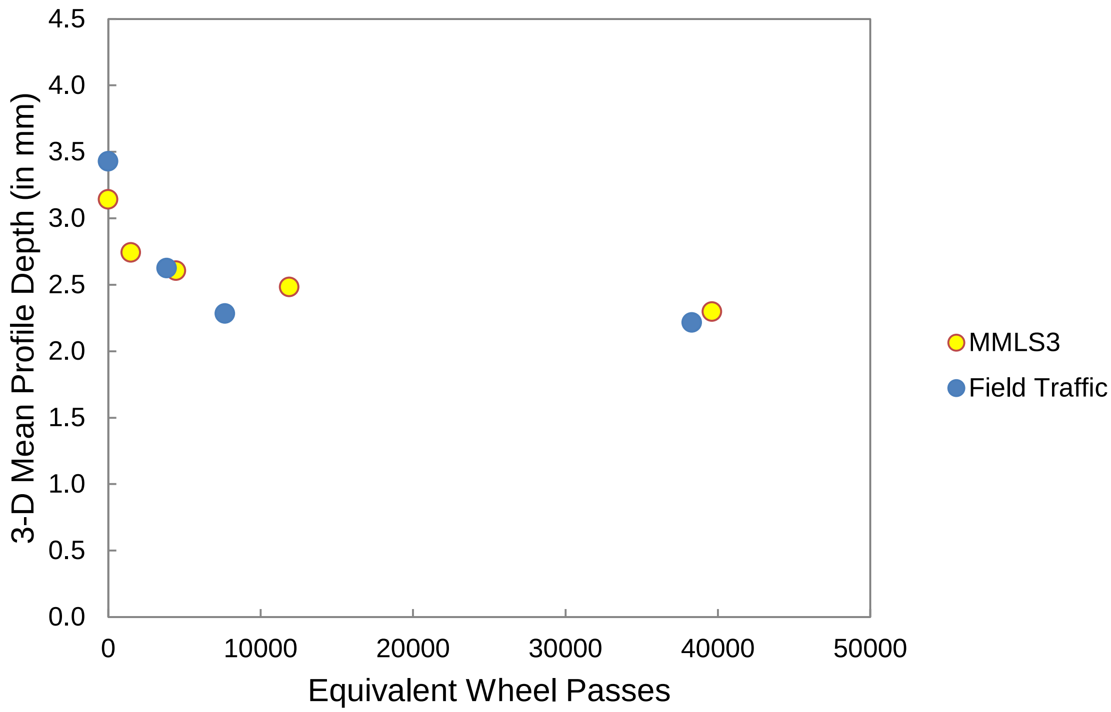

Figure 73 Section 9: lightweight aggregate

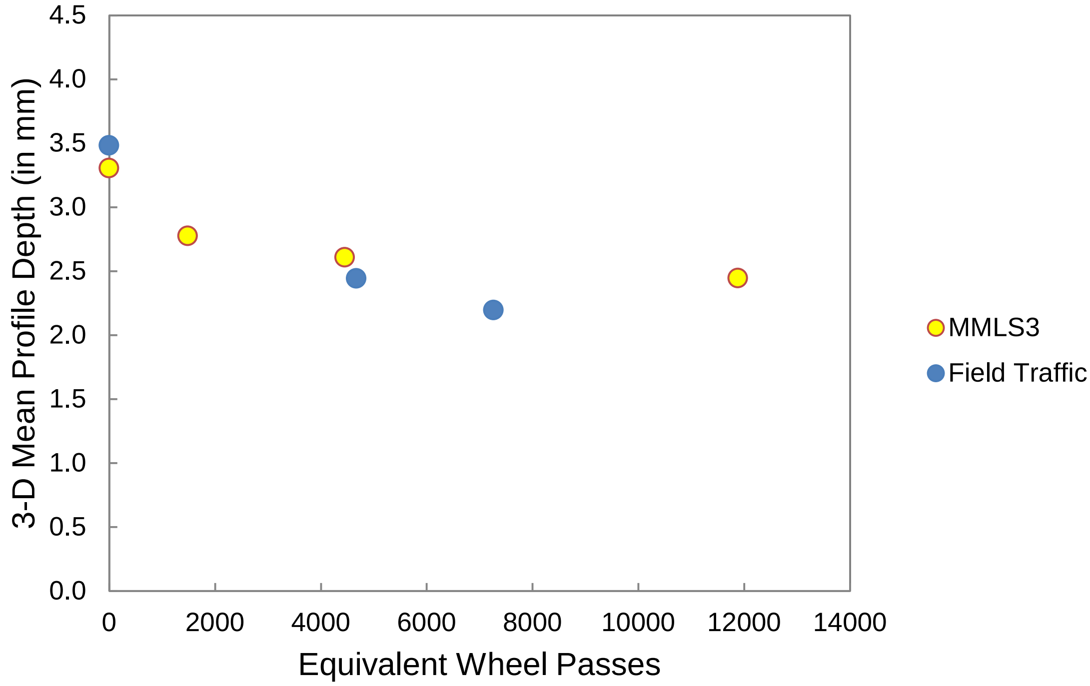

Figure 74 Section 10: granite 78M aggregate

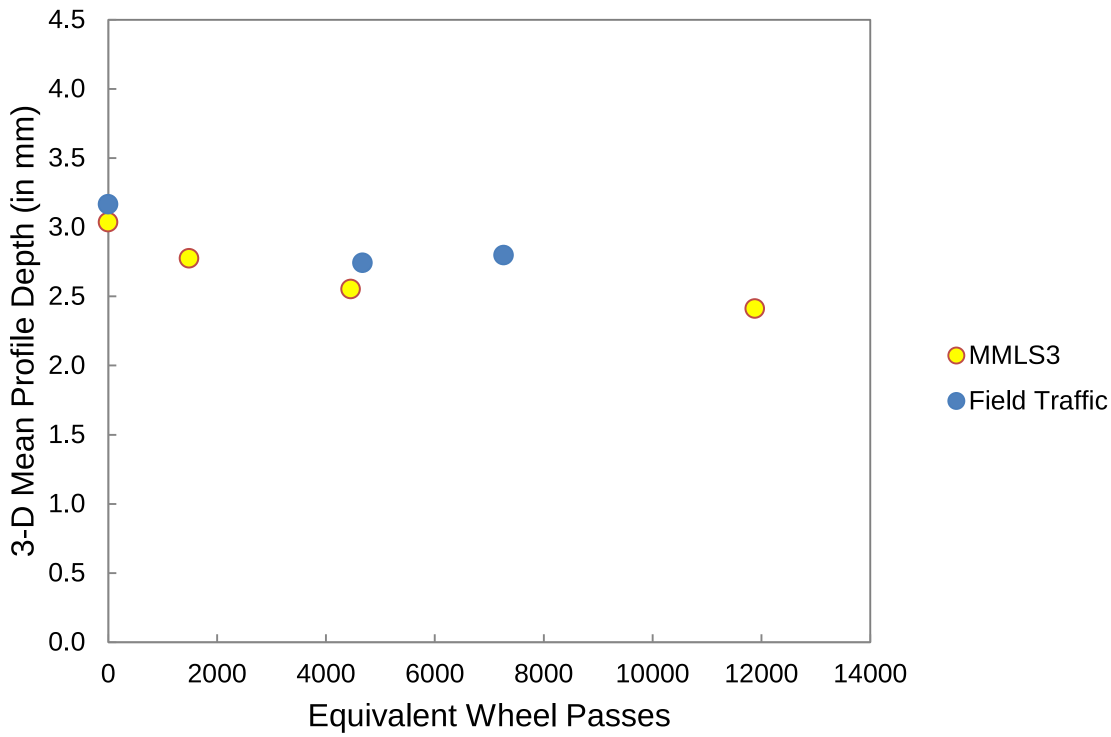

Figure 75 Section 11: granite 78M aggregate

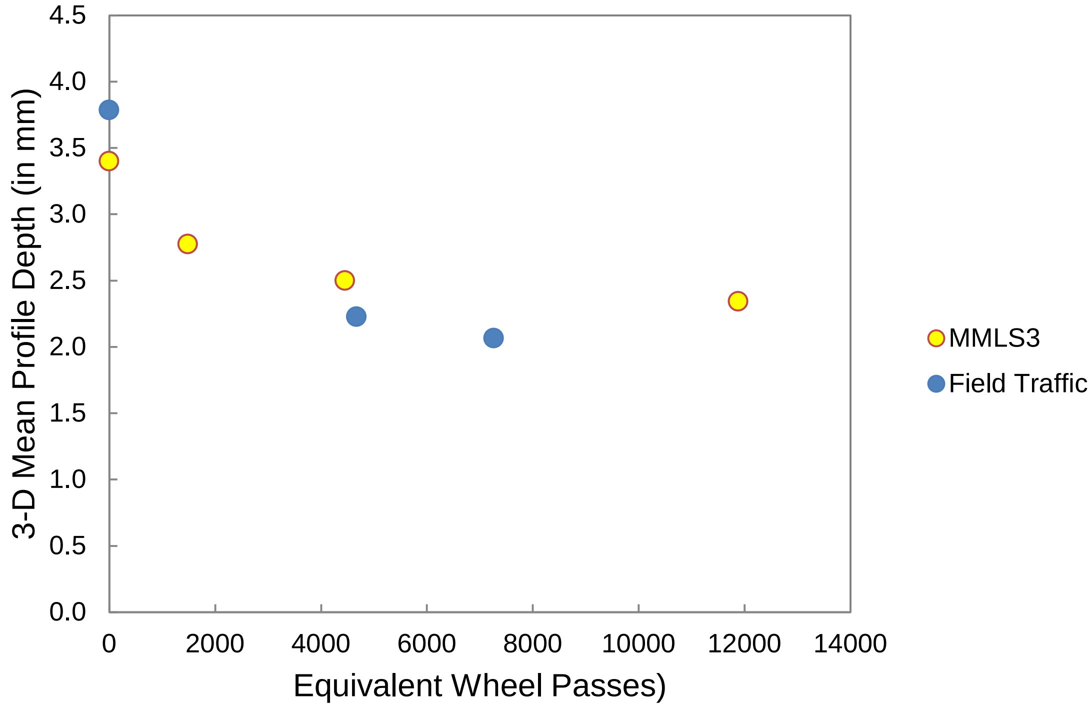

Figure 76 Section 12: granite 78M aggregate

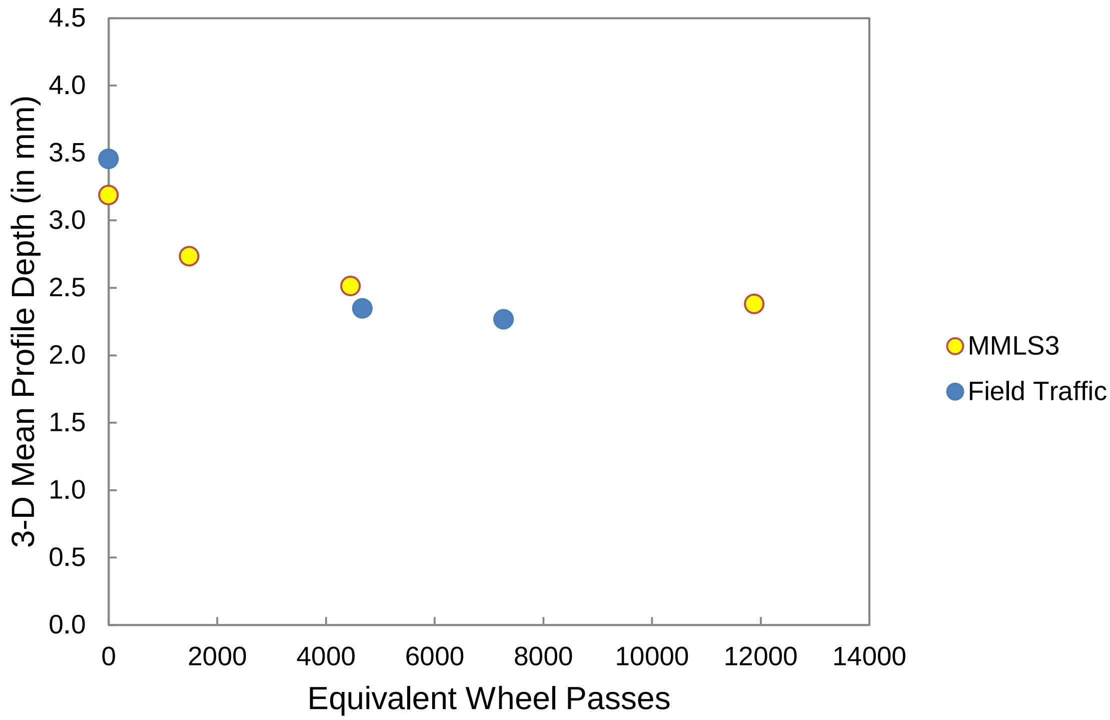

Figure 77 Section 13: lightweight aggregate

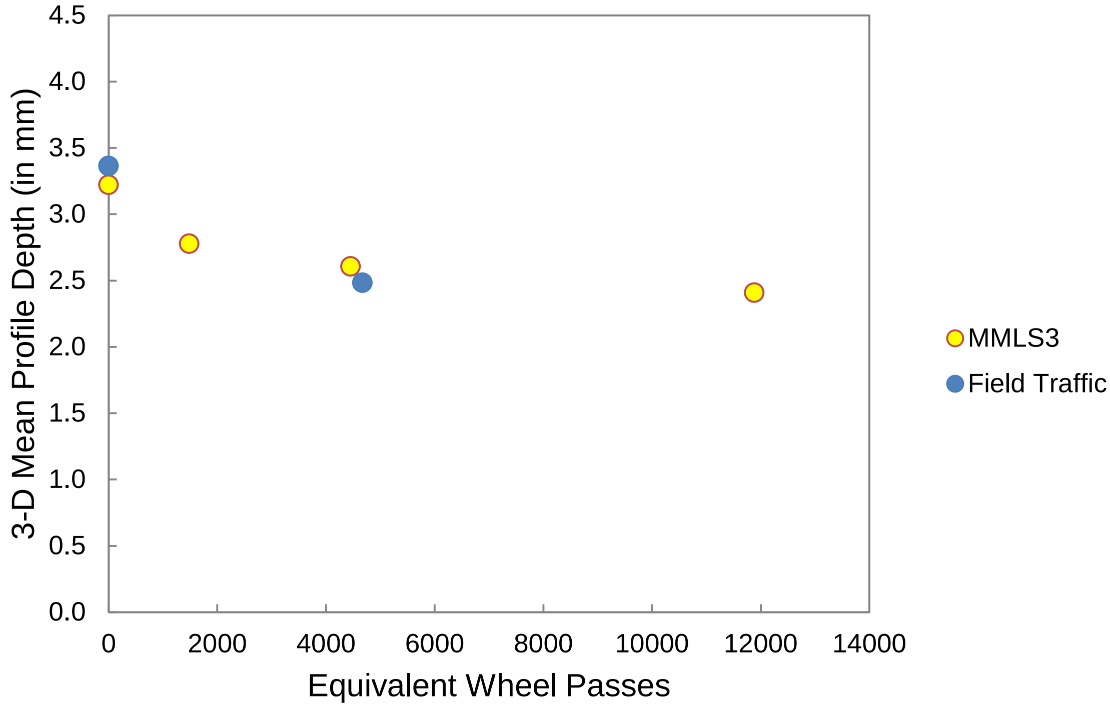

Figure 78 Section 14: lightweight aggregate

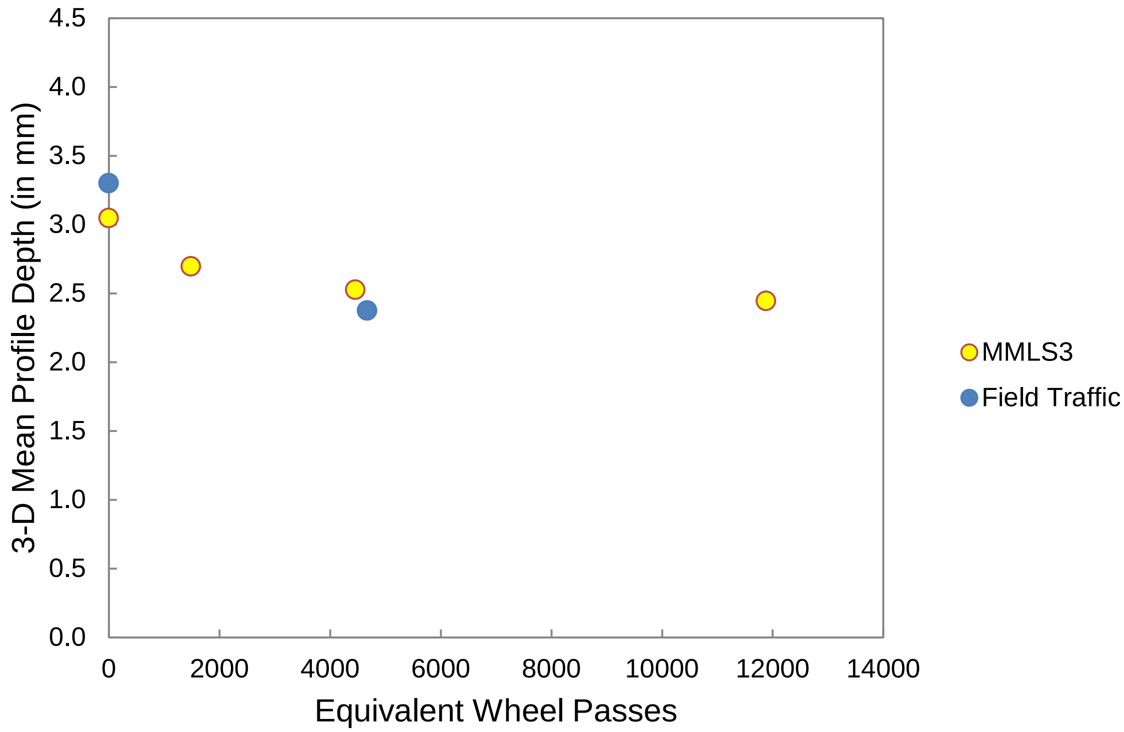

Figure 79 Section 15: lightweight aggregate

It should be noted that in almost all the sections (Figure 69 through Figure 79), the MPD curves for the field traffic-loaded sections descend faster initially (from the initial scan at 0 traffic to the second and third data points) than those of the MMLS3-loaded specimens. This occurrence most likely has to do with the difference in weight of the MMLS3 and actual traffic (which includes trucks and varying speeds). The speed at which the MPD curve changes is a function of the field traffic rate, but additionally, the rate has an effect on the final MPD value and how close that value is to the final MMLS3-trafficked MPD values. In almost all the medium volume sections, the final field-trafficked MPD value is extremely close to the final MMLS3 lab-trafficked MPD value. This finding indicates that the MMLS3 traffic load translates similarly to the medium volume field traffic rates. Also, because the complete amount of the field MPD change occurs within the first few days to a week, it can be said that a two-hour MMLS3 test simulates the first week of medium volume traffic. Likewise, this finding validates the aggregate loss findings that almost all loss occurs within the first 10,000 MMLS3 wheel loads (which is consistent with that seen in the field in the first few days, or 10,000 equivalent wheel loads). These findings affirm the research team's belief that the MMLS3 traffic loading results provide a reasonable prediction as to the changes in MPD and other performance parameters (which are related directly to embedment depth, as shown in the Delrin MPD vs. embedment depth study in this document) as the chip seal is traffic-loaded over time.

8.3 Long-Term MMLS3 Load Analysis Using Field Samples

Extended MMLS3 testing was performed in order to determine ways that the MPD changes over much longer periods of time than the normal two-hour MMLS3 test. The research team wanted to ensure that the two-hour MMLS3 testing was adequate to capture the final MPD as it reaches its asymptotic value. The results of that testing are shown in Figure 80. Figure 80 shows the average of multiple replicate field specimens that were MMLS3 traffic loaded, and the changes in the MPD during that traffic loading period. Under normal aggregate loss testing, samples are loaded using the MMLS3 for two hours (or the equivalent of 11,880 wheel passes at 990 wheel passes every 10 minutes). From Figure 80, it can be seen that after 11,880 wheel passes, the MPD no longer declines and starts to stabilize. Essentially, any MMLS3 traffic loading performed past two hours has little to no effect on the MPD parameter. This finding serves as justification that, with regard to MPD, the two-hour test used by the research team is adequate to capture the changes in embedment depth over the life of the chip seal surface treatment.

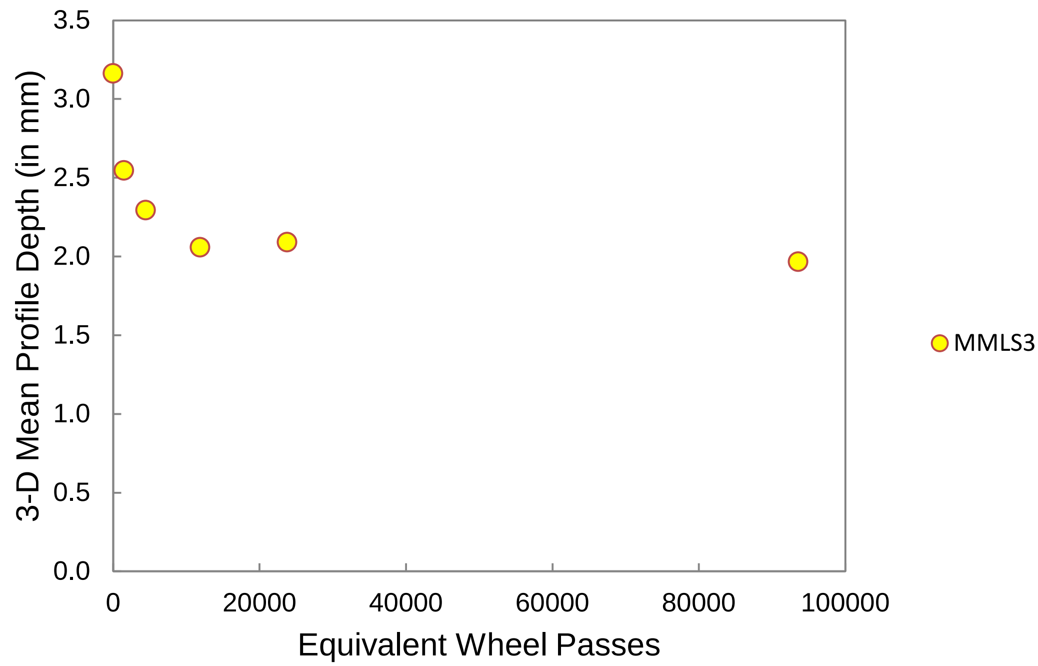

Figure 80 Section 1 Granite 78M aggregate long-term MMLS3 loading analysis

8.4 Field Section Performance Summary

In addition to the field MPD performance displayed in Figure 69 through Figure 79, evaluation of the field performance of the constructed chip seal sections involved a visual inspection of the chip seal sections two years after their initial construction to ascertain how the sections performed under field traffic loading and variable environmental conditions. The evaluation was performed on all of the single seal sections constructed of both lightweight and granite 78M aggregate types and for both low and medium traffic volumes. With regard to the field inspection, Mr. Averette Moore, a NCDOT field construction supervisor who constructs chip seal surface treatments and performs visual pavement inspections statewide, provided his expertise and experience in evaluating the condition of the given chip seal section (discussed hereafter). Each section was inspected visually for the estimated percentage of embedment as well as whether bleeding or aggregate whip-off occurred in the sections.

8.5 Section 1 through Section 3 – Granite 78M/Medium Traffic Volume

The first sections analyzed are medium volume (ADT of 4,500 vehicles) single seal sections constructed of granite 78M aggregate and CRS-2L emulsion. The chip seal design rates, aggregate loss, and visual observation comments are summarized in Table 17. The measured EARs and AARs were determined by oven-burning field samples extracted after chip seal construction in the field. During this process, the initial weight is measured, and the sample is burned in the oven, and the emulsion is burned from the sample. From this process, the emulsion weight can be determined, and the remaining aggregate can be measured to determine the aggregate application weight. This test was performed for multiple samples, and the results were averaged to determine the measured EAR and AAR for the respective sections.

Table 17 Performance of Sections 1-3 with Granite 78M Aggregate

Section	Visual Survey Condition	Target EAR (gal/yd^2)	Measured EAR (gal/yd^2)	Measured AAR (lb/yd^2)	% Aggregate Loss
1	Light Bleeding (not caused by whip-off); High Embedment Depth ~90%	0.30	0.24	19.42	5.4
2	Light Bleeding; Lower Embedment Depth ~75-80%	0.35	0.23	22.59	3.9
3	Light Bleeding; High Embedment Depth ~95%	0.40	0.29	22.2	2.6

In the evaluation of Sections 1 - 3, it was found that each section exhibited high embedment. Although aggregate whip-off did not appear to be a problem for any of the sections, each section exhibited some light bleeding in the wheel path, which can be seen in Figure 81 (a) and Figure 83 (a) where the reflection of the sun can be seen on the emulsion surface. Section 2 does not exhibit this bleeding as heavily (Figure 82 (a)). It should be noted from Table 17 that the measured EAR for Section 2 is the lowest of the three sections and shows the lowest estimated embedment percentage. Also, although Section 1 shows a similar measured EAR, the measured AAR is significantly lower, i.e., 19.42 for Section 1 versus 22.59 for Section 2. Therefore, Section 2 is the driest of the three sections and the only section that shows good embedment without bleeding. Therefore, it can be said that Section 2 approximates the optimal performance rates. Additionally, the aggregate loss is low for all the sections; i.e., all sections exhibit aggregate loss below 5.5% when field samples were extracted immediately after the initial construction site and tested using MMLS3 traffic loading. Figure 81 (b), Figure 82 (b), and Figure 83 (b) display the surface texture of each section, which in turn shows the exposure depth and estimated embedment depth of aggregate.

Figure 81 Section 1: (a) Traffic direction view and (b) Texture depth view

Figure 82 Section 2: (a) Traffic direction view and (b) Texture depth view

Figure 83 Section 3: (a) Traffic direction view and (b) Texture depth view

8.6 Section 7 through Section 9: Lightweight Aggregate/Medium Traffic Volume

Sections 7 to 9 are single seals constructed using lightweight aggregate and CRS-2L emulsion and are trafficked at a medium volume rate (located on the same road as Sections 1 to 3). The results of the visual observation, aggregate loss testing, and burn testing (to determine the measured EARs and AARs) are summarized in Table 18.

Table 18 Performance of Sections 7, 8, and 9 with Lightweight Aggregate

Section	Visual Survey Condition	Target EAR (gal/yd^2)	Measured EAR (gal/yd^2)	Measured AAR (lb/yd^2)	% Aggregate Loss
7	Light Bleeding; 80-90% Embedment	0.30	0.22	8.79	4.8
8	75-80% Embedment	0.35	0.24	9.6	6.2
9	70% Embedment	0.40	0.24	9.25	5.5

Table 19 shows the relationship between the AAR and the aggregate loss for these sections where the EAR values are similar. Lightweight aggregate is slightly more sensitive to fluctuations in AAR because it is a less dense material than granite 78M aggregate. Therefore, a jump in AAR requires more actual aggregate than it would if it were a more dense (heavier) material. Additionally, with regard to bleeding, only Section 7 shows bleeding in the wheel path (as displayed in Figure 84), whereas Sections 8 and 9 (shown in Figure 85 and Figure 86, respectively) do not exhibit bleeding. Looking at the rates presented in Table 18, Section 7 shows the lowest measured AAR of the three sections, which appears to make it the most susceptible to bleeding. In addition, Section 7 shows the lowest amount of aggregate loss (4.8%), despite having a slightly lower measured EAR than the other two sections. This result is likely due to the fact that a low aggregate rate raises the likelihood of bleeding and decreases the likelihood of aggregate loss. Additionally, the surface texture for each section, as detailed in Table 18, can be seen in Figure 84 (b), Figure 85 (b), and Figure 86 (b).

Figure 84 Section 7: (a) Traffic direction view and (b) Texture depth view

Figure 85 Section 8: (a) Traffic direction view and (b) Texture depth view

Figure 86 Section 9: (a) Traffic direction view and (b) Texture depth view

8.7 Comparison of Field Performance to NCSU Mix Design

Based on the visual condition survey shown in Table 17 and Table 18, the optimum rates for granite 78M chip seals and lightweight chip seals can be estimated. These field sections were constructed using gradation B in both aggregate types. Therefore, the field optimum rates and the NCSU mix design optimum rates for gradation B can be compared to evaluate how the laboratory based mix design results can be extended to the field condition. The NCSU mix design optimum rates and the field optimum rates based on the visual condition survey are summarized in Table 19.

Table 19 Summary of NCSU Mix Design Optimum Rates and Field Optimum Rates

	Granite 78M			Lightweight		
	Design	Field	% Diff.	Design	Field	% Diff.
AAR (lb/yd^2)	15.54	22.59	45%	6.65	9.25	39%
EAR (gal/yd^2)	0.18	0.23	28%	0.21	0.24	14%

Several observations can be made from Table 19. First, the field AARs are about 40% greater than the mix design AARs. There are three main reasons for this noticeable difference. One is different moisture contents between the aggregate used in the mix design (oven-dried condition) and the aggregate used in the chip seal construction (wet condition with unknown moisture content). Another reason is the wastage factor applied in the field AARs. The board test that is used to determine the optimum AAR in the mix design determines the amount of aggregate to form a single layer of stones without any extra aggregate. However, in the field AARs, extra aggregate is applied to ensure a complete coverage of pavement with aggregate particles and to account for the aggregate lost to the side of roadway due to initial passing of vehicles while the newly sprayed chip seal is still in its curing phase (so-called traffic whip-off). Reasonable values of the traffic whip-off factor are 5 to 10% depending on the traffic volume (McHattie 2001). The other reason is the loss of some aggregate particles due to their penetration to existing pavement surface, which is not included in the board test. Evaluation of each of these factors needs a well orchestrated laboratory-field calibration study, which could not have been done within the time and resources given to this study.

The difference between the mix design EARs and the field optimum EARs (ranging between 14 to 28%) is much smaller than that for the AARs. One of the reasons for the smaller difference in the EARs is that the wet and dry aggregate would have little to no effect on the NCSU mix design optimal EARs, as determined by the laser scan and volumetric analysis, because if the same aggregate and gradation are used, the aggregate moisture content would not affect the amount of emulsion required to fill the subsurface voids to 50 percent That is, the subsurface air voids between the aggregate particles are to be filled with emulsion ultimately, and this process is based only on AAR and aggregate gradation, not moisture content. Therefore, the amount of emulsion determined by the NCSU mix design that is needed to obtain 50% embedment would still be valid regardless of the moisture condition of the aggregate. The only adjustments needed would be for absorption into the existing pavement surface and absorption into the aggregate. Again, an additional laboratory-field joint study is needed to quantitatively evaluate the effects of these factors on the EARs.

8.8 Section 10 through Section 15 – Low Volume

Sections 10 to 15 feature both 78M aggregate and lightweight aggregate single seal sections that were constructed on a low volume roadway. These sections were not included in the visual observation analysis due to a construction project that began along the roadway in the middle of the study period. A large commercial development (similar in size to a school facility) began near the site, so large amounts of heavy vehicle traffic that were not present initially when the chip seal sections were constructed were introduced to the roadway. The new construction site can be seen in Figure 87. In addition, a large amount of red clay/mud was trafficked onto the surface of the road by vehicles entering and exiting the construction site, which affected the embedment depth determination.

Figure 87 Construction that began during field section study

Therefore, it was decided not to include the low volume sections in the visual observations and final performance analysis. All the previous MPD results shown for the low volume sections were obtained well in advance of this construction and, therefore, are not affected by this change in heavy traffic and remain valid.

9. CONCLUSIONS AND RECOMMENDATIONS FOR FURTHER RESEARCH

9.1 Conclusions

The research detailed here presents a performance-related chip seal mix design method to be used for constructing effective ASTs that perform well with regard to the major performance criteria studied, i.e., aggregate loss and bleeding. The mix design method detailed herein provides design EARs and AARs for the various aggregate and asphalt material types that are used in the construction of single layer chip seal surface treatments. This design method adopts the modified board test to determine the optimal AAR that is needed to cover the pavement surface with a single layer of given aggregate and the 50% initial embedment depth concept based on the surface texture measurements of the board test using the laser profiler. The following conclusions can be drawn from this study:

- The board test using a 305 mm by 508 mm board yields the least variability in AAR with statistically the same AAR as larger boards.
- A minimum of three board tests is necessary to obtain a representative AAR for the given aggregate.
- The laser profiler and associated algorithms developed by the NCSU research team seem to accurately capture the distance, area, and volume of the AST system subjected to laser testing.
- The reduction in MPD caused by the MMLS3 loading is similar to that under field traffic loading when one MMLS3 wheel pass is equated with one pass of an axle in field traffic. The MPD value becomes asymptotic after 2 hours of MMLS3 loading, and the final MPD values from the MMLS3 loading are very close to the final MPD values under field traffic loading for the medium volume traffic sections. Therefore, a two-hour MMLS3 test can simulate traffic loading during the first week of medium volume traffic.
- The performance uniformity coefficient (PUC) represents the uniformity of the aggregate gradation and is in good agreement with the aggregate loss performance of chip seals.
- MMLS3 aggregate loss and bleeding tests conducted on chip seals composed of two different aggregate types (granite 78M and lightweight aggregate) and CRS-2L emulsion suggest that the optimal EAR determined from the 50% initial embedment criterion provides the maximum allowable amount of asphalt binder without causing bleeding, and therefore, validates the 50% initial embedment concept as the critical mix design criteria.
- A comparison of the optimal rates from the mix design with the rates currently used by some Divisions reveals that the mix design AARs are about 40% less than the field AARs, and that the mix design EARs are about 14 to 28% less than the field EARs in some cases. The use of wet aggregate and traffic whip-off that have not been taken into account in the mix design process, but occur in actual field condition, account for portions of higher field AARs than the mix design AAR. The lower EARs from the mix design compared to the field values may be due to the absorption of the emulsion into aggregate and into the existing pavement surface.

9.2 Recommendations for Further Research

9.2.1 Further Calibration of Mix Design Model

As with any mix design, certain aspects of the model will involve refinement using further field assessment of its performance. Thus, the mix design detailed in this report should be performed and, after constructing the chip seal sections, the failure/success (and the failure mode in the case of potential failure) of the surface treatment over the life of the treatment should be determined. Ideally, this work should be performed for various climatic regions to help adjust the mix design to address environmental differences amongst regions and winter/summer extremes. Any future field calibration of the mix design model should compare the performance of the NCSU mix design yielded rates versus the field rates used by specific NCDOT divisions in order to validate the mix design performance under different environmental and traffic conditions and using different materials. Also, if resources are available to conduct a full study, these chip seals should be constructed on these existing surfaces using the full design algorithm to determine performance. This methodology could be used to further calibrate and refine the NCSU mix design absorption algorithm used for the existing pavement surfaces.

Additionally, a field study should be conducted to calibrate the absorption parameter of the mix design algorithm using different existing field surface conditions, and to determine the absorption adjustment given by the NCSU mix design procedure for each existing surface condition.

9.2.2 Construction Variability Study

During the field construction that was undertaken in this project, the need was clearly demonstrated for significant construction improvements in order to minimize construction variability. More specifically, during the field experimental design, analysis of the accuracy of the measured material application rates, when compared to the target rates, revealed an application rate inaccuracy that could lead to significant chip seal performance problems in the field. In this case, even with the use of an effective mix design procedure, the lack of control of the design material application rates would compromise the effectiveness of the mix design.

Improvements to the construction protocol for chip seal treatments will help ensure effective and consistent performance with regard to the performance parameters that are critical for chip seals. The research team recommends a study to be conducted that will identify the sources of variability and provide recommendations for improvements to the consistency and accuracy of asphalt surface treatment construction in the future. The recommended research would utilize both field construction and sampling efforts, as well as a laboratory experimental testing plan, in order to identify and quantify the variability associated with surface treatment construction.

9.2.3 Traffic Whip-Off Factor

As mentioned in the literature review, during the initial traffic passes on a newly paved chip seal, some traffic whip-off occurs that is caused by aggregate that has not completely bonded to the emulsion during the initial curing phase. This aggregate may need to be accounted for in the mix design to ensure that the AAR is not too low in some situations. If whip-off is not taken into account, it could lead to potential bleeding problems in the field. As previously discussed, the Alaska DOT suggests adding an additional 5% aggregate for low volume residential traffic areas, and 10% for higher speed roadways, such as county roads, because those roadways are likely to lose cover aggregate once they are opened to higher speed traffic after construction (McHattie 2001). This recommendation should be studied in the future to account for initial traffic whip-off in the field for different traffic volumes and speeds.

No whip-off factor was added to the optimal AAR used in the lab specimen mix design for the performance testing that was completed in this study. Because samples were undisturbed during the 24-hour curing phase for the lab-fabricated specimens, a whip-off factor applicable to the initial curing was deemed unnecessary. However, in the field, a whip-off factor should always be added to account for the opening of traffic during the initial curing phase.

9.2.4 MPD Long-Term Database Development

For different climatic regions, MPD scans of newly constructed ASTs should be performed and stored in a database to help determine the MPD at which bleeding/aggregate loss occurs in field situations. This database would require initial MPD scans of newly constructed sections. The associated failure mode and service life for those same respective sections would need to be recorded over a long period (years). This long-term database would allow highway agencies to develop intuition regarding MPD values that are likely to lead to performance problems during the life of the surface treatment, as was seen in the performance testing detailed in this study.

9.2.5 Further Aggregate Penetration Studies

Studies of the aggregate penetration ball test, and of ways that the NCSU mix design should be adjusted to account for various ball penetration values, would further strengthen the mix design flexibility for use under various existing surface conditions. This study would determine appropriate adjustments to the mix design EAR based on the softness of the existing substrate. Because the NCSU mix design uses volume to determine the design EARs, an increase in the aggregate volume in the mix design would be the most direct way to correct for ball penetration, based on the concept that any aggregate that is embedded into the substrate is no longer contributing aggregate volume to the chip seal being designed.

10. REFERENCES

Benson, F. J. and B. M. Gallaway. Study of Some Variables Affecting Retention of Aggregate by Asphalt Surface Treatments. *Roads and Streets*. 1954. pp. 113-1954.

Epps, J. A., B. M. Gallaway, and M. R. Brown. *Synthetic Aggregate Seal Coats*. Research Report 83-2F, Texas Transportation Institute, Texas A&M University, College Station. 1974.

Gransberg, D. D. and D. M. B. James. *Chip Seal Best Practices*. NCHRP Synthesis 342, Transportation Research Board, Washington, D.C. 2005.

Herrin, M., C. R. Marek, and K. Majidzadeh. *Surface Treatments: State-of-the-Art. Highway Research Board*. Special Report 96. 1968.

Hunter, R. N. *Asphalts in Road Construction* (first edition). London: Thomas Telford Publishing. 2000.

Jayawickrama, P. W. and B. Thomas. Correction of Field Skid Measurements for Seasonal Variations in Texas. *Transportation Research Record: Journal of the Transportation Research Board*, No 1639, TRB, National Research Council, Washington, D.C. 1997.

Kandhal, P. S. and J. B. Motter. *Criteria for Accepting Precoated Aggregates for Seal Coats and Surface Treatments*. Research Project 83-19, Final Report. Pennsylvania Department of Transportation. 1987.

Kearby, J. P. Tests and Theories on Penetration Surfaces. *Transportation Research Record: Journal of the Transportation Research Board*, No 271, TRB, National Research Council, Washington, D.C. 1953. pp. 232-237.

Ksaibati, K., M. Cole, and M. Farrar. Evaluation of Surface Treatment Practices in the United States. *Transportation Research Record: Journal of the Transportation Research Board*, No 1545, TRB, National Research Council, Washington, D.C. 1996. pp. 26-34.

Lee, J. S. and Y. R. Kim. *Performance-Based Evaluation of Asphalt Surface Treatments Using the Third Scale Model Mobile Loading Simulator*. NC State University, Raleigh, NC. 2007.

McHattie, R. L. *Asphalt Surface Treatment Guide*. Publication FHWA-AK-RD-01-03, Alaska Department of Transportation and Public Facilities. 2001.

McLeod, N. W. A General Method of Design for Seal Coats and Surface Treatments. *Proceedings of the Association of Asphalt Paving Technologists*, Vol. 38. 1969. pp. 537-630.

North Carolina Department of Transportation. *Standard Specifications for Roads and Structures*. N.C. Department of Transportation Design Services Unit. 2002.

Roque, R., M. Thompson, and D. Anderson. Bituminous Seal Coats: Design, Performance Measurements, and Performance Prediction. *Transportation Research Record: Journal of the Transportation Research Board*, No 1300, TRB, National Research Council, Washington, D.C. 1991. pp. 90-97.

Shuler, S. Chip Seal for High Traffic Pavements. *Transportation Research Record: Journal of the Transportation Research Board*, No 1259, TRB, National Research Council, Washington, D.C. 1990. pp. 24-33.

The Asphalt Institute. *Asphalt Surface Treatment and Asphalt Penetration Macadam*. Manual Series, No. 13 (MS-13) (First edition). 1964.

Transit New Zealand. *Chipsealing in New Zealand*. Controlling Authorities and Roading New Zealand. 2005.